A NEW METHOD FOR PRODUCING VAPOR GROWN CARBON FIBERS AT HIGH GROWTH RATES

SHIN MUKAI

1997

A NEW METHOD FOR PRODUCING VAPOR GROWN CARBON FIBERS AT HIGH GROWTH RATES

SHIN MUKAI

1997

CONTENTS

Chapter 1: General Introduction

1.1	Conventional Carbon Fibers	1
1.2	Vapor Grown Carbon Fibers (VGCFs)	3
	1.2.1 Growth Mechanism of VGCFs	3
	1.2.2 Physical Properties of VGCFs	5
	1.2.3 Production Methods of VGCFs	6
1.3	Objectives of this Work	10
	Literature Cited	12

Chapter 2: The Development of a New Method for the Rapid Production of Vapor Grown Carbon Fibers: The Liquid Pulse Injection Technique

2.1	Introduction	13
2.2	Concept of the Proposed Technique	14
2.3	Experimental	17
2.4	Results and Discussion	22
	2.4.1 As-grown VGCFs	22
	2.4.2 Morphology of VGCFs	22
	2.4.3 Growth Rates of VGCFs	27
	2.4.4 Electrical Resistivity	31
	2.4.5 Tensile Strength	33
	2.4.6 Oxidation Resistivity	33
2.5	Conclusion	33
	Nomenclature	36

Literature Cited 37

Chapter 3: The Effects of Reaction Conditions on the Growth Behavior of Vapor Grown Carbon Fibers Produced Using the Liquid Pulse Injection Technique

3.1 Introduction 38
3.2 Experimental 39
3.2.1 Effects of Reaction Conditions 39
3.2.2 Intermittent Liquid Pulse Injection 41
3.3 Results and Discussion 41
3.3.1 Reaction Temperature 41
3.3.2 Initial Carbon Source Concentration 43
3.3.3 Carrier Gas Line Velocity 47
3.3.4 Amount of Liquid Pulse 49
3.3.5 Intermittent Liquid Pulse Injection 52
3.4 Conclusion 54

Nomenclature 55
Literature Cited 56

Chapter 4: The Production of Vapor Grown Carbon Fibers from a Mixture of Benzene, Toluene and Xylene Using the Liquid Pulse Injection Technique

4.1 Introduction 57
4.2 Experimental 58
4.3 Results and Discussion 59
4.4 Conclusion 75

Nomenclature 76
Literature Cited 77

Chapter 5: Dominant Hydrocarbon which Contributes to the Growth of Vapor Grown Carbon Fibers

5.1 Introduction 78
5.2 Experimental 79
5.2.1 Fiber Production 79
5.2.2 Gas Analysis 80
5.3 Results and Discussion 82
5.3.1 As-grown VGCFs 82
5.3.2 Growth Rate Analysis 82
5.3.3 Gas Analysis 86
5.4 Conclusion 90

Nomenclature 91
Literature Cited 92

Chapter 6: The Influence of Catalyst Particle Size Distribution on the Yield of Vapor Grown Carbon Fibers Produced Using the Liquid Pulse Injection Technique

6.1 Introduction 93
6.2 Experimental 94
6.3 Model Equations 98
6.4 Results and Discussion 104
6.5 Conclusion 114

Nomenclature 115

Literature Cited 116
Appendix 117

Chapter 7: General Summary 123

List of Publications 127

Acknowledgments 129

CHAPTER 1

General Introduction

1.1 Conventional Carbon Fibers

Carbon fibers are widely used in various fields, *e. g.* from sporting goods such as golf clubs and tennis rackets, to advanced machinery such as military aircrafts and racing cars. The main reason that this material is widely used is their superior strength-to-weight properties. Some high performance carbon fibers possess tensile strengths up to 10 GPa, which is about 2.5 times that of steel wires, although their densities are approximately 2 g cm^{-3}, which is about 1/4 of that of iron. In extreme cases, like graphite whiskers grown in carbon arcs under high argon gas pressure, fibers (whiskers) which exhibit tensile strengths up to 20 GPa have also been produced (Bacon, 1960). This value is close to the theoretical value of ideal graphite.

The first utilized carbon fiber is said to be the ex-cotton carbon threads used as the filament of light bulbs invented by Edison about a century ago. Later the initial material of the fiber was changed to bamboo, and then regenerated cellulose. However, the usage of carbon fibers in this field did not make further progress, due to the development of tungsten filaments in the early 1900s.

Research in the carbon fiber field became active again in the sixties, after UCC demonstrated that high modulus fibers could be obtained by the hot stretching of rayon fibers at graphitization temperatures (Bacon *et al.*, 1966). This rayon based fiber is well known as "Thornel" fibers and is regarded as the "father" of ex-polymer fibers. These fibers are in most cases derived from organic precursors by extrusion into polymeric fibers, followed by heat treatment for stabilization, carbonization and further heat treatment up to 3000 °C in an inert atmosphere. Research on this fiber

was conducted in U. S. A., France and Germany, in view of the usage of this fiber as fillers in the place of boron fibers in various composites. However, as other low cost precursors appeared in the market, rayon based fibers gradually lost its competitive power, and finally disappeared from the market in 1978.

The hint that the carbonization of polymeric yarns leads to the formation of carbon fibers led Shindo to introduce polyacrylonitrile (PAN) as the precursor for carbon fibers (1961a, 1961b, 1964). This precursor was more economical than rayon, as PAN is one of the top three mass produced synthetic fibers, the others being nylon and polyester. Moreover, the carbon yield of PAN based carbon fibers is about 50 % whereas that of rayon based carbon fibers is less then 30%. PAN based carbon fibers are also known for their high tensile strengths. Shindo's early fibers possessed a tensile strength of approximately 1400 MPa, which value is quite low when compared with high performance fibers of today, but was three times that of rayon based fibers of the same period. Therefore, PAN based fibers rapidly took the market of carbon fibers. The development of PAN based fibers has made steady and continuous progress and at present, dominates most of the applications of carbon fibers.

Another precursor for fiber production is pitch produced from petroleum asphaltene or coal tar. Pitch based fibers were introduced to the market in 1970. These fibers were produced by the method based on the research of Ohtani *et al.* (1970). Potentially, pitch based fibers are more economical than PAN, as the fiber precursor is abundant and inexpensive. Moreover, the weight loss during processing of pitch based fibers is also smaller then fibers produced from other precursors. However, although pitch based fibers possess high thermal conductivity and oxidation resistivity compared to other carbon fibers, their mechanical strength is relatively poor. Therefore, further refinement of the fibers is necessary for pitch based fibers to become competitive with PAN based fibers.

1.2 Vapor Grown Carbon Fibers (VGCFs)

Another unique type of carbon fibers is vapor grown carbon fibers (abbreviated to VGCFs) which are produced by the chemical vapor deposition of a hydrocarbon in the presence of ultra-fine metal catalyst particles (*e. g.* Fe, Ni, Co). Although among several types of carbon fibers this type is the least known, it has the longest history, which exceeds over a hundred years. The early reports on VGCFs are those of Schützenberger and Schützenberger (1890), and Pelabon (1905). Hughes and Chambers (1889) achieved a patent for "hair-like carbon filaments" grown from methane in an iron crucible under a hydrogen atmosphere. These researchers focused on VGCFs for the usage of them as filaments for the newly invented electric light bulb. Unfortunately, the lack of technology of process control made them lose commercial interest in it. However, studies on VGCFs have been conducted in many laboratories ever since. These studies have been reviewed periodically by many authors (Hillert and Lange, 1958, Baker and Harris, 1978, Tibbetts *et al.*, 1986, Endo, 1988, Baker, 1989).

1.2.1 Growth Mechanism of VGCFs

The widely supported growth mechanism of VGCFs is schematically shown in Fig. 1-1. First, when a vapor of a hydrocarbon makes contact with a ultra-fine metal catalyst particle under a high temperature atmosphere, it is decomposed to carbon atoms on the surface of the catalyst. These carbon atoms dissolve into the catalyst and precipitate in the form of a hollow primary fiber. The fiber elongates as this process continues. In this process, a reduced atmosphere is essential to maintain the catalytic activity of the particle. Concurrently with the elongation process, pyrolytic carbon layers are deposited on the wall of the primary fiber through the thermal chemical vapor deposition (CVD) of the hydrocarbon, and thickens the fiber. So it could be said that VGCFs are formed by an integrated process of catalysis and CVD. Therefore, these fibers are frequently referred to as catalytic chemical vapor deposited (CCVD) filaments. Although many factors govern the elongation rate of VGCFs, the

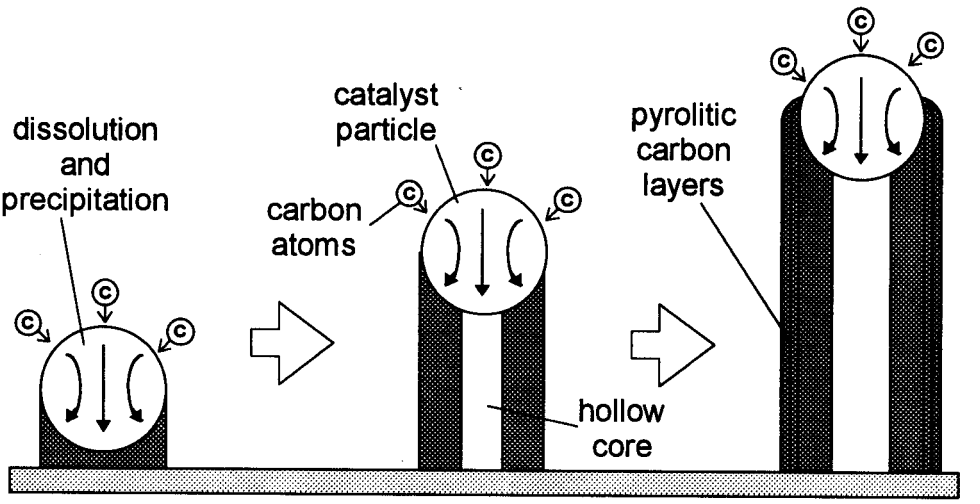

axial direction:	**catalysis**
radial direction:	**thermal CVD**

Fig. 1-1 Growth Mechanism of VGCFs

size of the catalyst particle seems to be the key. Only catalyst particles in a narrow size range lead to the growth of VGCFs. This size range is a few to about a hundred nanometers.

Baker *et al.* (Baker and Harris, 1970, Baker *et al.*, 1972, 1973) used a new technique of controlled atmosphere electron microscopy (CAEM) and directly observed the growth of VGCFs from the decomposition of acetylene on particles of nickel, iron, cobalt and chromium. These studies allowed the confirmation of the manner in which VGCFs grow, *i.e.* the important roles of a ultra-fine metal catalyst particle. They found that the catalyst particle always exists at the growing tip of the fiber, and half of the particle is exposed to the atmosphere whereas half is protected by the fiber. They also clarified that the growth of the fiber terminates when the catalyst particle is completely encapsulated by carbon layers.

There have been a lot of controversies about the nature of the driving force for carbon diffusion through the catalyst particle. Baker *et al.* (1972, 1973) suggested that carbon species diffuse from the hotter leading surface, on which hydrocarbons occurs, to the cooler rear faces, at which carbon is precipitated from solution, and that the driving force for carbon diffusion is the temperature gradient created in the particle by the exothermic decomposition of the hydrocarbon at the exposed front faces and endothermic deposition of carbon at the rear faces. On the other hand, Rostrup-Nielsen and Trimm (1977) insisted that the driving force for diffusion was due to the existence of a carbon concentration gradient rather than a temperature gradient within the particle. The latter opinion seems realistic, since the diameter of the catalyst particle is around 10 nm, and it is unlikely that a temperature gradient exists in such a small dimension.

1.2.2 Physical Properties of VGCFs

VGCFs possess a structure which reflects its unique growth mechanism. Basically, VGCFs are formed by carbon layers arranged like a tree-ring structure. However, a

single fiber can be divided into two regions, one, the core of the fiber which is formed by catalysis, and the other, the external region which is formed by thermal chemical vapor deposition. This structure was confirmed by Oberlin *et al.* (1976). The core is almost free from defects and is close to the structure of ideal graphite, though the carbon atoms are not arranged as flat layers, but as concentric tubes. On the other hand, the stacking manner of graphene sheets in the external region are quite random when compared with the core. Therefore as-grown VGCFs have a "sword and sheath" structure. Although the sheets of the outer region are stacked randomly, they are still roughly aligned to the axis of the fiber even at the as-grown state, so on heat treatment, their structure approaches that of the core. From this point of view, VGCFs are considered to be easy graphitizable materials.

If the production temperature of VGCFs is set as the same as the carbonization temperature of conventional carbon fibers, properties as tensile strength, electric and heat conductivity, oxidation resistivity of VGCFs are extremely superior to those of conventional ones. However, there is a lack in accurate values of such properties, as VGCFs are usually extremely short, and the values obtained are those of long fibers which were produced under extreme reaction conditions (Koyama, 1972, Koyama *et al.*, 1972).

1.2.3 Production Methods of VGCFs

The key of VGCF production is how to prepare the ultra-fine metal catalyst particles, which are essential for fiber growth. One easy way is to prepare particles on a substrate. Endo and Shikata (1985) have listed three possible methods of catalyst preparation, which are summarized in Fig. 1-2. The first method is to directly spray a dispersion of ultra-fine iron particles on a substrate followed by drying. The second method is to spray or paint a solution of an iron compound on a substrate. Catalyst particles can be obtained on the substrate through the thermal decomposition of the compounds. The last method is to form catalyst particles in the vapor phase through the decomposition of organic compounds of metals, and then deposit them on

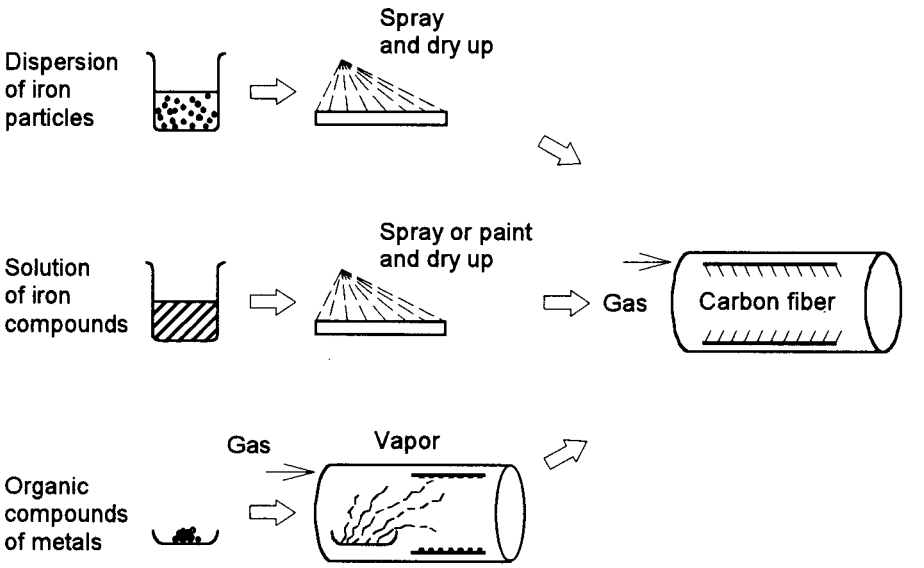

Fig. 1-2 Substrate Seeding Methods

a substrate. VGCFs are subsequently obtained by heating the substrate in an atmosphere of a mixture of hydrogen and hydrocarbon vapors. These methods are referred to as substrate seeding methods. The growth rate of thus obtained VGCFs is very low (30 to 50 $\mu m\ s^{-1}$) and their lengths are usually very short (a few to a few hundred microns), but if the carbon potential of the atmosphere is suppressed to a value which does not allow carbon deposition, extremely long VGCFs can be obtained. However after elongation in such an atmosphere, the obtained VGCFs need to be thickened in a atmosphere of higher carbon potential, a process which requires a long process time. The fact that fibers can only be obtained on a substrate, in other words that the production process is a semi-batch process, is a critical shortcoming for the commercialization of this process.

In the mid 1980s, Endo *et al.* introduced a new method for the production of VGCFs, the floating catalyst technique (Endo and Shikata, 1985) which is illustrated in Fig. 1-3. In this technique, ultra-fine metal catalyst particles are introduced into the reactor either directly or indirectly through the decomposition of organic metal compounds. Fiber growth takes place in the three dimensional space of the reactor. This method may become a promising technique for the mass production of VGCFs as this process can be continuously operated.

However, there are still many problems to solve before realizing this new method. For example, it is very difficult to reactivate the catalyst particles in the direct method. Moreover, in the indirect method, the vapors of the catalyst material and the carbon source is introduced into the reactor with the carrier gas, and since the temperature at the inlet of the reactor is very low in comparison with the decomposition temperature of the catalyst material, and the heat conductivity of the gas is very low, the catalyst material is gradually heated and slowly decomposes. This indicates that the generation of metal clusters is very gradual. There is a possibility that most of these clusters make contact with the carbon source and are completely covered with carbon layers before they grow up to catalyst particles which have suitable sizes for fiber

[Direct Seeding]

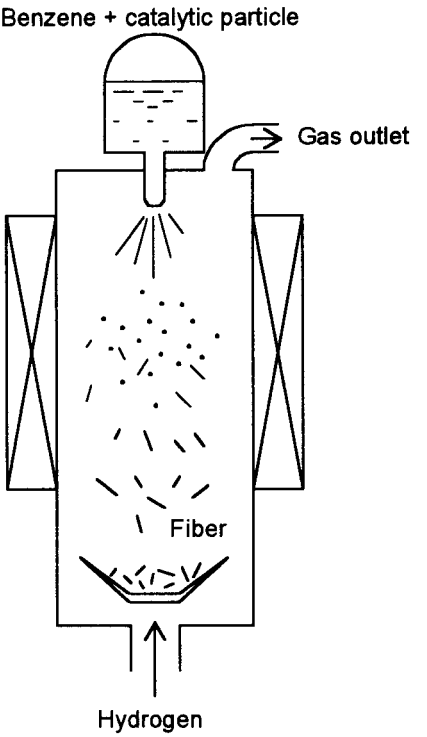

[Indirect Seeding]

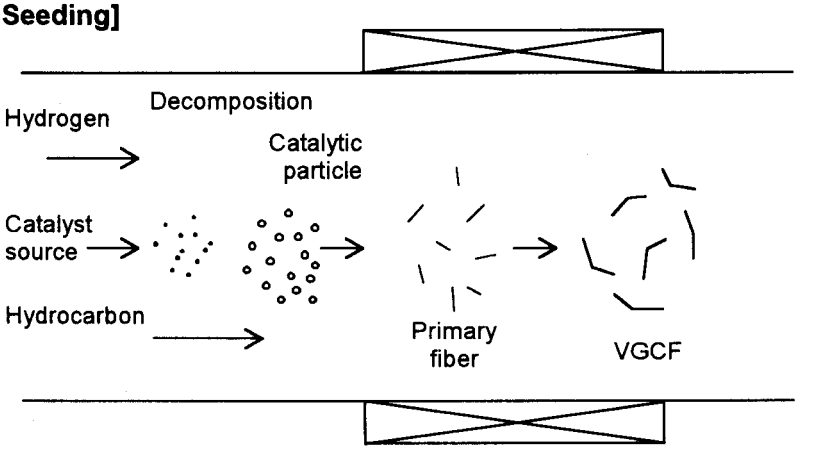

Fig. 1-3 Floating Catalyst Technique

growth. Therefore the growth rates of the fibers are extremely low, and it is seldom that the lengths of VGCFs produced using this method exceed 1 mm. This short length limits their usage.

1.3 Objectives of this Work

Research in the field of VGCFs has made continuous progress, but it is hard to say that VGCFs are presently commercially feasible, as although they possess extremely superior properties, the productivity of them is still low. This leads to a extremely high production cost. The main obstacle of feasibility is their low growth rate and attainable length.

The main objective of this work is to develop a new method to produce fairly long VGCFs at high growth rates. The aim is to produce VGCFs longer than 10 mm within 10 seconds. The key point is to control the number and size of the catalyst particles in the reaction zone of fiber growth. This was achieved by introducing the catalyst material into the reactor as a liquid pulse.

In chapter 2, first the concept of the new proposed method is described in detail. Then the experimental results are reported along with the physical properties of the obtained VGCFs.

As the growth of VGCFs is a very sensitive process, it is assumed that reaction conditions impose a great influence on the yield of the fibers. From this point of view, in chapter 3, the effects of reaction conditions on the behavior of VGCF growth is investigated. A method to achieve the continuous production of VGCFs is also proposed, and its possibility is experimentally verified.

In chapter 4, a low cost material for VGCF production is sought. In conventional

production processes of VGCFs, aromatics, namely benzene, is a popular material. Therefore, crude benzene, which is a mixture of benzene, toluene and xylene, was the target. First, the growth sequences of VGCFs when each component of the mixture was used individually was analyzed. Next, VGCFs were produced using mixtures with various compositions of the three hydrocarbons. Finally, fiber growth rate constants of each hydrocarbon were derived.

As active catalyst particles can be easily obtained using this new production method, there is a possibility that VGCFs can be obtained from a wide variety of hydrocarbons, even from those which were thought not to be suitable for fiber growth. In chapter 5 the possibility of producing VGCFs from light paraffins is investigated. Moreover, the actual hydrocarbon which contributes to fiber growth is verified, as it is unlikely that the hydrocarbon(s) which exist in the high temperature reaction zone are the same as the initial carbon source.

Chapter 6 focuses on the formation process of catalyst particles. First the influence of reaction conditions on the size distribution of the generated catalyst particles is examined. Next, a model which represents the particle formation process is derived using population balance equations. Finally, a procedure to predict optimal reaction conditions for efficient fiber production is proposed.

Chapter 7 gives the conclusion of this thesis. Remarks about further studies of this topic are also given.

Literature Cited

Bacon, R, *J. Appl. Phys.* **31**, 283 (1960)

Bacon, R., Pallozza, A. A., and Slosarik, S. E., *Society of Plastics Industry, 21st. Tech. and Management Conf.*, Section 8E (1966)

Baker, R. T. K. and Harris, P. S., *J. Phys. E.* **5**, 793 (1970)

Baker, R. T. K., Barber, M. A., Harris, P. S., Feates, F. S., and Waite, R. J., *J. Catal.* **26**, 51 (1972)

Baker, R. T. K., Harris, P. S., Thomas, R. B., and Waite, R. J., *J. Catal.* **30**, 86 (1973)

Baker, R. T. K. and P. S. Harris, In *Chemistry and Physics of Carbon* (Edited by Walker, Jr., P. L. and Thrower, P. A.), Vol. 14, pp. 83-165, Marcel Dekker New York (1978)

Baker, R. T. K., *Carbon* **27**, 315 (1989)

Endo, M. and Shikata, M., *Ohyo Butsuri* **49**, 563 (1985)

Endo, M., *CHEMTECH* **Sept.**, 568 (1988)

Hillert, M. and Lange, N., *Z. Kris.* **111**, 24 (1958)

Hughes, T. V., and Chambers, C. R., U. S. Patent No. 405,480 (1889)

Koyama , T., *Carbon* **10**, 757 (1972)

Koyama , T., Endo, M., and Onuma, Y., *Jpn. J. Appl. Phys.* **11**, 445 (1972)

Oberlin, A., Endo, M., and Koyama, T., *J. Cryst. Growth* **32**, 335 (1976)

Otani, S., Kokubo, and Y., Koitobashi, T., *Bull. Chem. Soc. Jpn.* **43**, 3291 (1970)

Pelabon, C. H., *C. R. Acad. Sci.* **137**, 706 (1905)

Rostrup-Nielsen, J. R. and Trimm, D. L., *J. Catal.* **48**, 155 (1977)

Shindo, A., *Osaka Kogyo Gijitsu Shikoku* **12**, 110, 119 (1961a)

Shindo, A., *Rep. Govt. Ind. Res. Inst., Osaka*, 317 (1961b)

Shindo, A., *Carbon* **1**, 391 (1964)

Schützenberger, P., and Schützenberger, L., *C. R. Acad. Sci.* **111**, 774 (1890)

Tibbetts, G. G., Endo, M., and Beetz, Jr., C. P., *SAMPE J.* **22**, 30 (1986)

CHAPTER 2

The Development of a New Method for the Rapid Production of Vapor Grown Carbon Fibers: The Liquid Pulse Injection Technique

2.1 Introduction

Vapor grown carbon fibers (VGCFs) have a high potential to significantly reduce the production cost of "discontinuous" carbon fibers, as they can be produced using a single entrained bed (Endo and Shikata, 1985). They also show a higher tensile strength, and higher electrical and thermal conductivities when compared to conventional carbon fibers produced at the same reaction temperature (*e.g.* 1373 K) (Koyama, 1972, Koyama *et al.*, 1972, Tibbetts *et al.*, 1986, Ishioka *et al.*, 1992, 1993). These advantages make them applicable to various composites.

The main factors, which may determine whether VGCFs are commercially applicable or not, are the attainable length and growth rate of the fibers. Lengths of at least 1 mm are required to use VGCFs as the filler of various composites. VGCFs with lengths over 10 mm could widen their applications to many new purposes. Conventional growth rates of VGCFs are said to be in the range 30 to 50 $\mu m\ s^{-1}$, although it has been suggested that growth rates up to 830 $\mu m\ s^{-1}$ can be attained (Endo, 1988).

In the 1980s, a new method called the floating catalyst technique was proposed for the mass production of VGCFs (Endo and Shikata, 1985). In this technique the catalyst material is directly introduced into the gas flow of a mixture of the carrier and carbon source (hydrocarbon). Catalyst particles are obtained from the following thermal decomposition process of the catalyst material. Organic metal compounds (*e.g.*

ferrocene) are usually used as the catalyst material. When the catalyst material decomposes, it releases primary metal particles (nuclei). They increase their size through the coalescence among them. When they reach the proper size for fiber growth (a few to about a hundred nanometers), fiber growth initiates. A high reaction temperature (over 1273 K) is required for this process to continue, as it includes the thermal decomposition of the catalyst material and carbon source (*e.g.* benzene). Presently, the maximum length of fibers obtained by this method is usually a few millimeters (Komatsu and Nakatani, 1988, Morimoto, S., 1988, Endo *et al.*, 1989).

The objective of this work is to develop a new method to obtain fairly long VGCFs at high growth rates. The aim is to obtain VGCFs longer than 10 mm within 10 s.

2.2 Concept of the Proposed Technique

Many researchers have devoted their work to specify the mechanism of fiber growth, and to find the key points for fiber production. Among various factors, the size of the catalyst particle seems to be one of the critical key points.

The range of the catalyst particle size which is suitable for fiber growth is very narrow, usually a few to about a hundred nanometers in diameter. Baker *et al.* (1989) have reported that the rate of fiber growth has an inverse square root dependence on catalyst particle size. Endo (1988) has pointed out that not only the growth rate, but also the fiber yield increases when smaller particles are used as the catalyst. Furthermore, Benissad *et al.* (1988) have suggested that the fiber yield and length depends on the particle size which was influenced by reaction conditions. However, the effect of the reaction conditions on the size of the catalyst particles obtained has not been well distinguished yet, because the formation process of particles is very complicated.

In the usual floating catalyst technique, the vapors of the catalyst material and the carbon source are introduced into the reactor with the carrier gas. Since the temperature at the inlet of the reactor is very low in comparison with the decomposition temperature of the catalyst material, and the heat conductivity of the gas is very low, the catalyst material is gradually heated and slowly decomposes. This indicates that the generation of metal clusters is very gradual. There is a possibility that most of these clusters make contact with the carbon source and are completely covered with carbon layers before they grow up to catalyst particles which have the suitable size for fiber growth.

The strategy to produce long VGCFs at high growth rates is as follows:

(1) Stabilization of the gas flow.
(2) Rapid raising of the temperature of the catalyst material above its decomposition temperature.
(3) Controlling of the contacting pattern between the generated catalyst particles and the carbon source.

The first point can be achieved by thoroughly preheating the carrier gas. The latter two points can be achieved by introducing the catalyst material to the reactor as a liquid pulse.

The introduction of the catalyst material to the reactor as a liquid pulse has a possibility to produce catalyst particles which lead to rapid fiber growth. The effectiveness of this method is demonstrated in Fig. 2-1. When the catalyst material, a benzene solution of ferrocene, is injected into the reactor, it hits the hot wall of the reactor. This liquid pulse evaporates simultaneously, since the heat transfer from the reactor wall to the liquid is very rapid. The following decomposition of ferrocene instantaneously occurs, and numerous primary iron clusters are formed. As the concentration of these clusters is very high, they rapidly coalesce and form particles.

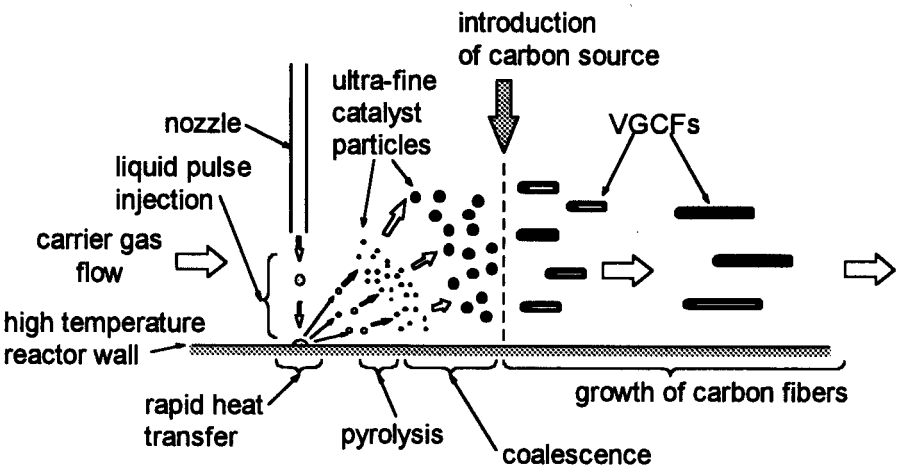

Fig. 2-1 Demonstration of the Effect of Liquid Pulse Injection

These particles increase in size, and make contact with the carbon source. VGCFs elongate through the catalysis of these metal particles.

This indicates that the sizes of the catalyst particles can be controlled by changing the time allowed for coalescence of the primary iron clusters before making contact with the carbon source. This can be achieved by changing the distance between the hitting point of the liquid pulse and the point where the particles make contact with the carbon source, or by changing the flow rate of the carrier gas.

The following experiment was conducted to investigate the effectiveness of this new liquid pulse injection (LPI) technique.

2.3 Experimental

Benzene (99.5% purity) was used as the carbon source and the solvent for the catalyst material. Ferrocene (98% purity) was used as the catalyst material. Nitrogen (99.999% purity) and Hydrogen (99.95% purity) were used as the reactor purging gas and carrier gas, respectively.

A schematic diagram of the apparatus and the reactor used for fiber production are shown in Figs. 2-2 and 2-3, respectively. The reactor was made from a quartz glass tube (*i.d.* 22 mm, length 1000 mm) and was composed of three zones, the gas preheating zone (zone A), the material introduction zone (zone B) and the reaction zone (zone C). A ceramic honeycomb (alumina, pitch: 3 mm) was placed in zone A in order to rapidly heat the carrier gas to the desired temperature. This stabilizes not only the gas phase temperature, but also the gas flow. A quartz glass inner tube was placed in zone C to catch the fibers and increase the residence time of the fibers in zone C.

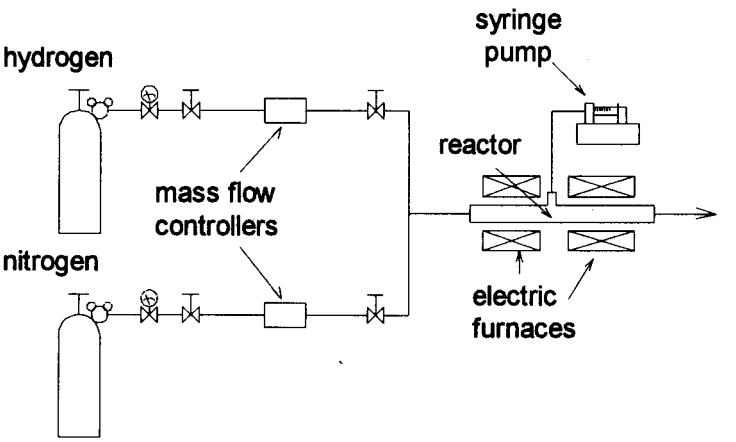

Fig. 2-2 Experimental Apparatus

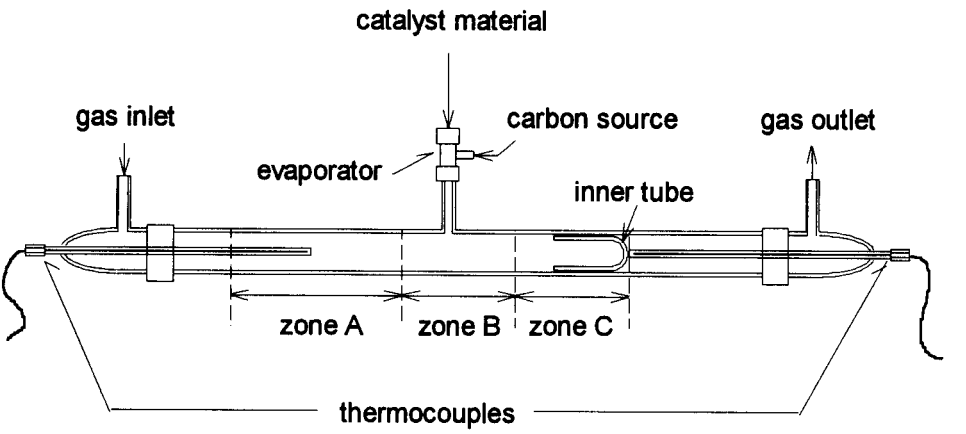

Fig. 2-3 Experimental Reactor

The reactor was purged with nitrogen for 30 min (flow rate: 300 (cm^3-NTP) min^{-1}) and then with hydrogen for 30 min (flow rate: 60 (cm^3-NTP) min^{-1})). The flow rate of hydrogen was kept constant throughout the experiment. After the reactor was purged thoroughly with hydrogen, the temperatures of zones A and C were respectively raised to 1073 K and 1373 K using electric furnaces. When each zone was heated to the desired temperature, liquid benzene (carbon source) was fed into the evaporator at a constant rate of 0.05 cm^3 min^{-1}, and then its vapor was introduced into the reactor from zone B. When a minute passed from the introduction of the carbon source, a nozzle for the injection of the catalyst material was inserted into zone B. 0.025 cm^3 of the catalyst material was injected as a liquid pulse from the nozzle to hit the hot reactor wall. After the injection, the nozzle was drawn out from the reactor. The catalyst material was a benzene solution of ferrocene. The weight percentage of ferrocene was 10 %. After the reaction was performed for a certain period (15 to 180 s), the electric furnaces were cut off, and the reactor was purged with nitrogen. When the reactor cooled down to room temperature, the inner tube was taken out and the produced fibers were recovered.

The length of the fibers were directly measured to obtain growth rates. The surface morphology of the obtained fibers were observed by scanning electron microscopy (Hitachi; S510).

VGCFs are known to possess high tensile strengths and electrical and thermal conductivities. This is due to their unique structure, *i.e.* VGCFs are formed by carbon layers arranged like a tree ring structure. There are some reports on the physical properties of VGCFs, but the number of data are few (Koyama, 1972, Koyama *et al.*, 1972, Tibbetts *et al.*, 1986, Ishioka *et al.*, 1992, 1993). This is due to the fact that most conventional VGCFs are very short. Conventional VGCFs are usually a few hundred micrometers in length. Therefore it is very difficult to handle them, and even if the properties of them could be measured, the obtained values are likely to lack accuracy. If long VGCFs could be obtained, it will become easy to

measure the physical properties of them. Therefore, the electrical resistivity, tensile strength and oxidation resistivity of the obtained VGCFs were also measured.

The electrical resistivity of the VGCFs obtained using the LPI technique were measured according to the method recommended in the Japanese Industrial Standard (JIS) R 7601. A single fiber was mounted on an insulator plastic sheet as shown in Fig. 2-4. The fiber was fixed to the plastic sheet using silver paste. The fiber diameter and the distance between the voltage terminals were measured using scanning electron microscopy. On the determination of the fiber diameter, a circular cross-section of the fibers was assumed. Measurements were conducted at room temperature.

Although the tensile strength of VGCFs (the strength per unit area of the cross section of a fiber) is relatively large, the diameter of it is extremely small, therefore it is impossible to use conventional equipment to measure the tensile strength of a single VGCF. Hence, the apparatus shown in Fig. 2-5 was constructed and used for the measurements of tensile strengths. The force loaded on the fibers was measured using a strain gauge (Kyowa Electronic Instruments; LTS-50GA). A single fiber was set on a plastic mount (Fig. 2-4) and was fixed to it using adhesives. The mount was set on the apparatus, and the plastic mount was cut using a hot knife. The fiber was pulled at a constant rate of 10 mm min^{-1}. The signal from the strain gauge was amplified and constantly recorded. After the fiber broke, its diameter was measured from the observation of the fractured cross section using scanning electron microscopy. The tensile strength of the fiber was calculated using the measured maximum force on the fiber before fractuation, and the measured diameter of the fiber.

The oxidation rate of the fibers was measured using a thermogravimetric analyzer (Shimadzu; TGA-50H). Air was used as the oxidizer. Approximately 2 mg of a sample was set in the analyzer. Experiments were conducted at a constant temperature increment rate of 5 K min^{-1}, and the weight loss of the sample was

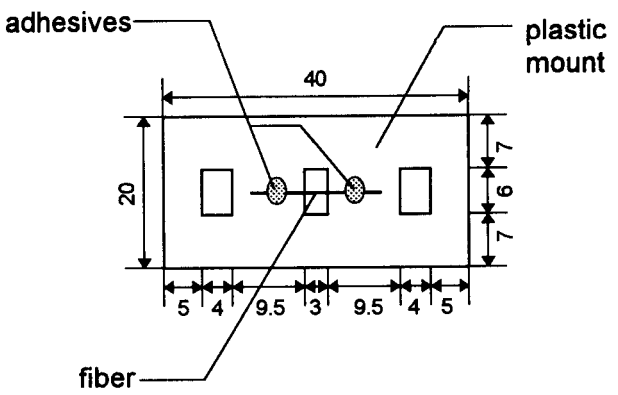

Fig. 2-4 Plastic Mount for Tensile Strength and Electric Conductivity Measurements

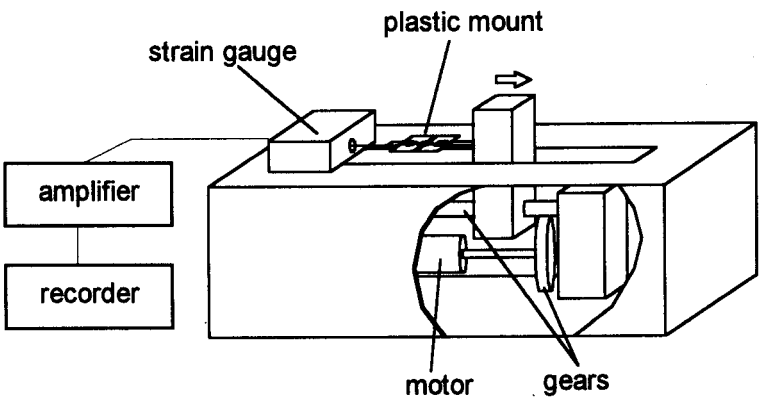

Fig. 2-5 Apparatus for Tensile Strength Measurements

recorded. The samples used in both experiments were VGCFs obtained in this work, commercially available VGCFs (produced using the floating catalyst technique), typical commercial PAN based carbon fibers and typical commercial pitch based carbon fibers.

2.4 Results and Discussion

2.4.1 As-grown VGCFs

Figures 2-6 and 2-7 are photographs and a SEM micrograph of typical as-grown VGCFs, respectively. Straight fibers with lengths up to 50 mm were obtained. The diameters of these fibers were 0.5 μm to 50 μm, mainly in the range 1 μm to 4 μm. This indicates that fibers with high geometric aspect ratios up to 100000 can be obtained using this new technique. The thicker fibers seem to grow through another process, which will be discussed later.

2.4.2 Morphology of VGCFs

Figure 2-8 shows the cross section of a typical thin VGCF obtained using the liquid pulse injection technique. Concentric rings can be observed, supporting the fact that the obtained VGCFs grow through the same mechanism as that of conventional VGCFs. Among the VGCFs, fibers adhered side by side (Fig. 2-9), and cross connected fibers (Fig. 2-10) were observed. This also reflects their growth mechanism. First a thin primary fiber elongates through the catalysis of a ultra-fine iron catalyst particle, then the primary fiber thickens through the chemical vapor deposition of the carbon source. Therefore, if two primary fibers are closely located before thickening terminates, connected fibers will be formed.

The thicker fibers had unique rough surfaces as shown by SEM images (Figs. 2-11 a-c). These fibers looked as if numerous carbon particles were attached to the surface of the fibers, leaving no space between them. The rapid thickening, as well as the

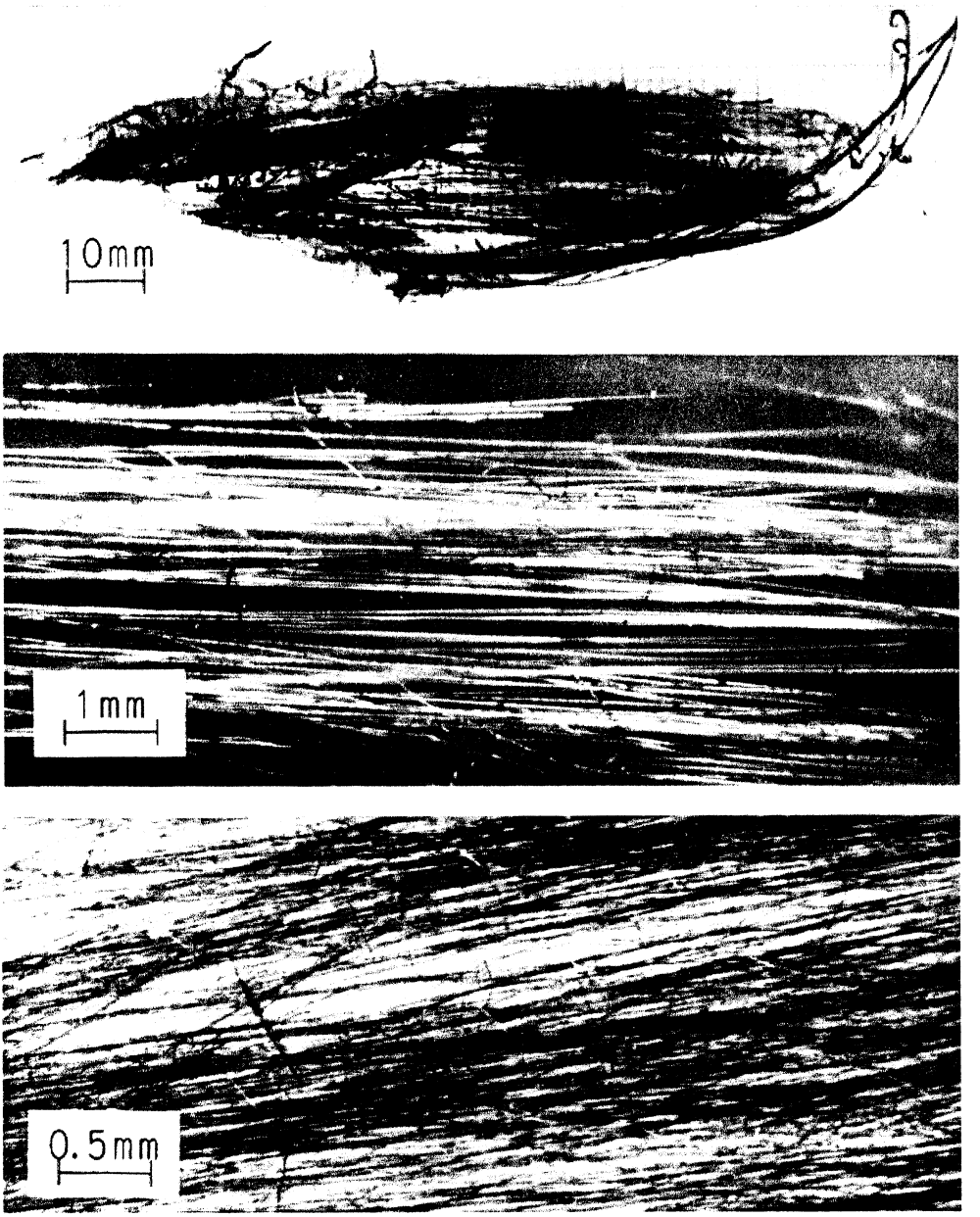

Fig. 2-6 Photographs of As-grown VGCFs

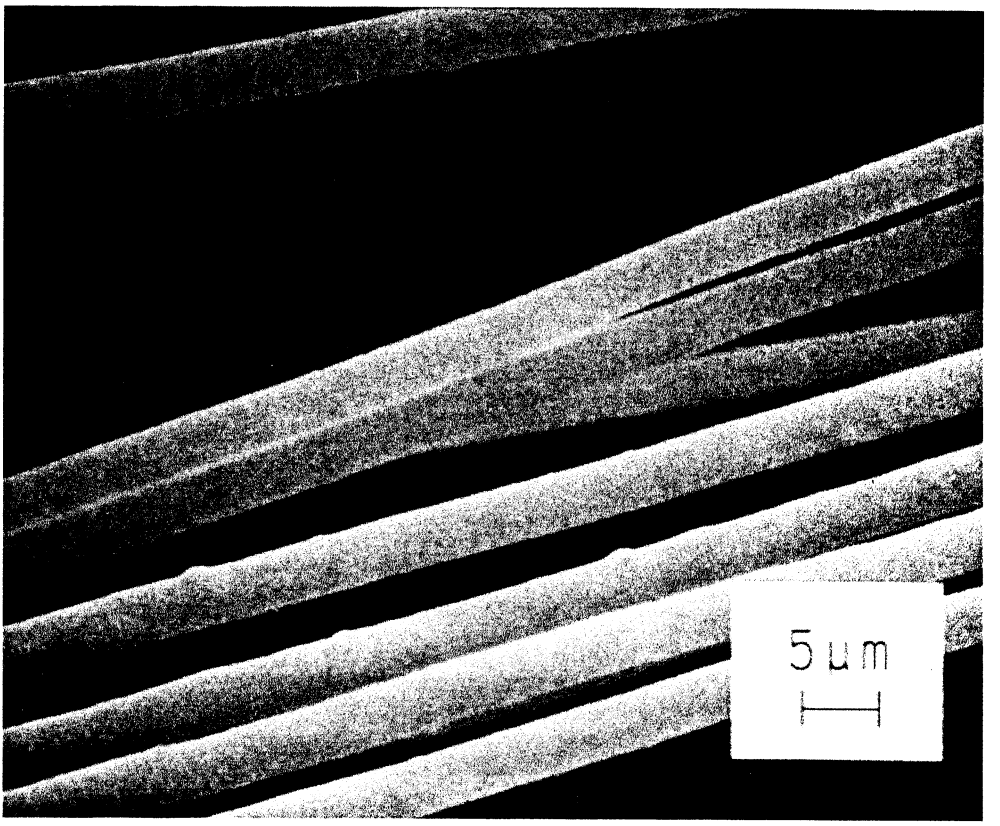

Fig. 2-7 SEM Micrograph of As-grown VGCFs

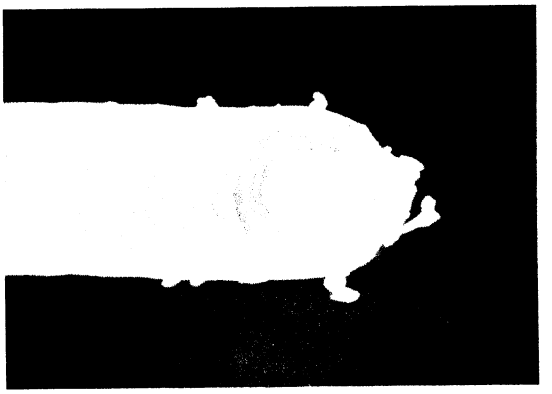

Fig. 2-8 Cross Section of a VGCF

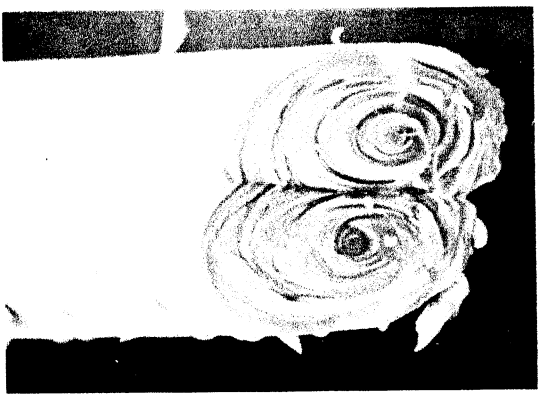

Fig. 2-9 Side Adhered VGCFs

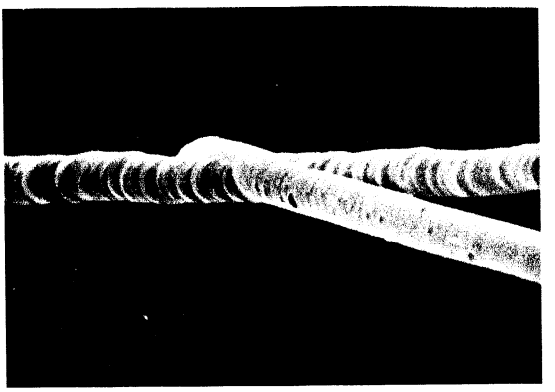

Fig. 2-10 Cross Connected VGCF

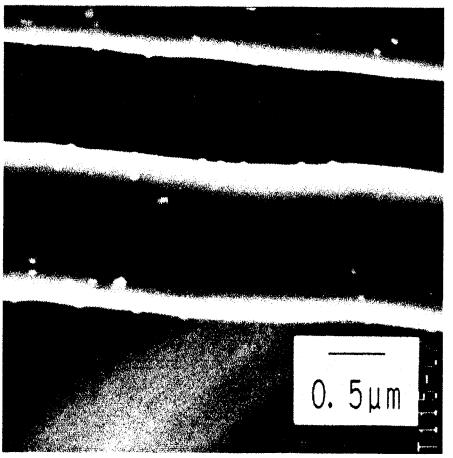

Fig. 2-11a Catalyst Particles Attached to the Surface of VGCFs

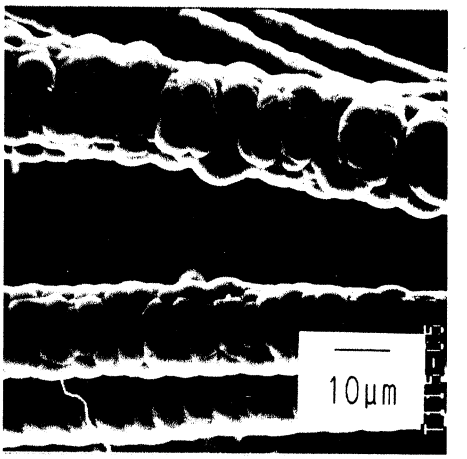

Fig. 2-11b Thick VGCFs

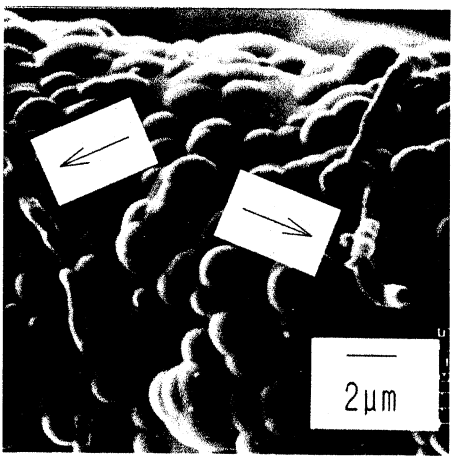

Fig. 2-11c Secondary Fibers Growing from the Surface of a Primary Fiber

formation of rough surfaces, can be explained by the following process.

Figure 2-12 is a demonstration of this process. In the LPI technique, many catalyst particles are instantaneously generated. Naturally, these particles have a distribution in size, since their sizes increase through a coalescence process. The larger particles, which do not lead to rapid fiber growth, adhere to the surface of the growing fibers. The carbon source is decomposed on the surface of these particles and forms hemispheric carbon layers. These layers grow and gradually fill the space between the particles. Hence, thick fibers which have rough surfaces are formed. This indicates that the thickening rate of the fibers can also be controlled by changing the ferrocene concentration and the reaction temperature of the proposed LPI technique. Moreover, the rough surfaces obtained through this process may act as an anchor to increase the adhesion of the fibers to the matrices when they are used as the filler of various composites.

Figures 2-11 a-c are a series of SEM images which show the fiber surface at each step of this process. Figure 2-11 a shows catalyst particles attached to the surface of the fiber, and Fig. 2-11 b shows carbon layers accumulated on the particles. Figure 2-11 c shows secondary fibers which grow from the surface of the fiber. The growth of secondary fibers is indirect evidence of the presence of iron catalyst particles on the surface of the fiber.

2.4.3 Growth Rates of VGCFs

Preliminary experiments were conducted by continuously introducing the vapor of the catalyst material to the reactor. VGCFs with lengths up to 10 mm were obtained. However, the growth rates of them were comparable to those of conventional VGCFs.

Figures 2-13 shows the growth sequence of VGCFs, where L is the fiber length, and t reaction time. The length of the fibers rapidly increase at the beginning of the reaction, and after a short reaction period, the growth rate drastically decreases and

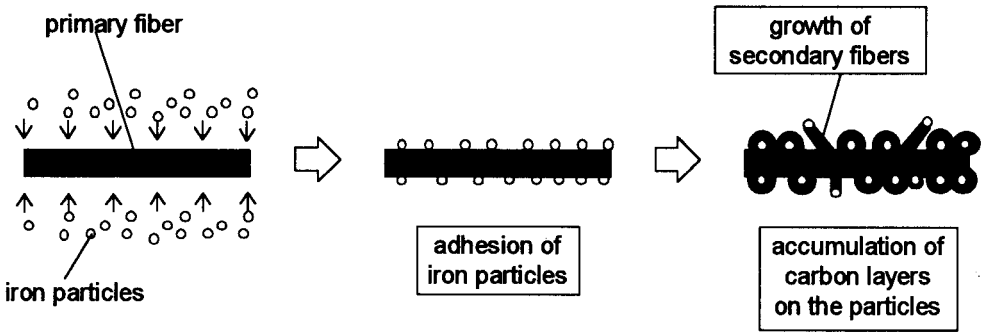

Fig. 2-12 Rapid Thickening Process

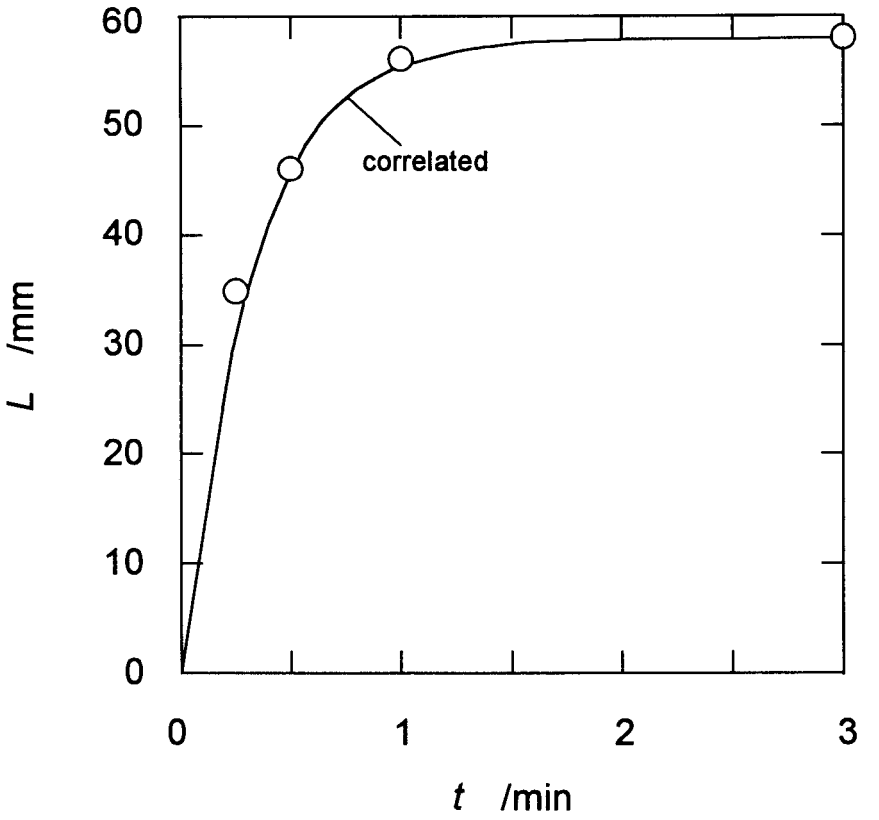

Fig. 2-13 Growth Curve of VGCFs

finally the growth of the fibers terminates. Maximum lengths up to 55 mm were obtained. It is obvious that fibers longer than 10 mm can be easily obtained within 10 seconds using this newly developed method

The rapid decrease in the growth rate of VGCFs is mainly due to the following two factors. First, the decrease in the concentration of the carbon source, which occurs after fiber growth initiation, as carbon is consumed by fiber elongation and thickening. The amount of consumption depends on the number of the growing fibers, which depends on experimental conditions and is not predictable. Second, the deactivation of the catalyst particle. This is due to the surface coverage of the particle by carbon layers. Both factors highly depend on the configuration of the reactor used for production. However, as the effects of both factors can be neglected at the beginning of the reaction, it is wise to evaluate the growth rate of the fibers by its initial value. Unfortunately, it is impossible to obtain this value experimentally, as it is difficult to conduct short reaction time experiments. Therefore, in this work, this value was obtained by first finding an empirical equation which well represents the growth behavior of VGCFs, and next, calculating the initial growth rate of the fibers by analysis of the obtained empirical equation.

Considering the rapid decrease in the growth rate of the fibers, it is expected that the transient change of the growth rate of the fibers can be expressed by the following empirical equation:

$$\frac{dL}{dt} = A\exp(-Bt) \qquad (2\text{-}1)$$

where L is the length of the fiber, t the reaction time, and A, B adjustable parameters. The integration of Eq. (2-1) gives the following equation, which represents the growth behavior of the fibers:

$$L = \frac{A}{B}\{1 - \exp(-Bt)\} \tag{2-2}$$

Note that parameter A gives the initial growth rate of the fibers ($r_{(t=0)}$):

$$r_{(t=0)} = \left.\frac{dL}{dt}\right|_{t=0} = A \tag{2-3}$$

and A/B gives the maximum length of the fibers (L_{max}) at a certain set of reaction conditions. This value can be experimentally obtained. First, parameter B was adjusted so that each growth curve would well represent experimental data by using Eq. (2-2), and the experimentally obtained maximum length of the fiber ($=A/B$). Then parameter A was determined by multiplying the A/B value with the obtained B value. The growth curve calculated by Eq. (2-2) and the obtained A and B values are also shown in Fig. 2-13. This line is in good agreement with the experimental data.

The obtained initial growth rate of the fibers was 3.1 mm s^{-1}. This value is approximately a hundred times larger than that of fibers obtained using conventional production methods. This shows that the LPI technique is an effective method for rapid VGCF production.

2.4.4 Electrical Resistivity

Figure 2-14 shows the electrical resistivities of VGCFs (ρ), measured at room temperature, plotted against the diameter of the fiber (d). The resistivity increases with the increase in the diameter of the fibers. This is due to the fact that although the core of the fiber formed by catalysis is highly graphitic, the degree of order of the carbon layers decreases towards the fiber surface, as the outer carbon layers of the fiber are formed through the chemical vapor deposition of the carbon source. The resistivity of fibers which diameters are less than 5 μm are comparable to those reported by several authors (Koyama *et al.*, 1972, Tibbetts *et al.*, 1986, Ishioka *et al.*,

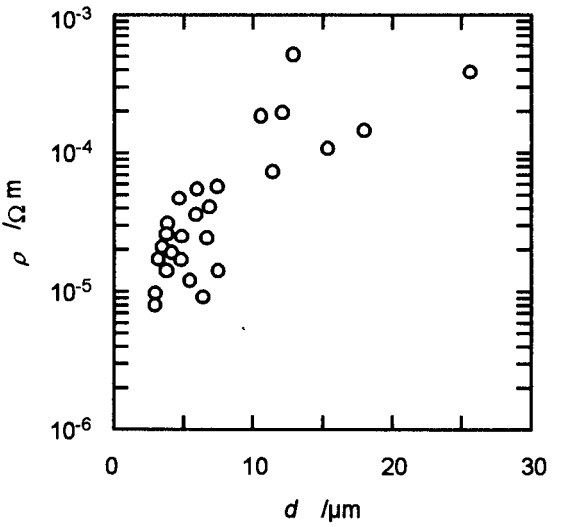

Fig. 2-14 Electrical Resistivities of VGCFs

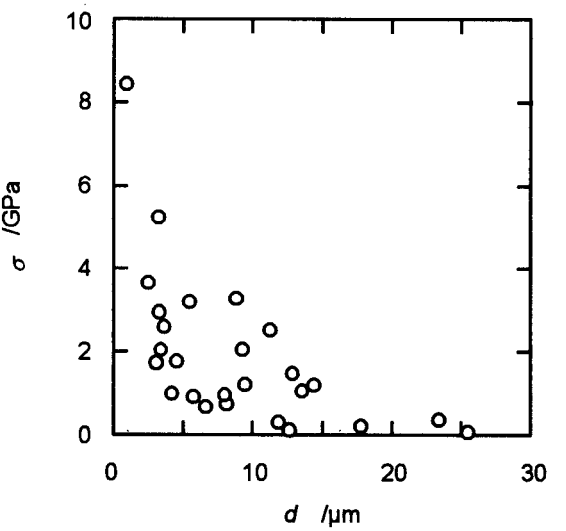

Fig. 2-15 Tensile Strengths of VGCFs

1993).

2.4.5 Tensile Strength

Figure 2-15 shows the plots of tensile strengths of VGCFs against the diameter of the fiber. The tensile strength of the fibers increase with the decrease in the diameter of the fibers. The core of the fiber is highly graphitic and the number of defects included in it is extremely small. The possibility of a defect to be formed drastically increases with the increase in diameter, as the fiber thickens through the deposition of the carbon source.

The average tensile strength of fibers which diameters are less than 5 μm is in the range 2500 to 3500 GPa. It is noteworthy that values over 5000 GPa can be attained, even though the fibers were produced at 1373 K.

2.4.6 Oxidation Resistivity

Figure 2-16 shows a typical weight loss curve of VGCFs obtained using the LPI technique, where W and W_0 are the weight and the initial weight of the sample, respectively. That of commercially available VGCFs is also shown for comparison. Apparently there is no difference among them.

Figure 2-17 compares the weight loss curves of VGCFs and typical PAN and pitch based carbon fibers. Although the heat treatment temperature of the latter two fibers (1273 K) is close to the production temperature of VGCFs (1373K) the initiation temperature of oxidation for the VGCFs is higher than those of the other fibers.

2.5 Conclusion

A new method to produce VGCFs, the liquid pulse injection technique, has been developed. This technique permits the production of long VGCFs at high growth

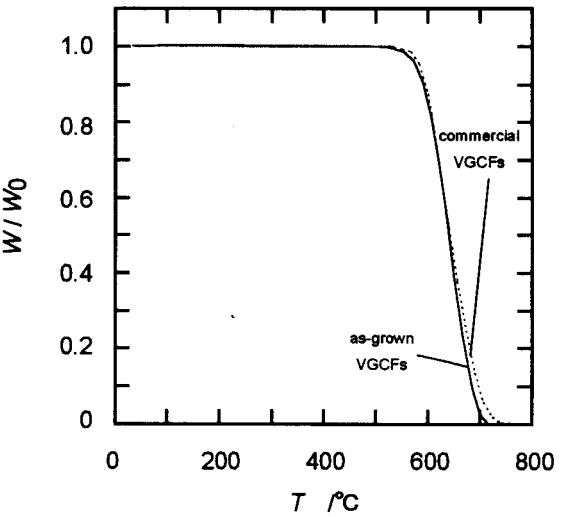

Fig. 2-16 Weight Loss Curves of VGCFs

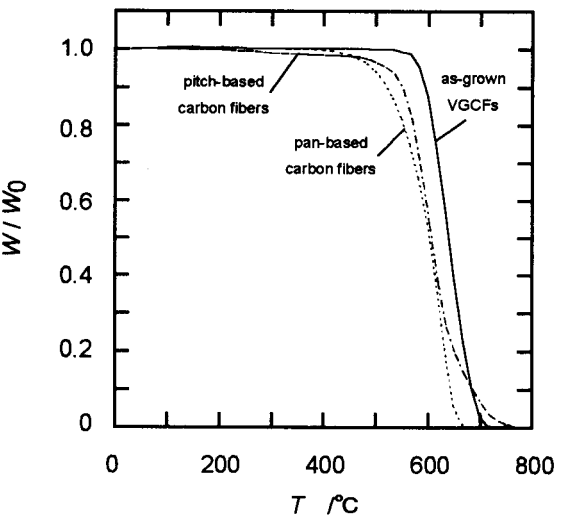

Fig. 2-17 Weight Loss Curves of Various Types of Carbon Fibers

rates. Fibers with lengths up to 55 mm can be produced within 30 s by employing this new technique.

Empirical equations, which well represent the growth sequence of the fibers, have been proposed.

The obtained VGCFs were found to have the same structure as VGCFs produced using conventional production methods. Even though they are rapidly grown, they possess the same superior quality as conventional VGCFs.

Nomenclature

A	=	Adjustable Parameter	[mm s^{-1}]
B	=	Adjustable Parameter	[s^{-1}]
d	=	Diameter of Fiber	[μm]
L	=	Length of Fiber	[mm]
L_{max}	=	Maximum Length of Fibers	[mm]
$r_{(t=0)}$	=	Initial Growth Rate of Fiber	[mm s^{-1}]
t	=	Reaction Time	[min]
T	=	Reaction Temperature	[°C]
W	=	Weight of Sample	[mg]
W_0	=	Initial Weight of Sample	[mg]

Greek Letters

ρ	=	Electrical Resistivity of Fiber	[Ω m]
σ	=	Tensile Strength of Fiber	[GPa]

Literature Cited

Baker, R. T. K., *Carbon* **27**, 315 (1989)

Benissad, F., Gadelle, P., Coulon, M., and Bonnetain, L., *Carbon* **26**, 61 (1988)

Endo, M. and Shikata, M., *Ohyo Butsuri* **49**, 563 (1985)

Endo, M., *CHEMTECH* **Sept.**, 568 (1988)

Endo, M., Ishioka, M., Nakazato, K., Okada, T., Okuyama, Y., and Matsubara, K., *Jpn. Kokai Tokkyo Koho*, JP 01,92,421 [89,92,421] (1989)

Ishioka, M., Okada T., and Matsubara, K., *J. Mater. Res.* **7**, 3019 (1992)

Ishioka, M., Okada T., Matsubara, K., Inagaki, M., and Hishiyama, Y., *J. Mater. Res.* **8**, 1866 (1993)

Komatsu, Y. and Nakatani, M., *Jpn. Kokai Tokkyo Koho*, JP 63,219,630 [88,219,630] (1988)

Koyama , T., *Carbon* **10**, 757 (1972)

Koyama , T., Endo, M., and Onuma, Y., *Jpn. J. Appl. Phys.* **11**, 445 (1972)

Morimoto, S., *Jpn. Kokai Tokkyo Koho*, JP 63,92,726 [88,92,726] (1988)

Tibbetts, G. G., Endo, M., and Beetz, Jr., C. P., *SAMPE J.* **22**, 30 (1986)

CHAPTER 3

The Effects of Reaction Conditions on the Growth Behavior of Vapor Grown Carbon Fibers Produced Using the Liquid Pulse Injection Technique

3.1 Introduction

In the previous chapter, a new method to produce vapor grown carbon fibers (VGCFs) was introduced, the liquid pulse injection (LPI) technique. Catalyst particles can be easily obtained in a highly dense state using this new method. Moreover, catalyst particles obtained using this method are very active, as high growth rates, up to a few hundred times larger than those of conventional methods, can be obtained. This indicates that only a small scale reactor is required for fiber production by employing this new method.

However, to realize the potential of this low cost process, the following requirements must be fulfilled:

(1) Efficient conversion of the carbon source to VGCFs.
(2) Continuous production of VGCFs.

In order to effectively convert the carbon source to VGCFs, active ultra fine catalyst particles must be dispersed in a uniform dense state throughout the reactor. This can be easily achieved using this new LPI technique. The sizes of the catalyst particles must also be controlled, because the activity of the catalyst has a strong dependency on its size (Benissad *et al.*, 1988a, Endo, 1988, Baker, 1989). The sizes of the catalyst particles have a high dependency on reaction conditions such as the line velocity of the carrier gas. We must also not forget that high reaction

temperatures (over 1273K) are required to produce VGCFs to activate the catalyst particles. However, at such high temperatures, the carbon source not only produces VGCFs, but also is decomposed and forms pyrolytic carbon and various gases. Hence, the effects of reaction conditions must be thoroughly investigated to optimize the operation conditions of this new production method.

To satisfy the second requirement, intermittent injection of the catalyst source into the reactor may be an effective method.

In this chapter, first, the effects of reaction conditions on the growth behavior of VGCFs is reported. The examined conditions were the reaction temperature, the carbon source flow rate, the line velocity of the carrier gas, and the amount of catalyst source injected into the reactor as a liquid pulse. The possibility of the continuous production of VGCFs by intermittent injection of the catalyst source was also investigated.

3.2 Experimental

Benzene (99.5% purity) was used for the preparation of the carbon source. Ferrocene (98% purity) was used as the source of the iron catalyst particles. Nitrogen (99.999% purity) and hydrogen (99.95% purity) were used as the purge gas and carrier gas, respectively.

3.2.1 Effects of Reaction Conditions

First the reaction temperature and initial carbon source concentration were varied and the optimal values were determined from the obtained growth curves. Those which give the highest growth rate were selected. Benzene was used as the carbon source. The reaction temperatures examined were 1223, 1273, 1323, 1373 and 1423 K. The carbon source flow rates were adjusted to 0.01, 0.03, 0.05, 0.07 and 0.10 cm^3

min^{-1}. The carrier gas flow rate was fixed to 60 (cm^3-NTP) min^{-1}. Therefore, each carbon source flow rate gives an inlet carbon source concentration of 1.80, 4.88, 7.65, 9.95, and 12.9 mol (m^3-NTP)$^{-1}$, respectively. The experimental apparatus and procedure, and other reaction conditions were the same as those of the previous chapter. The optimal reaction temperature and carbon source inlet concentration were determined to those which give the highest initial growth rate.

Next, the effects of the remaining reaction conditions on the yield of VGCFs were examined. The varied conditions were the flow rate of the carrier gas, and the amount of the liquid pulse injected into the reactor as the catalyst source (ferrocene dissolved in benzene). Both of them are the key conditions for controlling the size and number of the catalyst particles.

Benzene was used as the carbon source. The flow rates of the carrier gas were 30, 60, 90, 120, and 180 (cm^3-NTP) min^{-1}. The corresponding gas line velocities were 2.95, 5.93, 8.89, 11.9, and 17.8 mm s^{-1}, respectively. The amount of the catalyst source injected into the reactor as a liquid pulse were 0.010, 0.015, 0.020, 0.025 and 0.030 cm^3. The flow rate of the carbon source was fixed as to maintain the gas phase initial benzene concentration which was found to be optimal. The reaction time was fixed to 60 s. The formed VGCFs were collected after reaction, and the amount of them were measured.

Experiments were conducted three times at each set of conditions to confirm the reproducibility of each data. The yield of the VGCFs obtained under each set of reaction conditions (Y) was calculated using the following equation:

$$Y = \frac{\text{average weight of VGCFs}}{\text{amount of carbon introduced during the time of reaction}} \quad (3\text{-}1)$$

3.2.2 Intermittent Liquid Pulse Injection

The possibility of the continuous production of VGCFs by the intermittent liquid pulse injection of the catalyst source was investigated. One of the important factors of this technique is the interval of the injections. If the intervals are too short, the iron particles produced from the preceding liquid pulse will not be completely swept out from the reaction zone by the carrier gas before the following liquid pulse. Hence, the flow pattern of the particles will be disturbed, and the time allowed for the particles to grow before encountering the carbon source will be altered (this time will be referred to as "encounter time" hereafter). Therefore, the number of active catalyst particles will decrease. If the intervals are too long, the productivity of the reactor will decrease. Considering these points, the effect of the injection interval on the amount of VGCFs obtained was also investigated.

The flow rate of the carrier gas, and the amount of the catalyst source injected into the reactor as a liquid pulse were adjusted to the optimized conditions obtained from the first experimental series described above.

Five liquid pulses of the catalyst source were intermittently injected into the reactor at a certain interval. The intervals were 10, 15, 20, and 30 s. The weight of the fibers obtained was measured, and the amount produced per liquid pulse injection was calculated.

3.3 Results and Discussion

3.3.1 Reaction Temperature

Figure 3-1 shows the growth curves of VGCFs produced at different reaction temperatures, where L is fiber length and t, reaction time. The initial carbon source concentration was set to 9.95 mol $(m^3\text{-NTP})^{-1}$ in this series. Although there is a difference in the growth rates, the trend of the curves of each reaction temperature are

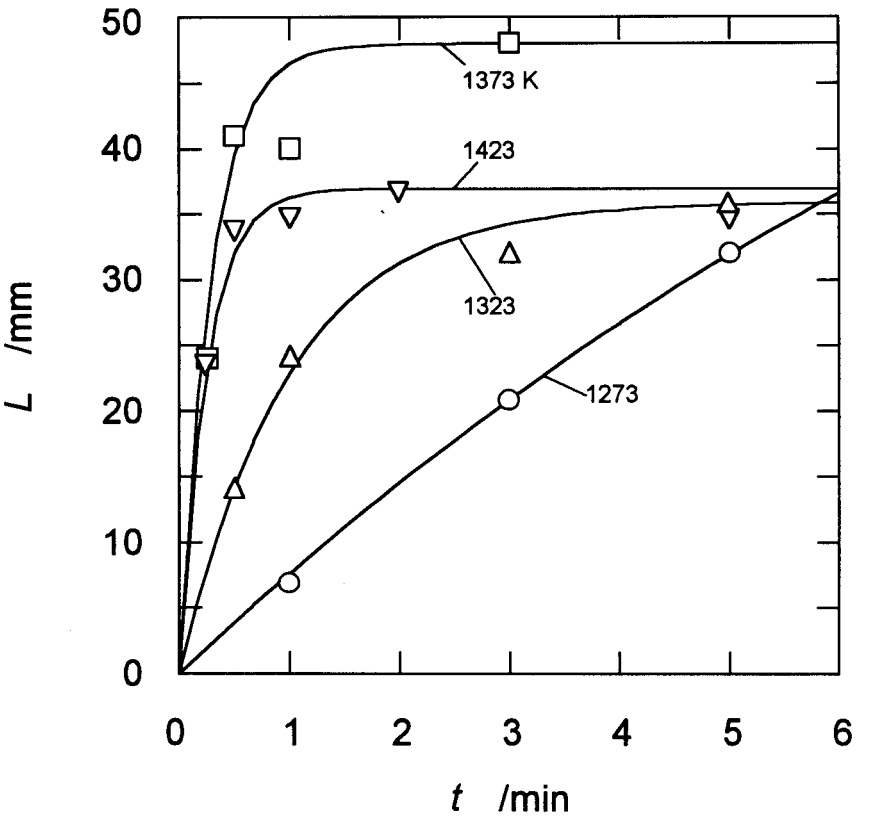

Fig. 3-1 Growth Curves of VGCFs

(Initial Carbon Source Concentration: 9.95 mol $(m^3\text{-NTP})^{-1}$)

basically the same. The initial growth rate of the fibers ($r_{(t=0)}$) at each reaction temperature (T) was determined according to the method described in the previous chapter. They are plotted against the reaction temperature in Fig. 3-2. Rapid fiber growth could not be observed at temperatures below 1273 K, but the initial growth rate drastically increases at temperatures over 1300 K. It is inevitable that the catalyst particle is in the molten state for it to rapidly produce VGCFs, so it is assumed that the catalyst particles are in the liquid phase. The melting point of bulk iron is 1808 K, and the eutectic point of iron with carbon is 1426 K, so bulk iron can not melt at a temperature of 1300 K. This melting phenomena can be explained by the fact that the melting point decreases as the diameter of the catalyst particle decreases (Benissad *et al.*, 1988b).

The initial growth rate suddenly drops as reaction temperatures exceed 1400 K. At high temperatures as this, a large portion of the carbon source is consumed by thermal decomposition and deposition. Therefore, it is assumed that even though the catalyst particles are very active, the attainable initial growth rate drops as the concentration of the carbon source which exist in the reaction zone is lower than those of lower reaction temperatures. Here it is concluded that the optimal reaction temperature for VGCF growth is 1373 K.

3.3.2 Initial Carbon Source Concentration

Figure 3-3 shows growth curves of VGCFs produced at different initial carbon source concentrations (C_0), where L is fiber length and t reaction time. The reaction temperature was set to 1373 K in this series, the optimal temperature determined in the previous section. The initial growth rates obtained at each initial concentration were determined and are summarized in Fig. 3-4. The initial growth rate of the fibers increase with the increase in the initial concentration of the carbon source, but after reaching a maximum value, it starts to decrease. Considering the reaction temperature, the carbon source is likely to thermally decompose, but as experiments were conducted under a hydrogen atmosphere, this decomposition was suppressed.

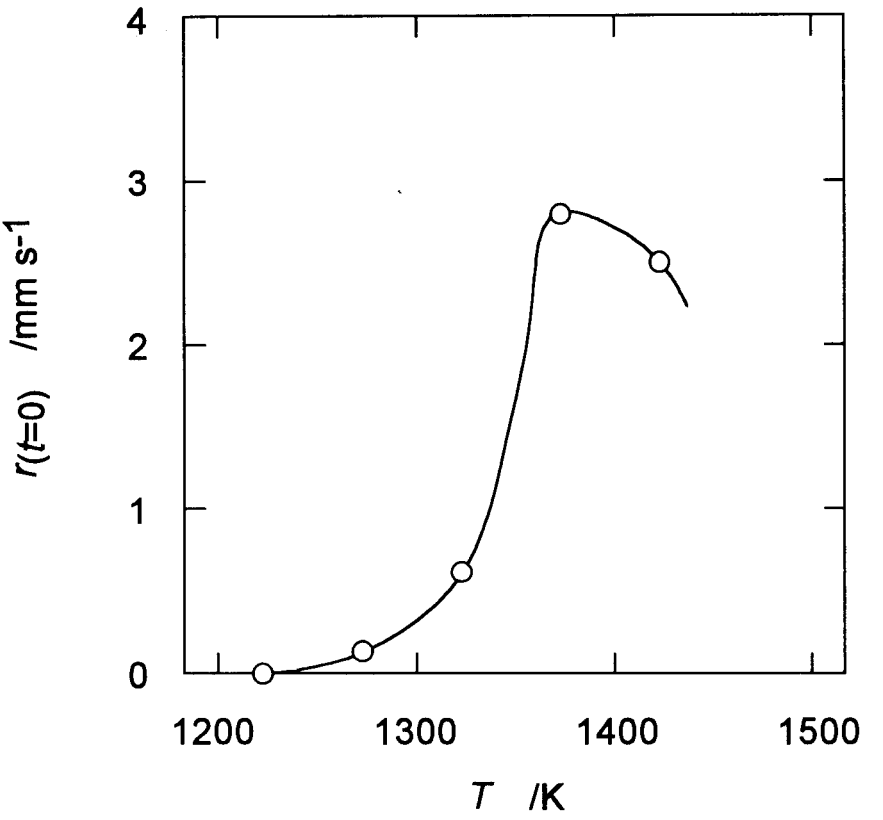

Fig. 3-2 Initial Growth Rates of VGCFs

(Initial Carbon Source Concentration: 9.95 mol $(m^3\text{-NTP})^{-1}$)

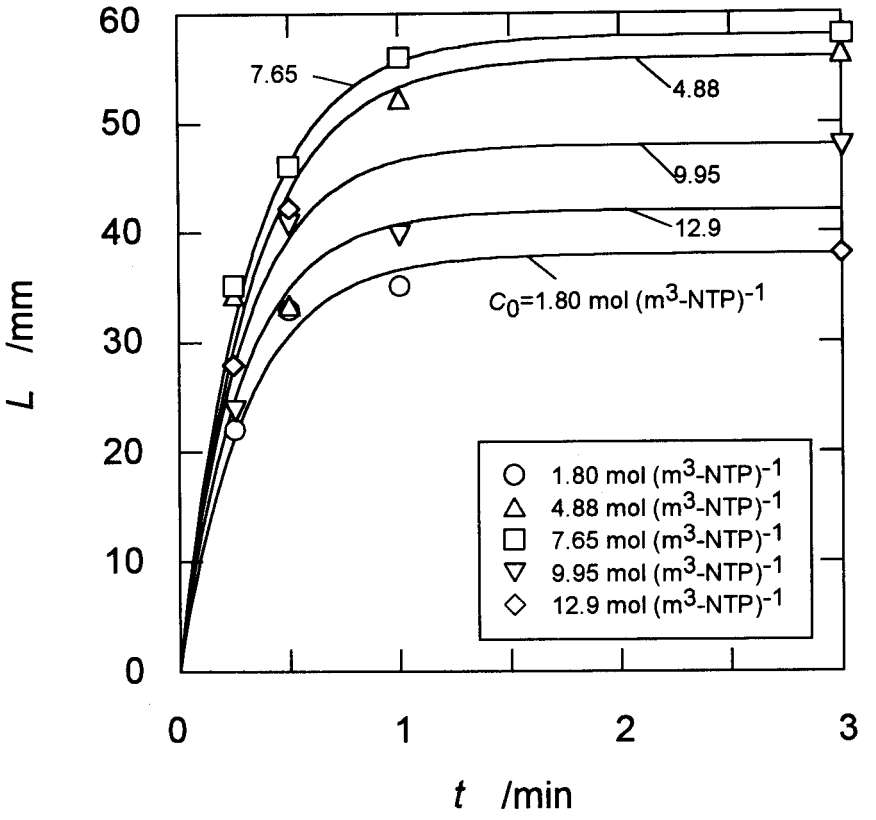

Fig. 3-3 Growth Curves of VGCFs
(Reaction Temperature: 1373 K)

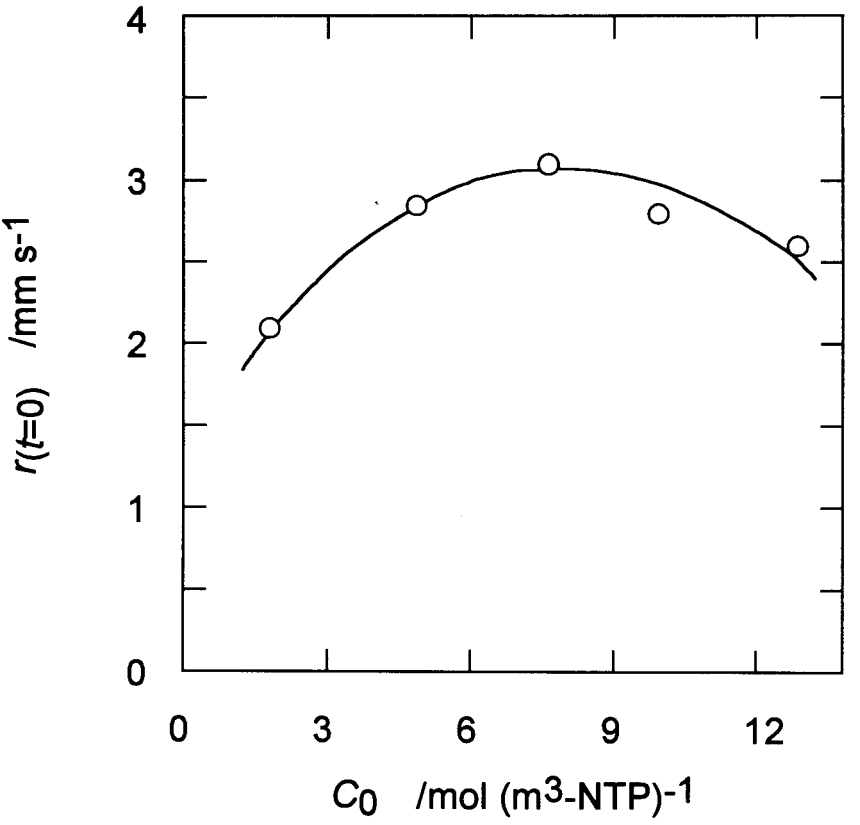

Fig. 3-4 Initial Growth Rates of VGCFs
(Reaction Temperature: 1373 K)

However, the degree of suppression drops as the initial concentration of the carbon source increases. Therefore, there is a high possibility that when the initial carbon source concentration is high, even if the flow rate of the carbon source is increased, the actual amount of carbon source in the reaction zone decreases. So it can be concluded that the optimal initial carbon source inlet concentration is 7.65 mol $(m^3\text{-NTP})^{-1}$

In the experiments conducted hereafter, the reaction temperature and initial carbon source inlet concentration were set to 1373 K and 7.65 mol $(m^3\text{-NTP})^{-1}$, respectively.

3.3.3 Carrier Gas Line Velocity

VGCFs grow in the axial direction through the catalytic action of ultra-fine particles of iron catalysts. The favorable diameters of these particles lay in the range from a few to about 50 nm (Benissad *et al.*, 1988, Endo, 1988, Baker, 1989, Ishioka *et al.*, 1993). Any particle which has the diameter above or below this range will not act as a catalyst for the production of VGCFs. Hence, it is important to increase the number of particles which have the favorable size in order to enhance the yield of VGCFs.

In the LPI technique, the catalyst source is rapidly heated and is decomposed, yielding iron clusters. These clusters coalesce and form particles. The size of the particles increases till they encounter the carbon source, due to further coalescence. Thus, the number of particles which have the favorable size for the production of VGCFs is considered to be strongly influenced by the encounter time.

Figure 3-5 schematically represents the change of the distribution of the particle size at different encounter times τ ($\tau_1<\tau_2<\tau_3$). The size of the catalyst particles will increase with the increase in the encounter time (τ_i). The size distribution of the particles will also become broader.

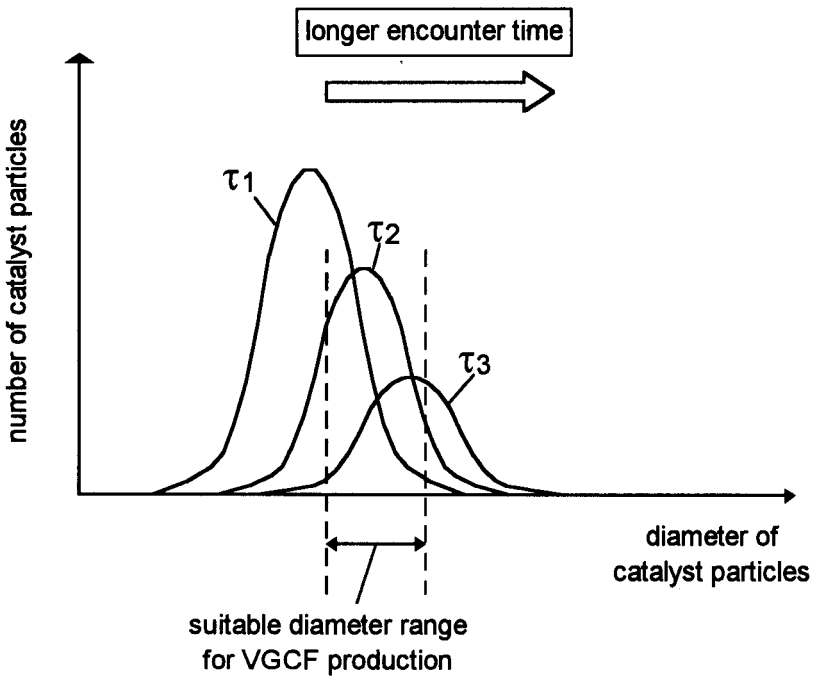

Fig. 3-5 Change of the Size Distribution of Catalyst Particles

Considering that the yield of VGCFs is proportional to the number of catalyst particles which have the suitable size for the production of VGCFs, it is expected that the yield of VGCFs will increase as the encounter time is increased (τ_1 to τ_2), and after reaching a maximum value (τ_2), it will start to decrease (τ_2 to τ_3). At encounter times which are too short or too long, there are no particles which have the suitable size for VGCF production, and it is difficult to obtain VGCFs. The effect of the encounter time on the yield of VGCFs can be experimentally examined by varying the line velocity of the carrier gas. A faster carrier gas velocity corresponds to a shorter encounter time.

Figure 3-6 shows the effect of the line velocity of the carrier gas (u) on the yield of VGCFs (Y). As was expected, when the velocity of the carrier gas is increased, the yield of VGCFs increased and reached a maximum value, and then started to decrease. No VGCFs were obtained at the maximum and minimum velocities, 2.95 mm s^{-1} and 17.8 mm s^{-1}.

3.3.4 Amount of Liquid Pulse

Figure 3-7 shows the effect of the amount of the catalyst source injected into the reactor (Q), on the yield of VGCFs (Y). It is expected that the yield of VGCFs will increase with the increase of the catalyst source injected into the reactor. This trend can be seen at lower amounts of the catalyst source injected into the reactor. However, the results show that the yield will decrease after reaching a maximum value. This decrease is considered to occur as it becomes difficult to rapidly increase the temperature of the liquid pulse when its amount is increased. In the LPI technique, it is essential to rapidly heat the liquid pulse up to the decomposition temperature of the catalyst source.

From the above discussions, the optimized reaction conditions for VGCF production are, carrier gas velocity: 5.93 mm s^{-1} (carrier gas flow rate 60 (cm^3-NTP) min^{-1}), and amount of the catalyst source injected into the reactor: 0.020 cm^3. However,

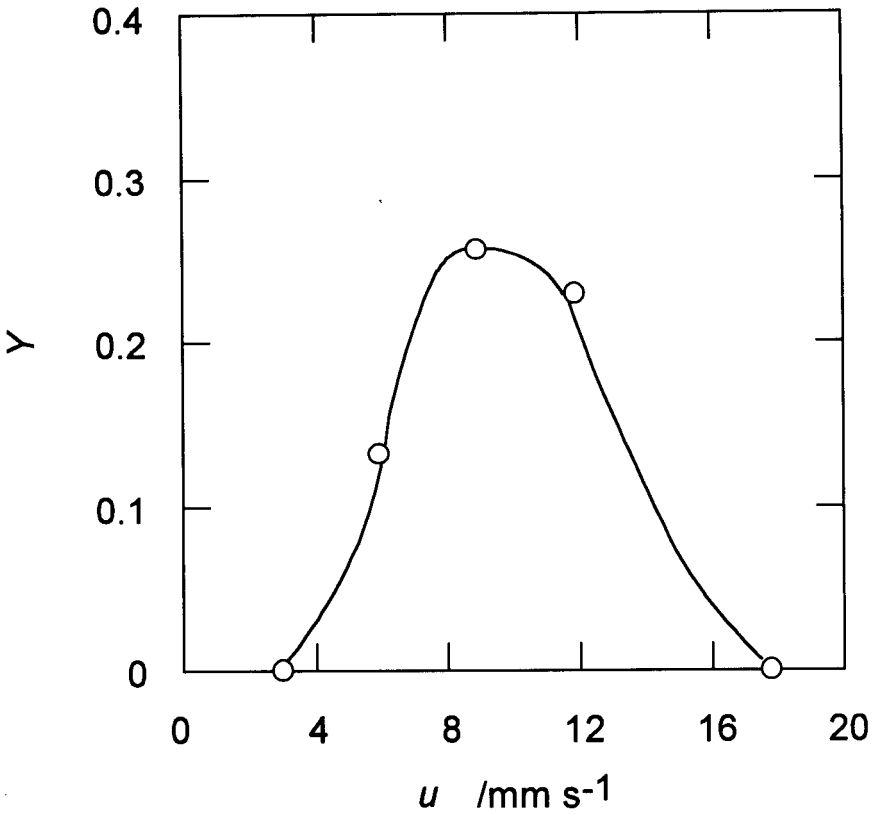

Fig. 3-6 Effect of the Line Velocity of the Carrier Gas on the Yield of VGCFs (Amount of Liquid Pulse: 0.020 cm^3)

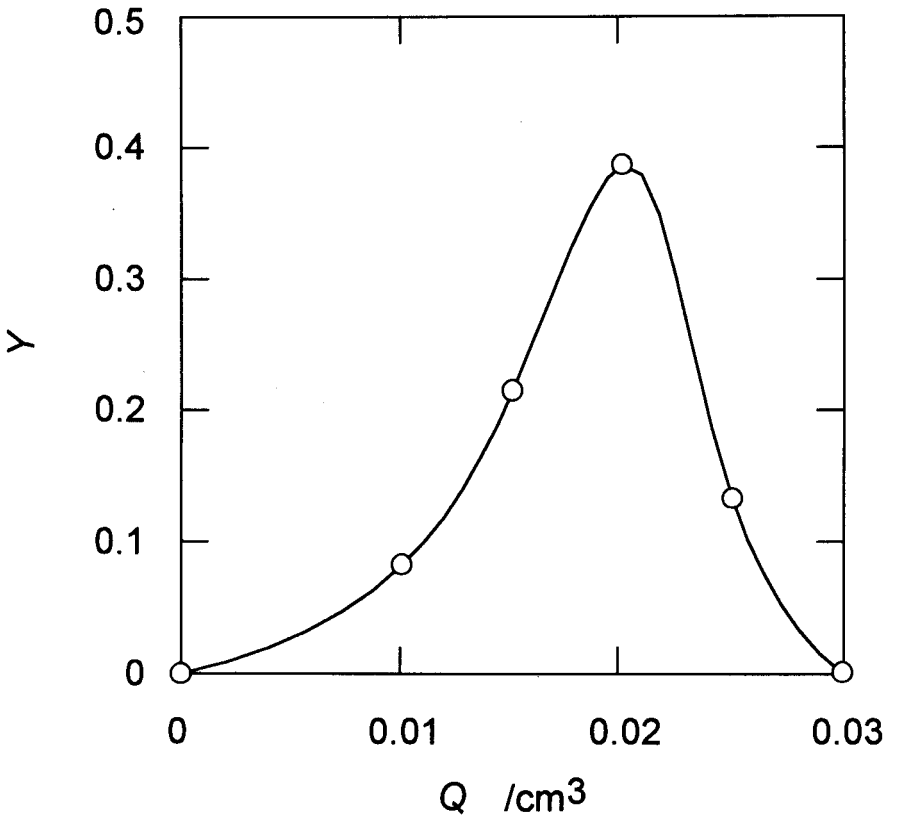

Fig. 3-7 Effect of the Amount of Liquid Pulse Injection on the Yield of VGCFs (Carrier Gas Line Velocity: 5.93 mm s^{-1})

these optimized conditions are pertinent to this experimental apparatus, and they will change when apparatus of different configurations are used.

3.3.5 Intermittent Liquid Pulse Injection

The carrier gas flow rate, and the amount of the catalyst source injected into the reactor were adjusted to the optimized reaction conditions obtained in the experimental series described above. They were 60 (cm^3-NTP) min^{-1} and 0.020 cm^3, respectively.

VGCFs were successfully obtained by intermittently introducing the catalyst material into the reactor as liquid pulses. The VGCFs obtained were fairly straight and had the maximum length which was comparable to the fibers obtained from single pulse experiments. This shows the potential of using this technique for the continuous production of VGCFs.

Figure 3-8 shows the amount of VGCFs obtained per pulse of catalyst source injection (W) at different intervals of liquid pulse injection (t_i). The values obtained from single pulse injection experiments are also shown at the right hand side of the figure. This amount increases as the intervals are increased, and is predicted to approach the amount obtained at single pulse injection experiments. This fact indicates that there is some interaction among the liquid pulses when the intervals are too short, and that a certain interval is necessary for efficient VGCF production. However, the productivity of the reactor will decrease at long intervals.

Figure 3-8 also shows the maximum length of the VGCFs (L_{max}) obtained at different intervals of liquid pulse injection (t_i). This value slightly decreases as the interval of pulse injection is increased. When the catalyst particle formation efficiently proceeds, the VGCF yield increases. This leads to the rapid decrease of the benzene concentration of the gas phase, and the decrease in the attainable maximum length.

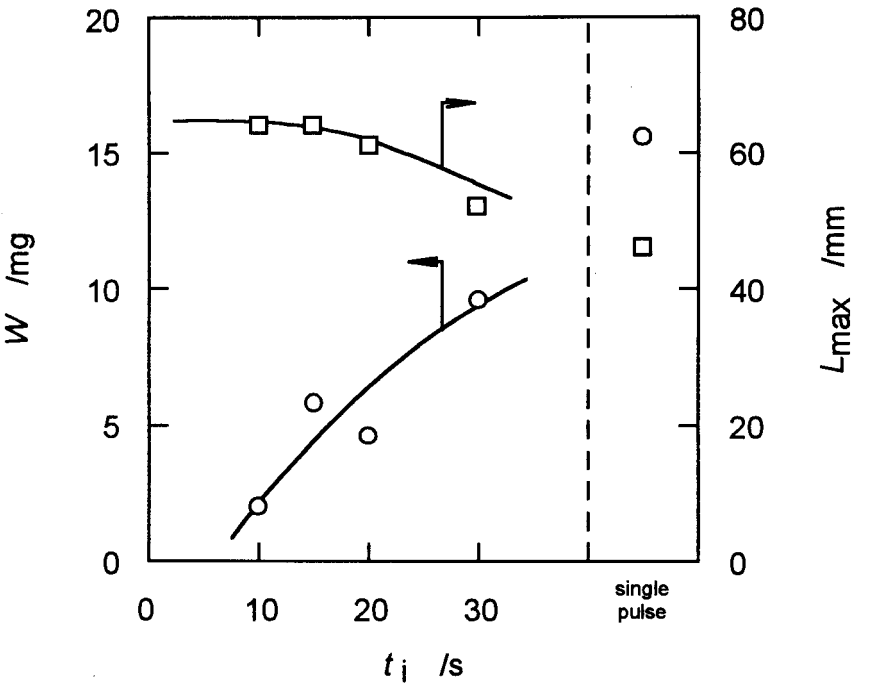

Fig. 3-8 Amount of VGCFs per Pulse of Catalyst Source and Maximum Length of VGCFs Obtained at Different Intervals

3.4 Conclusion

The effects of reaction conditions on the growth behavior of VGCFs were investigated using the LPI technique. The optimized reaction temperature, carbon source inlet concentration, flow rate of the carrier gas, and amount of the catalyst source injected into the reactor as a liquid pulse were 1373 K, 7.65 mol $(m^3\text{-NTP})^{-1}$ 60 $(cm^3\text{-NTP})\ min^{-1}$ and 0.020 cm^3, respectively.

VGCFs were successfully obtained by intermittently introducing the catalyst material into the reactor as liquid pulses. This shows the possibility of the continuous production of VGCFs.

Nomenclature

C_0	=	Initial Concentration of Carbon Source	[mol $(m^3\text{-NTP})^{-1}$]
L	=	Length of Fiber	[mm]
L_{max}	=	Maximum Length of Fibers	[mm]
Q	=	Amount of Liquid Pulse Injection	[cm^3]
$r_{(t=0)}$	=	Initial Growth Rate of Fiber	[mm s^{-1}]
t	=	Reaction Time	[min]
t_i	=	Interval of Liquid Pulse Injection	[s]
T	=	Reaction Temperature	[K]
u	=	Carrier Gas Line Velocity	[mm s^{-1}]
W	=	Amount of VGCF per Pulse	[mg]
Y	=	Yield of Fibers	[-]

Greek Letters

τ	=	Encounter Time	[s]

Literature Cited

Baker, R. T. K., *Carbon* **27**, 315 (1989)

Benissad, F., Gadelle, P., Coulon, M., and Bonnetain, L., *Carbon* **26**, 61 (1988a)

Benissad, F., Gadelle, P., Coulon, M., and Bonnetain, L., *Carbon* **26**, 425 (1988b)

Endo, M., *CHEMTECH* **Sept.**, 568 (1988)

Ishioka, M., Okada T., and Matsubara, K., *Carbon* **31**, 699 (1993)

CHAPTER 4

The Production of Vapor Grown Carbon Fibers From a Mixture of Benzene, Toluene and Xylene Using The Liquid Pulse Injection Technique

4.1 Introduction

In chapter 2, a new method to produce vapor grown carbon fibers (VGCFs) at high growth rates was introduced. In the previous chapter, the possibility of the continuous production of VGCFs was shown. In this chapter, a low cost carbon source for VGCF production is sought.

In conventional processes of VGCF production, high purity benzene is a popular carbon source. Assuming that the benzene ring is inevitable for rapid fiber growth, one will immediately think up of a mixture of benzene, toluene and xylene as an alternative carbon source. This mixture is relatively inexpensive, and is easily obtained in various petrochemical processes. Although Onuma and Koyama (1963) showed that VGCFs could be obtained from toluene, no one has attempted to grow VGCFs from xylene, nor has anyone analyzed the growth curves obtained using various hydrocarbons as the carbon source.

The objective of this work is to investigate the possibility of the usage of a mixture of benzene, toluene and xylene as the carbon source for VGCF production. First, the growth sequences of VGCFs, when each carbon source was used individually, were analyzed. Next, VGCFs were produced using mixtures of these hydrocarbons. Finally, the fiber growth rate constants using benzene, toluene and xylene as the carbon source were estimated, assuming that the growth rate is expressed by a first order reaction rate equation.

4.2 Experimental

Benzene (99.5 % purity), toluene (98 % purity), xylene (*o*-, *m*-, *p*-, 98 % purity) and methane (99 % purity) were used for the preparation of the carbon source. Ferrocene (98 % purity) was used as the source of the ultra-fine iron catalyst particles. Nitrogen (99.999 % purity) and hydrogen (99.95 % purity) were used as the purge gas and carrier gas, respectively.

The apparatus and experimental procedure used for fiber production was the same as those of the previous chapters. The temperatures of the gas preheating zone and reaction zone, which were measured by inserting a thermocouple into each zone, were 1073 K and 1373 K, respectively. The flow rate of the carrier gas was 60 (cm^3-NTP) min^{-1}. The amount of the catalyst source (10 wt% benzene solution of ferrocene) introduced into the reactor was 0.020 cm^3 per each pulse. These values are the optimal conditions which were obtained in the previous chapter. The reaction times were set in the range of 15 to 180 s.

First, VGCFs were produced using toluene and xylene as the carbon source. Production experiments using methane, which may be generated through the thermal decomposition of the former two hydrocarbons were also conducted. The initial concentration of the carbon source was in the range 1.80 mol (m^3-NTP)$^{-1}$ to 12.9 mol (m^3-NTP)$^{-1}$. Secondly, VGCFs were produced using three mixtures of benzene, toluene and xylene as the carbon source. The weight ratios of the three hydrocarbons in the mixtures were, 1:1:1, 1:1:4 and 1:5:7. The initial concentration of the carbon source was set in the range of 4.28 mol (m^3-NTP)$^{-1}$ to 11.6 mol (m^3-NTP)$^{-1}$. After each experiment, the produced VGCFs were collected, and the lengths of them were measured. The initial growth rates of the fibers were determined from the growth curves of the fibers. The surface morphology of the fibers were observed by scanning electron microscopy (Hitachi; S510).

The rate constant of the deposition of pyrolytic carbon was determined from the deposition rate measured using a thermogravimetric apparatus (Shimadzu; TG-30) as shown in Fig. 4-1. The rate was assumed to be expressed by a first order rate equation. The inner diameter of the quartz glass reactor was the same as that used for fiber production. An infrared furnace (ULVAC; RHL-E416) was employed to obtain a uniform temperature throughout the reaction zone. A quartz glass rod was hung at the center of the furnace. Benzene was fed to the evaporator using a syringe pump, and was introduced into the reactor. Hydrogen was used as the carrier gas. The transient change of the weight of the quartz glass rod, caused by carbon deposition, was measured under the same conditions as those of fiber production experiments. Reaction temperatures, which were measured using a thermocouple, were 1173, 1223, 1273 K. The carbon deposition rate was calculated from the weight change of the quartz glass rod.

4.3 Results and Discussion

VGCFs were successfully obtained when toluene and xylene were used as the carbon source. Figures 4-2 and 4-3 show photographs and SEM micrographs of VGCFs obtained from toluene and *m*-xylene, respectively. There was apparently no difference among the VGCFs obtained from these two carbon sources, and those obtained from benzene in the previous chapters. No VGCFs could be obtained when methane was used as the carbon source. Figures 4-4 and 4-5 are the growth curves of the VGCFs obtained respectively using toluene and *m*-xylene as the carbon source, where L is the fiber length and t is the reaction time. The growth curves were similar to those obtained when benzene was used as the carbon source. The fibers grow rapidly at the beginning of the reaction. After a short reaction period, the growth rate drastically decreases and finally the growth of the fibers terminates. Figure 4-6 shows the results when each xylene isomer was used separately as the carbon source. No significant difference could be observed among the isomers.

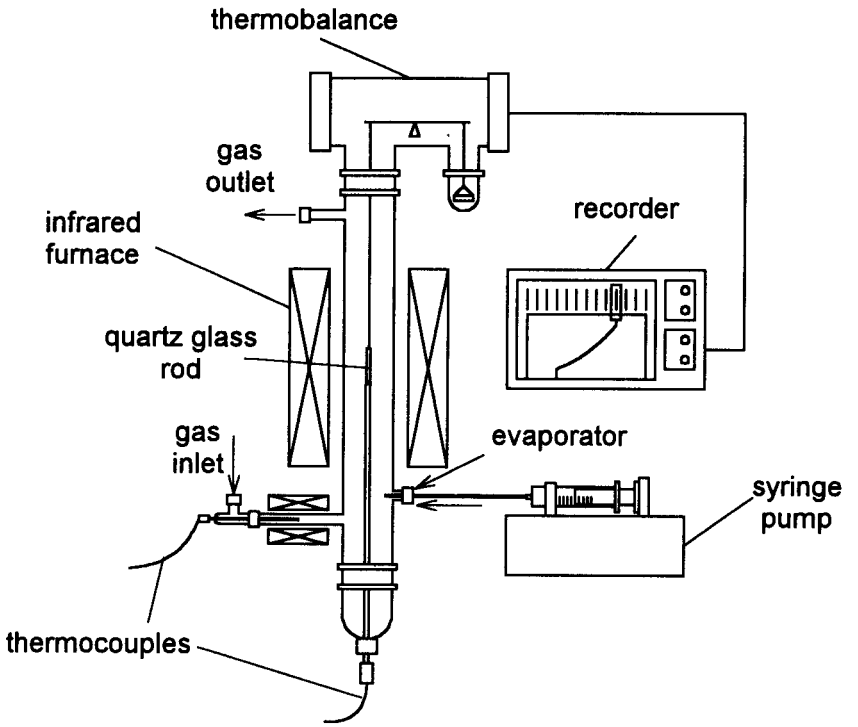

Fig. 4-1 Experimental Apparatus for Carbon Deposition

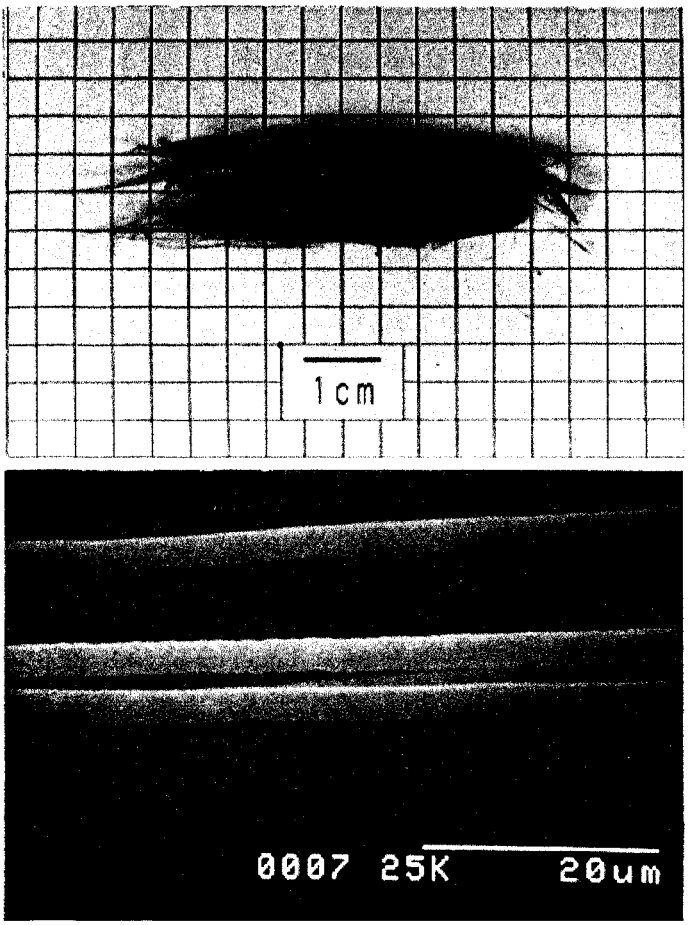

Fig. 4-2 Photograph (Upper) and SEM Micrograph (Lower) of VGCFs (Carbon Source: Toluene)

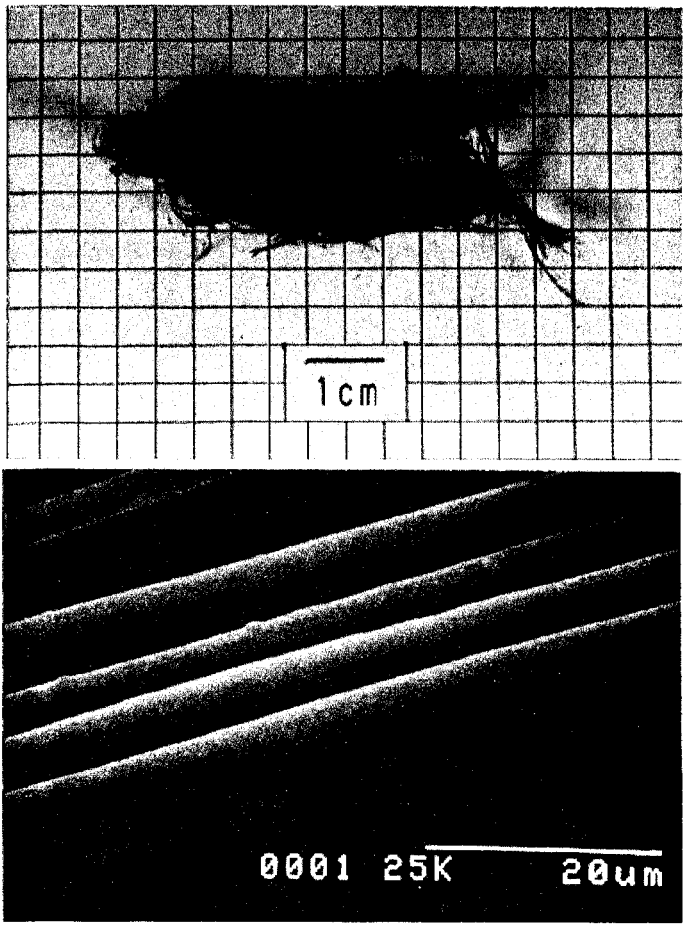

Fig. 4-3 Photograph (Upper) and SEM Micrograph (Lower) of VGCFs (Carbon Source: *m*-xylene)

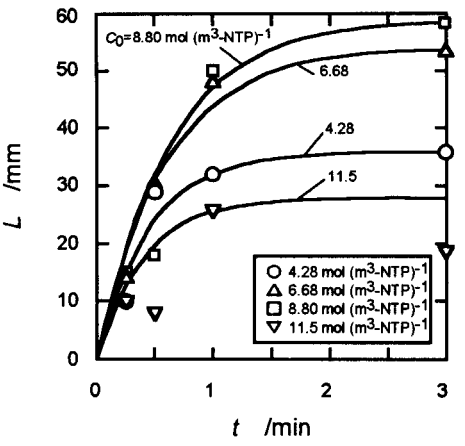

Fig. 4-4 Growth Curves of VGCFs
(Carbon Source: Toluene)

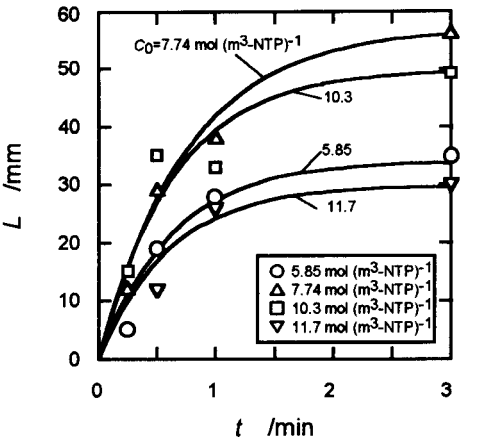

Fig. 4-5 Growth Curves of VGCFs
(Carbon Source: *m*-Xylene)

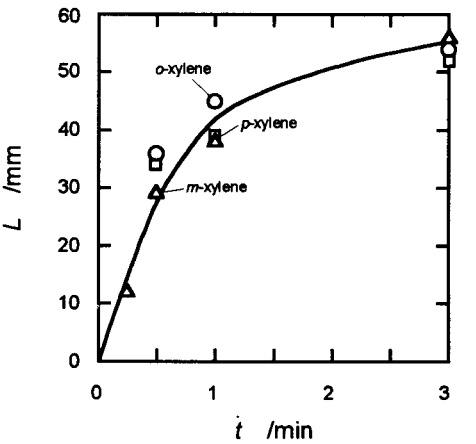

Fig. 4-6 Growth Curves of VGCFs
(Carbon Source: Xylene Isomers)

In chapter 2, it was found that the growth curves of VGCFs could be well represented by the following empirical equations:

$$\frac{dL}{dt} = A\exp(-Bt) \tag{2-1}$$

$$L = \frac{A}{B}\{1-\exp(-Bt)\} \tag{2-2}$$

where L is the fiber length, t the reaction time and A, B adjustable parameters. Parameter A gives the initial growth rate of the fibers ($r_{(t=0)}$). The initial growth rates of the fibers were determined according to the method described in chapter 2.

Figure 4.7 shows the plots of the initial growth rates of the fibers ($r_{(t=0)}$) against the initial concentration of the carbon source (C_0). The results of benzene are also shown in the figure. Although the initial growth rate decreases in the order of benzene, toluene and xylene, a minimum value close to 1 mm s^{-1} was obtained. This value is extremely higher than those obtained using conventional production methods.

Long VGCFs were also obtained using mixtures of benzene, toluene and xylene as the carbon source. Figure 4-8 shows a photograph and a SEM micrograph of typical VGCFs obtained. The VGCFs were apparently the same as those obtained when each hydrocarbon was used separately as the carbon source. Figure 4-9 a-c show typical growth curves obtained when mixtures of benzene, toluene and xylene were used as the carbon source. The growth curves show similar trends as those obtained when pure hydrocarbons were used as the carbon source. The initial growth rate of each growth curve is also shown in Fig. 4-7. High growth rates are attainable using mixtures of benzene, toluene and xylene as the carbon source, and are comparable to those of benzene, toluene and xylene. Thus, it can be concluded that this mixture is an effective carbon source for VGCF production.

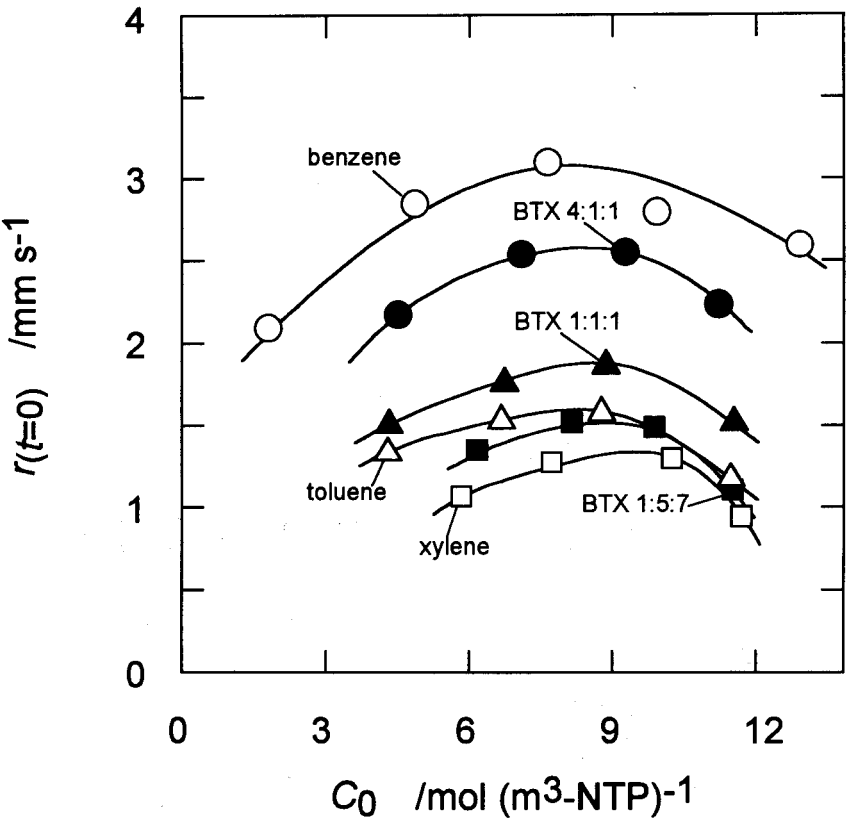

Fig. 4-7 Dependence of Initial Growth Rate on Initial Concentration of the Carbon Source

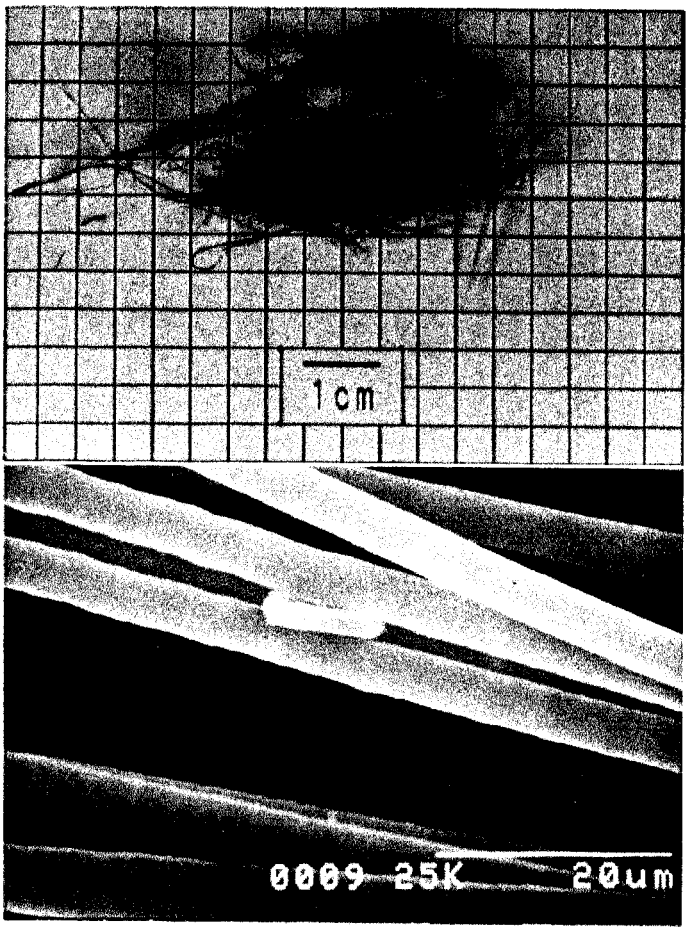

Fig. 4-8 Photograph (Upper) and SEM Micrograph (Lower) of VGCFs (Carbon Source: Mixture of Benzene, Toluene and Xylene)

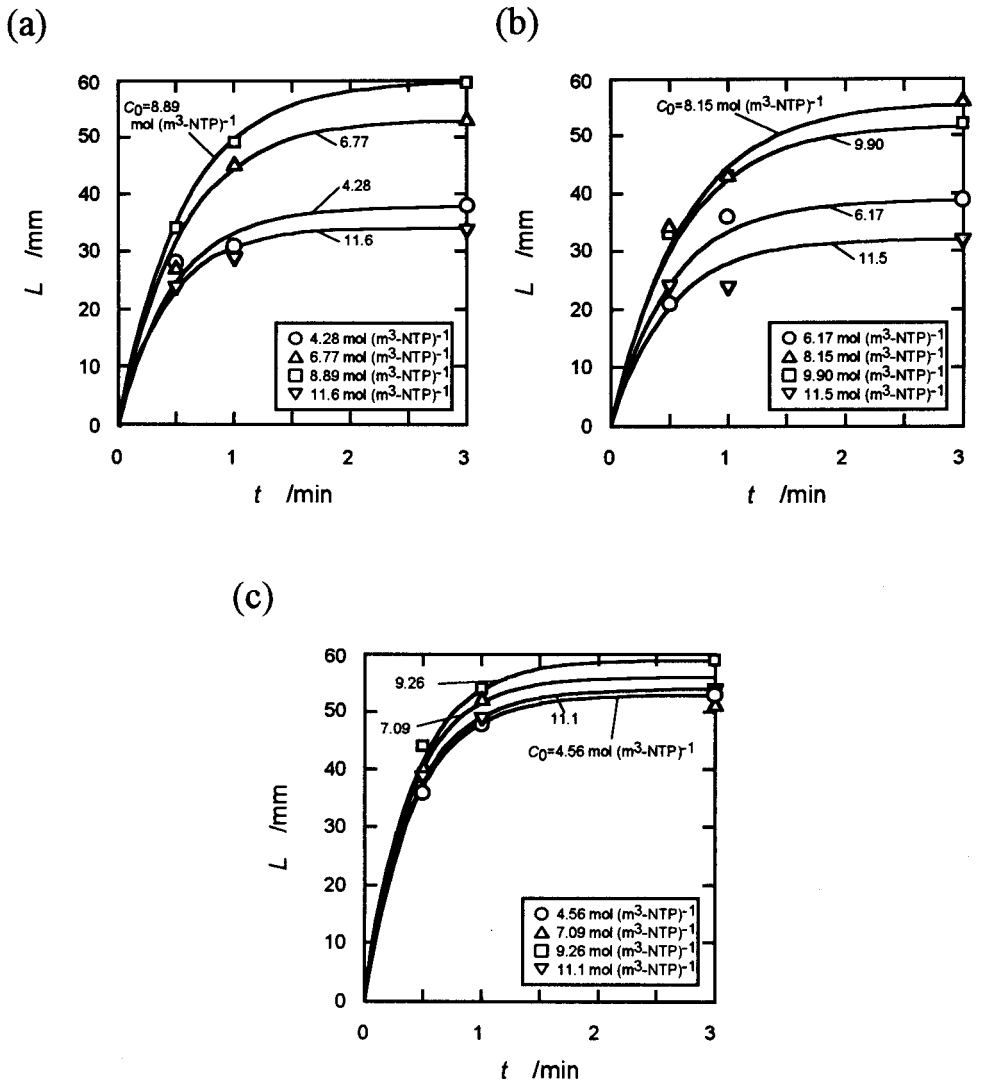

Fig. 4-9 Growth Curves of VGCFs

(Carbon Source: Mixtures of Benzene (B), Toluene (T) and Xylene (X)
(a) B:T:X=1:1:1 (b) B:T:X=1:5:7 (c) B:T:X=4:1:1)

There are two noteworthy points in Fig. 4-7. One is that the initial growth rate of the fibers increases with the increase of the initial concentration of the carbon source, but in the higher concentration region, the rates decrease. The other is that at the same initial concentration of the carbon source, the initial growth rate decreases as the average number of methyl group per benzene ring of the carbon source increases. In order to explain these results, the growth rate constants of each hydrocarbon were estimated. First, the concentrations of hydrocarbons at the position in the reactor, where the growth of VGCFs initiate, were calculated under the following assumptions:

(1) The contribution of methane, which is produced by the pyrolysis of toluene and xylene, to VGCF growth can be ignored because VGCFs were hardly obtained using methane.

(2) In a nitrogen atmosphere at temperatures above 1173 K, aromatics are thermally decomposed through various reaction mechanisms such as ring opening. However, the following reactions dominate in a hydrogen atmosphere (Benson and Shaw, 1967, Poutsma, 1990).

$$C_7H_8 + H_2 \xrightarrow{r_1} C_6H_6 + CH_4 \qquad r_1 = k_{CT} C_T C_H^{0.5} \qquad (4\text{-}1)$$

$$C_8H_{10} + H_2 \xrightarrow{r_2} C_7H_8 + CH_4 \qquad r_2 = k_{CX} C_X C_H^{0.5} \qquad (4\text{-}2)$$

$$C_6H_6 \xrightarrow[wall]{r_3} pyrolytic\ carbon \qquad r_3 = k_{DW} C_B \qquad (4\text{-}3)$$

$$C_7H_8 \xrightarrow[wall]{r_4} pyrolytic\ carbon \qquad r_4 = k_{DW} C_T \qquad (4\text{-}4)$$

$$C_8H_{10} \xrightarrow[wall]{r_5} pyrolytic\,carbon \qquad r_5 = k_{DW}C_X \qquad (4\text{-}5)$$

where r is the reaction rate, k is the reaction constant and C is the concentration of the materials. Subscript C indicates cracking, D, deposition, B, benzene, T, toluene, X, xylene, H, hydrogen and W, reactor wall.

The rate constants obtained by Burr *et al.* (1964a, 1964b) were used for k_{CT} and k_{CX}. They were:

$$k_{CT} = 2.3 \times 10^6 \exp(\frac{-193 \times 10^3}{R_g T}) \qquad (mol^{-0.5}m^{1.5}s^{-1}) \qquad (4\text{-}6)$$

$$k_{CX} = 6.3 \times 10^{10} \exp(\frac{-280 \times 10^3}{R_g T}) \qquad (mol^{-0.5}m^{1.5}s^{-1}) \qquad (4\text{-}7)$$

where T is absolute temperature and R_g is the gas constant, 8.314 J $mol^{-1}K^{-1}$. The k_{DW} value was determined from the experimental results of carbon deposition in this work. First the deposition rate was calculated from the transient weight change of the quartz glass rod. The concentration of the carbon source was calculated from the concentration at the reactor inlet and the deposition rate. Finally, the reaction rate constant was calculated assuming that the deposition rate can be expressed by a first-order reaction rate. The carbon deposition rate on the rod is assumed to be the same as that on the quartz glass reactor wall. Hence, the reaction rate constant thus obtained using benzene as the carbon source was used to represent the k_{DW} value, and is expressed as:

$$k_{DW} = 1.144 \times 10^9 \exp(\frac{-321 \times 10^3}{R_g T}) \qquad (m\,s^{-1}) \qquad (4\text{-}8)$$

Gas flowed as a laminar flow in the reactor, as the Reynolds' number was calculated to be approximately 0.1. Under this condition, the mass balance equations could be represented by a dispersed plug flow model (Levenspiel and Bischoff, 1963), where the gas flow pattern is simplified to be a plug flow which can be represented by a mean velocity, and the axial and radial dispersions of gas components are considered. The temperature distribution along the axial direction of the reactor, which was set at the same conditions as fiber production experiments, was measured using a thermocouple. The temperature at any axial position was assumed to be uniform in the radial direction at the value measured experimentally. These assumptions enable us to ignore the dispersions of gas components in the radial direction of the reactor, and give the following mass balance equations:

$$D_L \frac{d^2C_B}{dz^2} - u\frac{dC_B}{dz} + k_{CT}C_T C_H^{0.5} - a_v k_{DW} C_B = 0 \qquad (4\text{-}9)$$

$$D_L \frac{d^2C_T}{dz^2} - u\frac{dC_T}{dz} + k_{CX}C_X C_H^{0.5} - k_{CT}C_T C_H^{0.5} - a_v k_{DW} C_T = 0 \qquad (4\text{-}10)$$

$$D_L \frac{d^2C_X}{dz^2} - u\frac{dC_X}{dz} - k_{CX}C_X C_H^{0.5} - a_v k_{DW} C_X = 0 \qquad (4\text{-}11)$$

$$D_L \frac{d^2C_H}{dz^2} - u\frac{dC_H}{dz} - k_{CX}C_X C_H^{0.5} - k_{CT}C_T C_H^{0.5} = 0 \qquad (4\text{-}12)$$

$$D_L \frac{d^2C_M}{dz^2} - u\frac{dC_M}{dz} + k_{CX}C_X C_H^{0.5} + k_{CT}C_T C_H^{0.5} = 0 \qquad (4\text{-}13)$$

where z is the length from the carbon source inlet of the reactor, u is the velocity of the gas, and a_V the surface area per unit length of the reactor. D_L is the dispersion coefficient, which was calculated as 4.52×10^{-4} m^2s^{-1} by the method reported by Levenspiel and Bischoff (1963). Subscript M denotes methane.

Preliminary experiments of fiber production were conducted at different temperatures to determine the temperature at which fiber growth initiates. VGCFs could not be

obtained when the temperature of the reaction zone was lower than 1223 K. Therefore, it was concluded that the growth of VGCFs initiates at 1223 K. The axial position in the reactor, where the temperature reached 1223 K, was determined from the experimentally measured temperature distribution, and was found to be 0.125 m from the carbon source inlet of the reactor. Hence, the concentration distribution of each gas component was numerically calculated from the carbon source inlet to the position of 0.125 m from the inlet using the Runge-Kutta-Gill method. The measured temperature profile in the reactor was directly used for the calculation of the reaction rates at any axial position in the reactor.

Figure 4-10 shows a typical result of the calculated hydrocarbon concentration distribution within the reactor, where C is the hydrocarbon concentration, T the measured temperature and z the length from the carbon source inlet of the reactor. In this case, *m*-xylene was used as the initial carbon source. The temperature profile in the reactor is also shown in the figure. The concentration of *m*-xylene decreases due to the thermal expansion of the gases. This decrease is accelerated, as *m*-xylene decomposes to toluene and methane. Toluene decomposes and yields benzene. Therefore, although *m*-xylene is the initial carbon source, a mixture of *m*-xylene, toluene and benzene is the actual carbon source for fiber growth.

The fiber growth rate constant of each carbon source was estimated using the calculated concentrations of each carbon source at the point of fiber growth initiation. It was assumed that the growth rate could be expressed by a first order reaction equation. Therefore:

$$r_{(t=0)} = k_B C_B + k_T C_T + k_X C_X \qquad (4\text{-}14)$$

where k is the fiber growth rate constant. The values of $r_{(t=0)}$ have already been from the experimental data. Therefore, k_B can be estimated from the data of benzene and the calculated C_B value, because when benzene is used as the initial

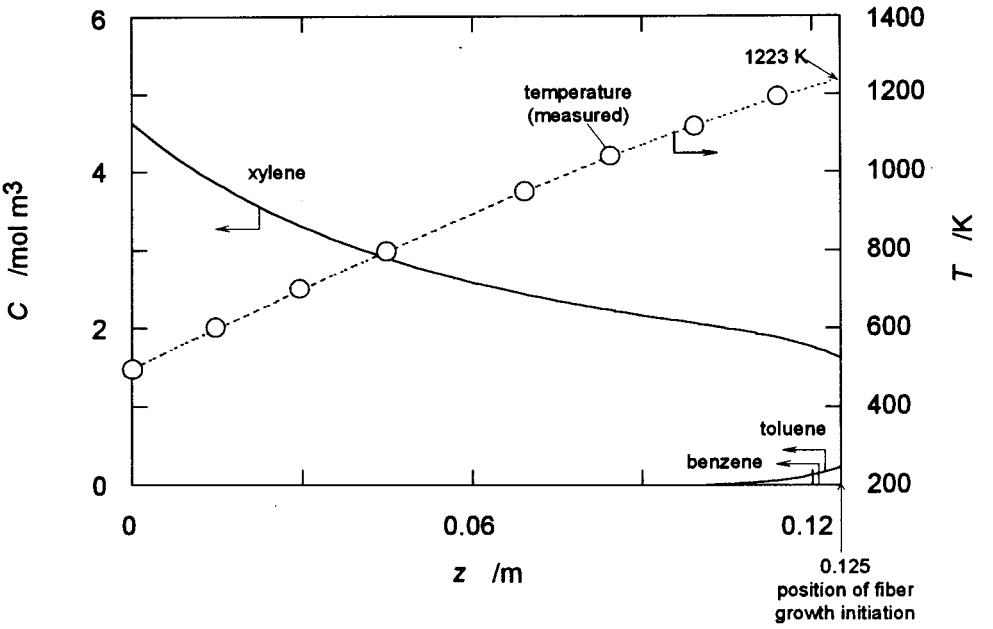

Fig. 4-10 Distribution of Temperature and Carbon Source Concentration (Initial Carbon Source: *m*-xylene)

carbon source, C_T and C_X are zero. Secondly, k_T was calculated using the data of toluene and the previously obtained k_B value, and the calculated C_B and C_T values, as C_X is zero when toluene is used as the initial carbon source. Finally, k_X was evaluated using the data of xylene and the obtained k_T, k_B values, and the calculated C_B, C_T and C_X values.

Figure 4-11 shows the plots of the obtained rate constants against the hydrocarbon concentration at the point of growth initiation, where k is the growth rate constant and C the hydrocarbon concentration. The results obtained by a plug flow model neglecting the dispersion are also shown by broken lines in the figure. This suggests that the effect of dispersion is small in the reaction system in this work. Each rate constant tends to decrease at higher concentration regions. This is considered to be due to the neglecting of ring opening reactions in the calculations, leading to the overestimation of the higher concentrations. Therefore, in this region the rate constants are considered to be underestimated. The average rate constant values of benzene, toluene and xylene were obtained to be 1.69×10^{-3}, 0.85×10^{-3} and 0.65×10^{-3} $m^4mol^{-1}s^{-1}$, respectively.

The growth rate constants decrease in the order of benzene, toluene and xylene. This decrease in the growth rate may be attributed to the electron donor ability of the methyl group. Compared to hydrogen, the methyl group is a stronger electron donor. The methyl groups of toluene and xylene are thought to stabilize the π-electrons of the benzene ring resulting in the strengthening of the bonds between the carbon atoms. This leads to the decrease of the decomposition rate of the hydrocarbon, resulting in the decrease of the growth rate of the fiber. Therefore, when high growth rates are required, a carbon source with a high fraction of benzene is required.

However, considering the fact that fibers as long as 10 mm, which meets the requirements of most of the applications of short carbon fibers, can be obtained within 15 s even using xylene as the carbon source, any mixture of benzene, toluene

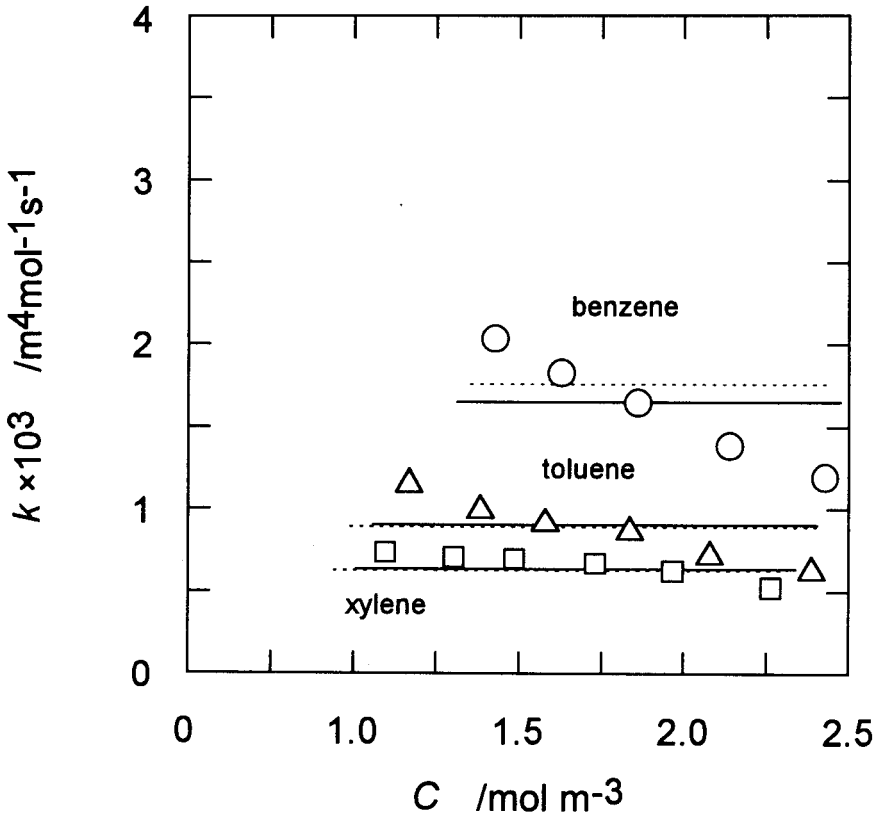

Fig. 4-11 Growth Rate Constants of VGCFs

(— Calculated by Dispersed Plug-Flow Model
- - - Calculated by Plug-Flow Model)

and xylene is thought to be an effective low cost carbon source for VGCF production.

4.4 Conclusion

VGCFs were produced using toluene and xylene as the carbon source. From the analysis of the obtained growth curves, the initial growth rate of VGCFs was found to decrease in the order benzene, toluene and xylene.

VGCFs were successfully produced using mixtures of benzene, toluene and xylene as the carbon source. Considering the low cost of this material, this mixture is an effective carbon source in VGCF production.

The fiber growth rate constants of benzene, toluene and xylene were estimated. They decrease in the order of benzene, toluene and xylene. This decrease may be attributed to the growth inhibiting effect of the methyl group.

Nomenclature

a_V	=	Surface Area per Unit Length of the Reactor	[m^2m^{-3}]
A	=	Adjustable Parameter	[mm s^{-1}]
B	=	Adjustable Parameter	[s^{-1}]
C	=	Concentration	[mol m^{-3}]
D_L	=	Dispersion Coefficient	[m^2 s^{-1}]
k	=	Reaction Constant	
L	=	Length of Fiber	[mm]
r	=	Reaction Rate	
$r_{(t=0)}$	=	Initial Growth Rate of Fiber	[mm s^{-1}]
t	=	Reaction Time	[min]
T	=	Reaction Temperature	[K]
u	=	Velocity of Gas	[m s^{-1}]

Subscripts

B	=	Benzene
C	=	Cracking
D	=	Deposition
H	=	Hydrogen
M	=	Methane
T	=	Toluene
W	=	Reactor Wall
X	=	Xylene
0	=	Initial

Literature Cited

Benson, S.W. and Shaw, R., *J. Chem. Phys.* **47**, 4052-4055 (1967)

Burr, J.G., Meyer, R.A. and Strong, J.D., *J. Am. Chem. Soc.* **86**, 3846-3850 (1964a)

Burr, J.G., Meyer, R.A. and Strong, J.D., *J. Am. Chem. Soc.* **86**, 5065-5068 (1964b)

Levenspiel, O. and Bischoff, K. B., *Adv. Chem. Eng.* **4**, 95 (1963)

Onuma, Y. and Koyama, T., *Ohyo Butsuri* **32**, 857 (1963)

Poutsma, M.L., *Energy & Fuels* **4**, 113-131 (1990)

CHAPTER 5

Dominant Hydrocarbon which Contributes to the Growth of Vapor Grown Carbon Fibers

5.1 Introduction

Benzene is the most popular carbon source for vapor grown carbon fiber (VGCF) production (Onuma and Koyama, 1963, Koyama, 1972, Koyama and Endo, 1973, Oberlin *et al.*, 1976). In the previous chapter, it was shown that aromatic compounds such as toluene and xylene are also suitable hydrocarbons for the production of VGCFs. Katsuki *et al.* (1981) have shown that VGCFs can be obtained from naphtalene. Acetylene, is also a popular carbon source for VGCFs (Baker *et al.*, 1972, 1973, 1975). Recently, it was found that VGCFs could also be obtained from low cost sources such as coal derived hydrocarbons like 1-methylnaphthalene (Kato *et al.*, 1993).

Benissad *et al.* (1988) have obtained VGCFs from methane. Tibbetts and coworkers (Tibbetts, 1983, Bradley and Tibbetts, 1985) have produced VGCFs from natural gas, which main component is methane (~97%). However, attempts to produce VGCFs from other light paraffins are few. The lengths and growth rates of VGCFs produced using methane as the carbon source were extremely small compared to those produced from benzene using the liquid pulse injection technique. Moreover, it was shown in the previous chapter that VGCFs could not be rapidly produced using methane as the carbon source.

When VGCFs are produced from various hydrocarbons, it is unlikely that they grow directly from the initial carbon source, as the production temperature of the fibers is extremely high (*e.g.* over 1273 K). Secondary products generated from the

decomposition of the initial carbon source are thought to actually contribute to fiber growth. Therefore, in order to efficiently produce VGCFs from various hydrocarbons, it is necessary to identify the actual hydrocarbon which contributes to fiber growth.

The aim of this work is to first, rapidly produce VGCFs using light paraffins as the carbon source. The second objective is to clarify the hydrocarbon(s) which actually contributes to fiber growth when various hydrocarbons are used as the initial carbon source for VGCF production.

Firstly, fiber production experiments were conducted using several light paraffins as the initial carbon source to determine the initial growth rate of the fibers under various reaction conditions. Secondly, the gas at the reaction zone of fiber growth was sampled and analyzed to find the composition and concentration of the hydrocarbons which were generated from the initial carbon source. Finally, the actual contributor was clarified by investigating the relationship between the concentration of the hydrocarbons which exist at the reaction zone, and the obtained initial growth rate of the fibers.

5.2 Experimental

5.2.1 Fiber Production

The rapid production of VGCFs were attempted using ethane, propane, *i*-butane, *n*-pentane and *n*-hexane as the initial carbon source. The experimental procedures were the same as those of the previous chapters. The temperatures of the gas preheating zone and the reaction zone were set to, 1073 K and 1373 K, respectively. The initial concentration of each carbon source was in the range 4.88 to 13.7 mol $(m^3\text{-NTP})^{-1}$, and the reaction time was set in the range 15 to 180 s. After each experiment, the fibers were collected for measurements of their lengths. The

morphology of the obtained fibers were observed by scanning electron microscopy (Hitachi; S510).

5.2.2 Gas Analysis

Figure 5-1 shows the apparatus used for gas sampling. The preheating zone and the reaction zone of the reactor used had the same size and shape as that used for fiber production, but a gas sampler was inserted into the reaction zone. Therefore, the reactant gas could be rapidly quenched to terminate further gas phase reactions and be easily collected.

The paraffins which allowed the rapid production of VGCFs were employed as the initial carbon source. Experiments using benzene as the initial carbon source were also conducted. Hydrogen was used as the carrier gas, and the temperature of the gas preheating zone and the maximum temperature within the reaction zone were set to 1073 K and 1373 K, respectively. The initial concentration of each initial carbon source was in the range of 4.88 to 13.7 mol $(m^3\text{-NTP})^{-1}$. These conditions are the same as those used for fiber production. From temperature measurements, it was found that the temperature dropped rapidly from 1373 K to 323 K within the gas sampler at the reaction zone. This allows the rapid termination of gas phase reactions. Hence, the collected gas well represents the state of the gas phase at the reaction zone of fiber production.

After the reactor was thoroughly purged with the carrier gas, and the temperatures of the electric furnaces reached a steady state, the initial carbon source was introduced into the reactor. After 2 minutes from this introduction, the three way valve located at the gas outlet of the reactor was rotated to lead the gas stream to the liquid and gas traps. Gas was collected for 30 minutes. The low boiling point fraction of the collected gas was trapped in the liquid trap which was cooled with a mixture of dry ice and dichloromethane. The high boiling point fraction of the gas was collected in the gas trap. The components of the sampled gas were identified using mass

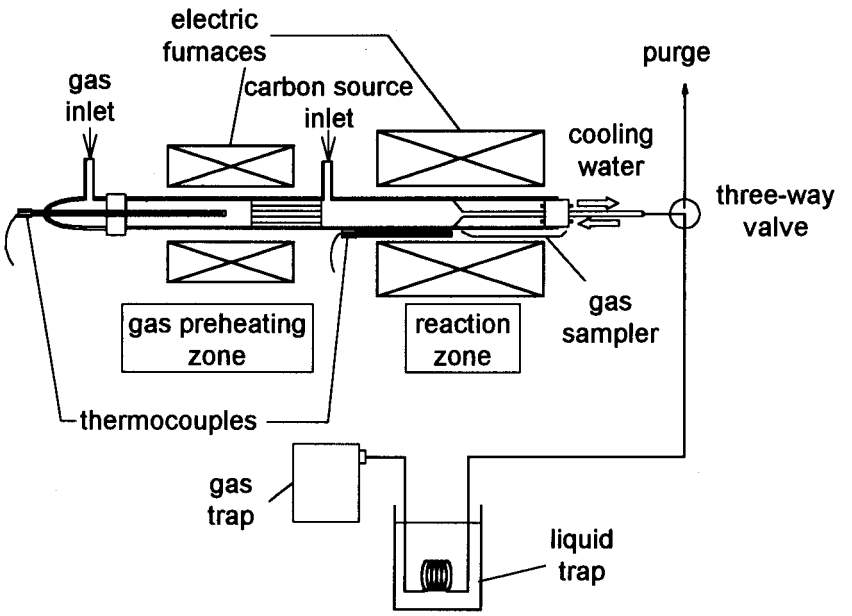

Fig. 5-1 Apparatus for Gas Sampling

spectroscopy (Shimadzu; QP-5000), and quantitatively analyzed using gas chromatography (Shimadzu; GC 14A). The column packings used were Porapak Q and OV-101 for gas and liquid analysis, respectively.

5.3 Results and Discussion

5.3.1 As-grown VGCFs

VGCFs were obtained from *i*-butane, *n*-pentane, and *n*-hexane. A few fibers could be occasionally obtained when propane was used as the carbon source, whereas no fibers could be obtained using ethane.

Figures 5-2 to 5-4 show typical SEM micrographs of VGCFs obtained from different carbon sources. The fibers were fairly straight and were apparently the same as those obtained using aromatic compounds as the carbon source.

5.3.2 Growth Rate Analysis

Figures 5-5 to 5-7 show growth profiles when different light paraffins were used as the carbon source. The same trend as the growth curves of benzene can be seen in these curves. Although under certain reaction conditions the initial growth rate tends to be lower than others, fibers longer than 10 millimeters were obtained within 15 s under any reaction condition. This length satisfies most applications of short fibers.

It is obvious that the growth profiles of the fibers can be expressed by Eqs. (2-1) and (2-2). The initial growth rates of the fibers ($r_{(t=0)}$) were determined by the method described in chapter 2. They are plotted against the carbon source initial concentration in Fig. 5-8. For comparison, the results of benzene are also shown in this figure. Although the $r_{(t=0)}$ values of light paraffins are smaller than those of benzene, the minimum value is over 1 mm s^{-1}, which is at least ten times larger than those of VGCFs produced by conventional production methods using benzene as the

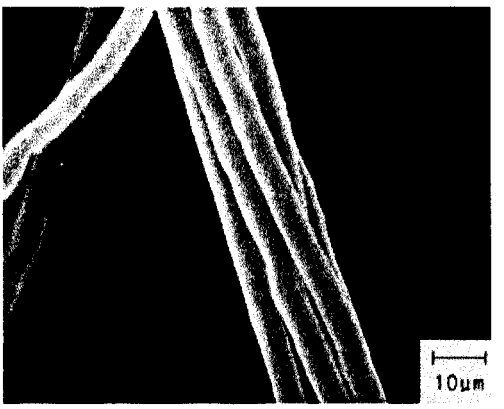

Fig. 5-2 SEM Micrograph of VGCFs
(Carbon Source: *i*-Butane)

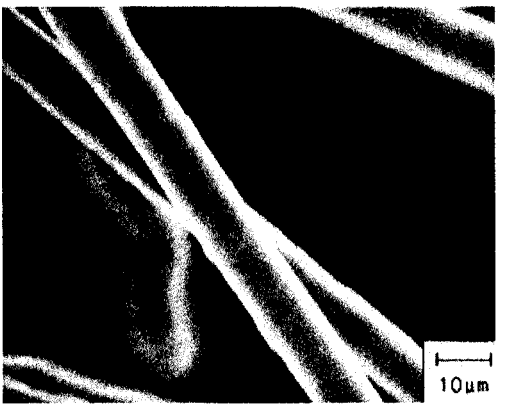

Fig. 5-3 SEM Micrograph of VGCFs
(Carbon Source: *n*-Pentane)

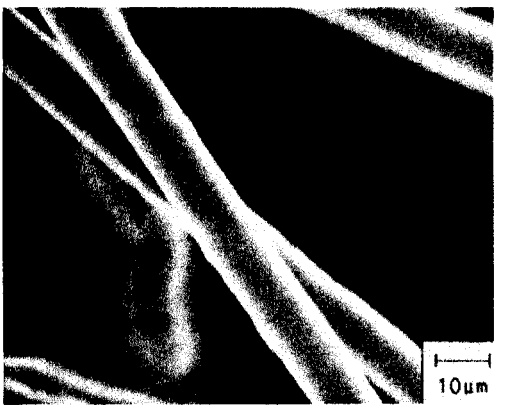

Fig. 5-4 SEM Micrograph of VGCFs
(Carbon Source: *n*-Hexane)

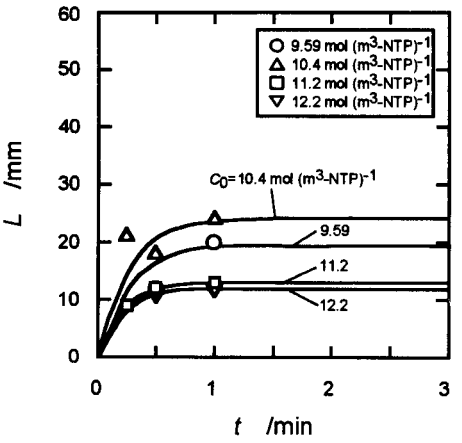

Fig. 5-5 Growth Curves of VGCFs
(Carbon Source: *i*-Butane)

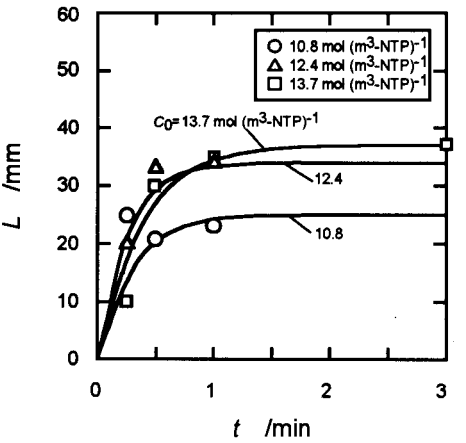

Fig. 5-6 Growth Curves of VGCFs
(Carbon Source: *n*-Pentane)

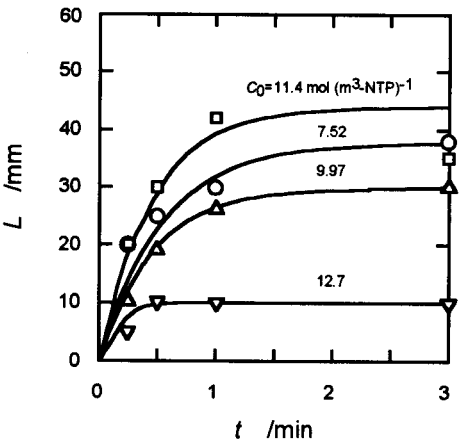

Fig. 5-7 Growth Curves of VGCFs
(Carbon Source: *n*-Hexane)

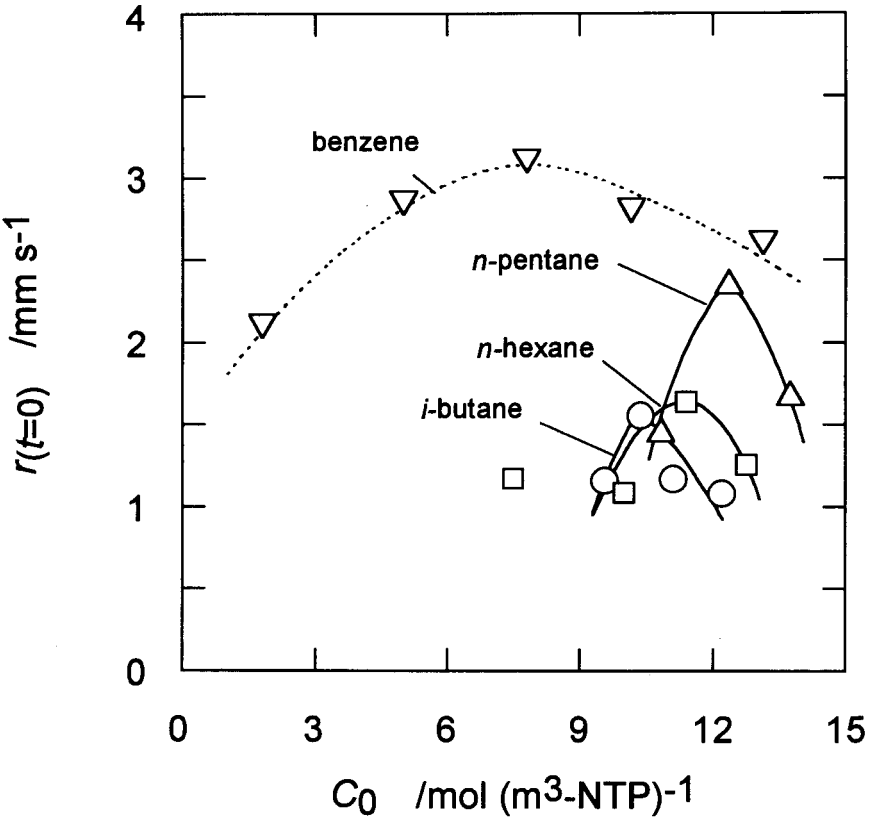

Fig. 5-8 Initial Growth Rates of VGCFs

carbon source. In these methods, it is very difficult to obtain VGCFs from light paraffins. It is noteworthy that values over 2 mm s^{-1}, which is close to those of benzene, can be attained when *n*- pentane is used as the initial carbon source.

5.3.3 Gas Analysis

Typical results of gas analysis are summarized in Fig. 5-9. Although the initial carbon source was different, the main hydrocarbons obtained from each initial carbon source were benzene, methane and ethylene. Here we will try to clarify the hydrocarbon which actually contributes to fiber growth.

We attempted to verify the actual contributor by investigating the relationship between the concentration of each main hydrocarbon and the initial growth rate of the fibers. The change in the concentration of the actual contributor should significantly have influence on the initial fiber growth rate. This is a rough but simple method for verification.

Figure 5-10 shows the influence of the concentration of methane (C_M) on the initial growth rate of VGCFs ($r_{(t=0)}$). Apparently there is no relationship between them. This result is consistent with fiber production experimental results, where no fibers could be obtained using methane as the carbon source. Figure 5-11 shows the influence of the concentration of ethylene (C_E) on the initial growth rate of VGCFs ($r_{(t=0)}$). Here also no relationship can be seen between them. Therefore, it may be concluded that ethylene does not contribute to fiber growth. Figure 5-12 shows the influence of the concentration of benzene (C_B) on the initial growth rate of VGCFs ($r_{(t=0)}$). Although the initial carbon sources are different, the results lay well on one straight line indicating that benzene is the actual contributor to fiber growth.

The results shown in Fig. 5-8 supports this result, where VGCFs could be obtained in a wide initial concentration range when benzene was used as the initial carbon source, but could only be obtained in a narrow range when light paraffins were used. When

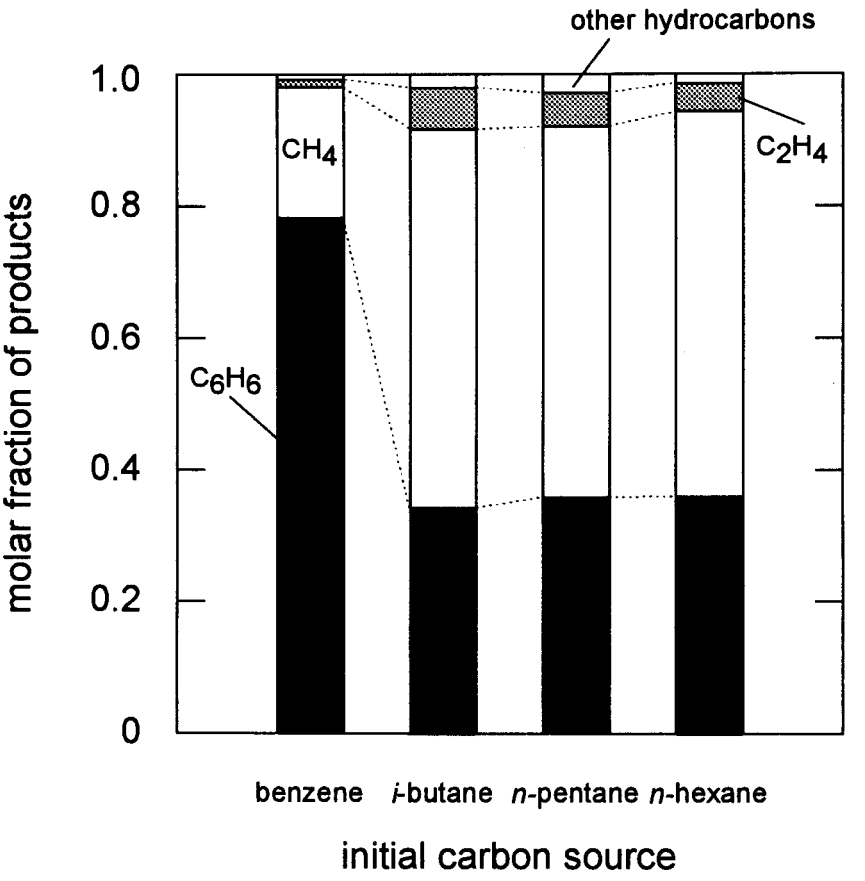

Fig. 5-9 Typical Results of Gas Analysis

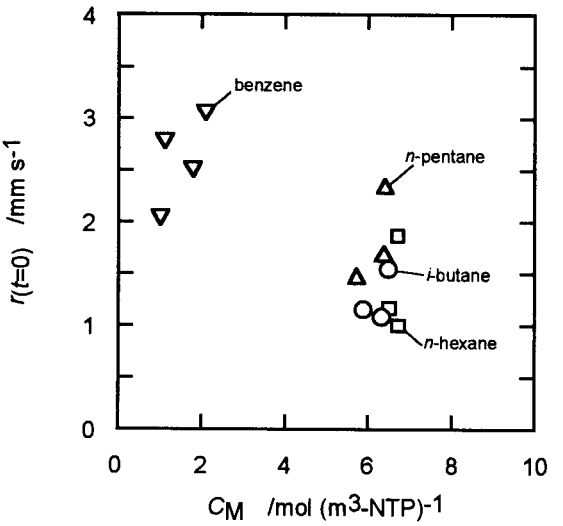

Fig. 5-10 Influence of the Concentration of Methane on the Initial Growth Rate of VGCFs

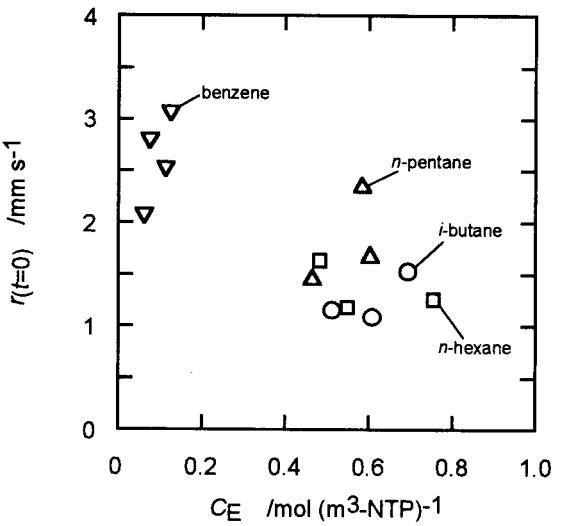

Fig. 5-11 Influence of the Concentration of Ethylene on the Initial Growth Rates of VGCFs

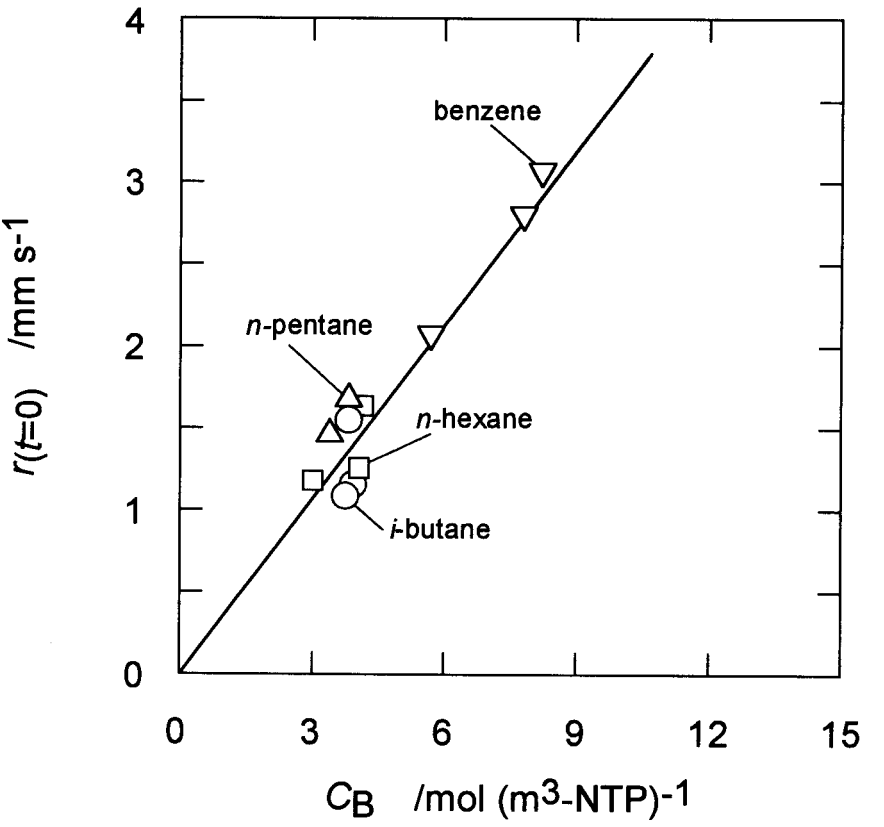

Fig. 5-12 Influence of the Concentration of Benzene on the Initial Growth Rate of VGCFs

benzene is used, the concentration of benzene is high at the upstream of the reactor and gradually decreases due to decomposition, so the concentration of it is maintained relatively high throughout the reaction zone under a wide range of initial concentrations. In the cases when light paraffins are used, benzene is only formed through the decomposition of the initial hydrocarbon. The produced benzene undergoes further decomposition. Therefore, the region in the reaction zone, where the concentration of benzene is significantly high, is rather narrow. The position of this region differs when the initial concentration of the paraffin is changed. Therefore, VGCFs can be obtained only at limited initial concentration ranges as they can grow only when the concentration of benzene is high at the position where the catalyst particles reveal their activity.

The above results show the possibility that VGCFs can be produced from a wide variety of hydrocarbons which generate benzene under reaction conditions suitable for fiber growth. The key point for efficient VGCFs production is to prepare active catalyst particles in the region where the concentration of benzene is high. This can be easily achieved using the newly developed liquid pulse injection technique.

5.4 Conclusion

Long VGCFs were successfully obtained at high growth rates from various light paraffins using the liquid pulse injection technique. From the analysis of the gas at the reaction zone, the hydrocarbon which actually contributes to fiber growth was found to be benzene. Therefore, VGCFs can be produced from a wide variety of hydrocarbons which generate benzene during decomposition. The liquid pulse injection technique is a promising method to prepare active catalyst particles where the concentration of benzene is high, which is the key point for efficient VGCF production.

Nomenclature

C	=	Concentration	[mol m^{-3}]
L	=	Length of Fiber	[mm]
$r_{(t=0)}$	=	Initial Growth Rate of Fiber	[mm s^{-1}]
t	=	Reaction Time	[min]

Subscripts

B	=	Benzene
E	=	Ethylene
M	=	Methane
0	=	Initial

Literature Cited

Baker, R. T. K., Barber, M. A., Harris, P. S., Feates, F. S., and Waite, R. J., *J. Catal.* **26**, 51 (1972)

Baker, R. T. K., Harris, P. S., Thomas, R. B., and Waite, R. J., *J. Catal.* **30**, 86 (1973)

Baker, R. T. K. and Waite, R. J., *J. Catal* **37**, 101 (1975)

Benissad, F., Gadelle, P., Coulon, M., and Bonnetain, L., *Carbon* **26**, 61 (1988)

Bradley, J. R. and Tibbetts, G. G., *Carbon* **23**, 423 (1985)

Kato, T., Matsumoto, T., Saito, T., Hayashi, J., Kusakabe, K., and Morooka, S., *Carbon* **31**, 937 (1993)

Katsuki, H., Matsunaga, K., Egashira, M. and Kawasumi, S., *Carbon* **19**, 148 (1981)

Koyama , T., *Carbon* **10**, 757 (1972)

Koyama, T. and Endo, M., *Ohyo Butsuri* **42**, 690 (1973)

Oberlin, A., Endo, M., and Koyama, T., *J. Cryst. Growth* **32**, 335 (1976)

Onuma, Y. and Koyama, T., *Ohyo Butsuri* **32**, 857 (1963)

Tibbetts, G. G., *Appl. Phys. Lett.* **42**, 666 (1983)

CHAPTER 6

The Influence of Catalyst Particle Size Distribution on the Yield of Vapor Grown Carbon Fibers Produced Using the Liquid Pulse Injection Technique

6.1 Introduction

Vapor grown carbon fibers (VGCFs) grow in the axial direction through the catalytic action of ultra-fine metal catalyst particles. The axial growth rate of VGCFs is very sensitive to the activity of the catalyst.

Among various factors, the diameter of the catalyst particle has a significant influence on its catalytic activity. Baker *et al.* (1978, Baker, 1989) have reported that the axial growth rate of a VGCF has an inverse square root dependency on catalyst particle size. This indicates that a smaller catalyst particle leads to a higher growth rate, but a particle which is too small will probably not show any catalysis, because it is difficult to form a cylindrical graphitic tube with a small diameter. Endo (1988) has reported that not only the growth rate, but also the fiber yield increases when smaller catalyst particles are used. The suitable catalyst particle size seems to be a few to about 20 to 30 nm (Benissad *et al.*, 1988; Endo, 1988; Baker, 1989; Ishioka *et al.*, 1993). However, it was very difficult to generate catalyst particles in this size range in a highly dense state.

The liquid pulse injection (LPI) technique is a very promising method to generate very active ultra-fine metal particles in a highly dense state. However, the change in the reaction conditions varies the size distribution of the generated catalyst particles, leading to the change in the yield of VGCFs. Therefore, the effects of reaction conditions on the yield of VGCFs were investigated in chapter 3. However, the

actual distribution of the generated particles has not yet been experimentally obtained .

From transmission electron microscopy observations of VGCFs produced using the LPI technique, the size of the catalyst particles of the fibers were in the range of 20 to 30 nm. It is premature to conclude from observations of a few particles that this is the suitable size range of the catalyst particles, but it is unrealistic to determine statistically the range, as it is very difficult to obtain a micrograph of a catalyst particle encapsulated within a fiber. This range of 20 to 30 nm was verified in a different way.

The main objectives of this chapter are to measure the size distribution of the catalyst particles produced using the LPI technique, and to develop a model to predict this size distribution. Particles produced under the same conditions as VGCF production were collected at the position in the reactor where fiber growth initiates, and were withdrawn from the reactor. Their size distribution was determined from transmission electron microscope observations. The size range of the catalyst particles which is suitable for VGCF production can be verified by combining the data of the obtained distribution curves with the yield of VGCFs produced under the same reaction conditions. Moreover, using population balance equations, a model was developed to predict the size distribution of particles produced under various reaction conditions.

6.2 Experimental

In the liquid pulse injection technique, a liquid pulse of the catalyst material (benzene solution of ferrocene) is injected into the reactor and impinges on its hot wall. This pulse rapidly evaporates and decomposes, releasing numerous iron clusters. These clusters coagulate and form catalyst particles. VGCF growth initiates when these catalyst particles grow up to the suitable size for fiber growth and make contact with

the carbon source (*e. g.* benzene vapor) and reach the appropriate temperature. The catalytic activity of the catalyst particle depends on several factors, especially on their size. In order to obtain the size distribution of the catalyst particles at the position where VGCFs grow, the following points were taken into account:

(1) The growth of VGCFs was suppressed by not providing the carbon source to the reactor, since once fiber growth initiates, the catalyst particles will be encapsulated by carbon layers, and it will become very difficult to measure their actual sizes.

(2) The size distribution of catalyst particles which are collected from the reactor must represent that of the position where fiber growth initiates. Therefore, a new reactor was designed for this purpose.

Figure 6-1 shows a schematic of the reactor used for particle production and collection. The reactor used for VGCF production is also shown for comparison. The reactor was made with a 22 mm *i.d.* quartz tube. The configuration of the reactor was basically the same as that used for VGCF production. However, the following two points were reformed.

(1) The reactor was tapered at the position where fiber growth usually initiates. This increases the line velocity of the flowing gas, and allows the quick sweep out of the generated particles from the reaction zone. This position was determined in chapter 4.

(2) A quencher was set downstream of the position where VGCF growth usually initiates, to rapidly cool the flowing gas and particles to avoid further growth of particles.

From the measurement of the temperature profile within this new reactor, it was

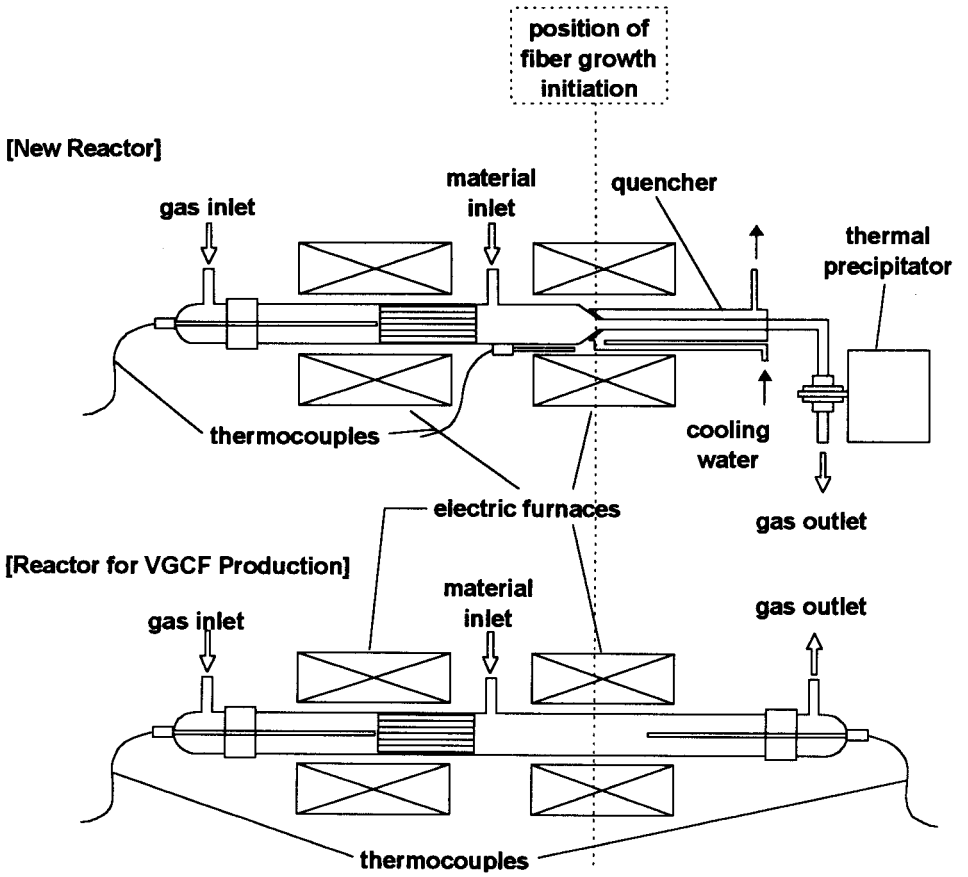

Fig. 6-1 Experimental Apparatus

confirmed that the profile from the reactor inlet to the position where fiber growth usually initiates was identical to that of the reactor for VGCF production. Moreover, the temperature rapidly drops from 1323 K to below 473 K within only 20 mm from this position. Therefore particle growth is rapidly suppressed at this position. This new reactor enables us to collect the catalyst particles without any change in particle size, and the distribution curve of the collected particles represents that of the actual reactor for fiber production.

The reactor was purged with nitrogen for 30 min (flow rate 120 (cm^3-NTP) min^{-1}) and then with hydrogen for 30 min (flow rate 60 (cm^3-NTP) min^{-1}). The reactor was heated up to the desired temperature. After the flow of the carrier gas and the temperatures of the electric furnaces reached a steady state, a liquid pulse of the catalyst particle material was injected into the reactor. The carrier gas and the catalyst particle material were hydrogen and a benzene solution of ferrocene, respectively. This injection was continued for 40 times at an interval of 60 s, because the amount of catalyst particles obtained from a single pulse is extremely small. It was confirmed in chapter 3 that there is no significant interaction among pulses at this interval. The generated catalyst particles were quickly cooled at the quencher. Due to thermophoresis, they stick to the wall of the quencher. Particles which could not be trapped at the quencher were caught using a thermal precipitator (Shibata; L-2), which was set at the outlet of the reactor. After each experiment, the collected particles were dispersed in acetone. A fraction of the dispersed particles was set on a copper grid for transmission electron microscopy (TEM) observation (Hitachi; H-9000NAR). The size distributions of the particles were determined from TEM micrographs.

The varied reaction conditions were the line velocity of the carrier gas, and the amount and the concentration of the liquid pulse of the benzene solution containing ferrocene, which was used as the catalyst particle precursor. They were set in the range 1.02 to 6.62 (mm-NTP) s^{-1}, 0.010 to 0.025 cm^3 and 3 to 10 wt%-ferrocene, respectively.

The yield of VGCFs grown under the same set of reaction conditions was also obtained using the reactor for fiber production.

6.3 Model Equations

In order to simulate the growth process of catalyst particles, it was assumed that the growth proceeds through the process summarized in Fig. 6-2. When a liquid pulse of the catalyst particle material is injected into the reactor, it hits the hot reactor wall and instantaneously evaporates. This vapor forms a "cell" and is pushed downstream of the reactor by the carrier gas. The mixing of components between the cell and carrier gas was neglected. The cell changes its volume according to the temperature profile within the reactor. The catalyst particle material starts to decompose and generates iron clusters of volume v^*. These clusters coagulate and form catalyst particles. The size distribution of the particles in the cell, which reached the position where fiber growth initiates, was calculated on the basis of this process. Usually this distribution is calculated in the form of particle concentration, but as the volume of the cell changes according to the temperature profile within the reactor, the size distribution was calculated in terms of number of particles within the cell.

The population balance equation for clusters which have a volume of v^* is given by,

$$\frac{\partial}{\partial t}\{n(v^*,t)\} = V\left\{r_{\text{birth}} - \frac{n(v^*)}{V}\int_{v^*}^{\infty}\beta(v^*,\tilde{v})\frac{n(\tilde{v})}{V}\mathrm{d}\tilde{v}\right\} \qquad (6\text{-}1)$$

whereas that for particles which have a volume of v is written as,

$$\frac{\partial}{\partial t}\{n(v,t)\} = V\left\{\frac{1}{2}\int_{v^*}^{v}\beta(\tilde{v},v-\tilde{v})\frac{n(\tilde{v})}{V}\frac{n(v-\tilde{v})}{V}\mathrm{d}\tilde{v} - \frac{n(v)}{V}\int_{v^*}^{\infty}\beta(v,\tilde{v})\frac{n(\tilde{v})}{V}\mathrm{d}\tilde{v}\right\} \qquad (6\text{-}2)$$

injection of catalyst particle material

- simultaneous evaporation
- formation of cell

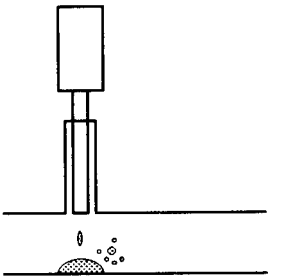

shift of cell

- shift of cell with carrier gas
- change of cell temperature

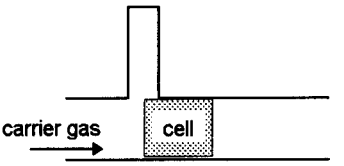

formation of ultra-fine catalyst particles

- formation of clusters through the thermal decomposition of catalyst material
- formation of particles through the coagulation of clusters

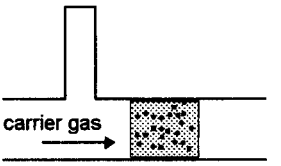

prediction of the size distribution of particles at the position of fiber growth initiation

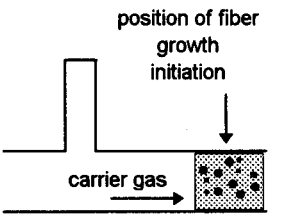

Fig. 6-2 Outline of the Process of Particle Formation

$n(v,t)/V$ is the density distribution function, where $n(v,t)dv$ gives the number of particles which have volumes between v and $v+dv$ at time t, V the volume of the cell, r_{birth} a term which expresses the birth of clusters, and $\beta(u,v)$ the coagulation coefficient between particles having volumes u and v. Considering the temperature distribution within the reactor, V can be expressed as follows:

$$V = \frac{T}{T_0} V_0 \tag{6-3}$$

where T is the temperature of the position where the cell is located at, and T_0 and V_0 are the initial temperature and initial volume of the cell, respectively. As we are dealing with iron particles, the clusters which are initially generated by the decomposition of the particle material, can be taken as iron atoms. Therefore, r_{birth} can be expressed using the following decomposition rate of ferrocene, r_v*,

$$r_v * = kC_{ferrocene} \tag{6-4}$$

where, k is the decomposition rate constant of ferrocene, and $C_{ferrocene}$ the number of ferrocene molecules per unit volume within the cell. The temperature dependence of k was determined from the experimental data of Dyagileva *et al.* (1979) and Lewis and Smith (1984) as,

$$k = 5.01 \times 10^{10} \exp(-2.50 \times 10^5 / R_g T) \quad [s^{-1}] \tag{6-5}$$

The sizes of the particles in this system are about one tenth of the mean free path of the gases, therefore the coagulation coefficient, $\beta(u,v)$ can be expressed as follows (Friedlander, 1977):

$$\beta(u,v) = a\sqrt{T}(u^{\frac{1}{3}} + v^{\frac{1}{3}})^2(u^{-1} + v^{-1})^{0.5} \tag{6-6}$$

Among the above equations, a is the only unknown parameter.

The population balance equations must be solved numerically. Among various numerical methods, the discrete-sectional model (DSM), which was presented by Wu and Flagan (1988), was employed, since this method can be applied to a wide particle diameter range, and allows us to calculate the distribution in a rather short time compared to other methods.

In the DSM, the spectrum of the size distribution of the particles is separated into two parts as illustrated in Fig. 6-3. The first part of the spectrum, starting from a cluster (atom), is described by the number of particles (in the cell) containing i clusters, n_i, where $1 \le i \le k$. The second part is described by the numbers contained in sections, N_l ($1 \le l \le M$), into which the rest of the particle size space is divided. The particle size in this sectional regime is represented by x which is the logarithmic value of particle diameter, and is,

$$x = \frac{1}{3}\log(\frac{6v}{\pi}) \tag{6-7}$$

For the lth section ($1 \le l \le M$), the number, N_l, in the corresponding interval, $x_{l-1} \le x < x_l$, is,

$$\frac{N_l}{V} = \int_{x_{l-1}}^{x_l} \frac{m(x)}{V} dx \tag{6-8}$$

where $m(x)/V$ is the density distribution function and $m(x)dx$ is the number of particles which have diameters between x and $x+dx$.

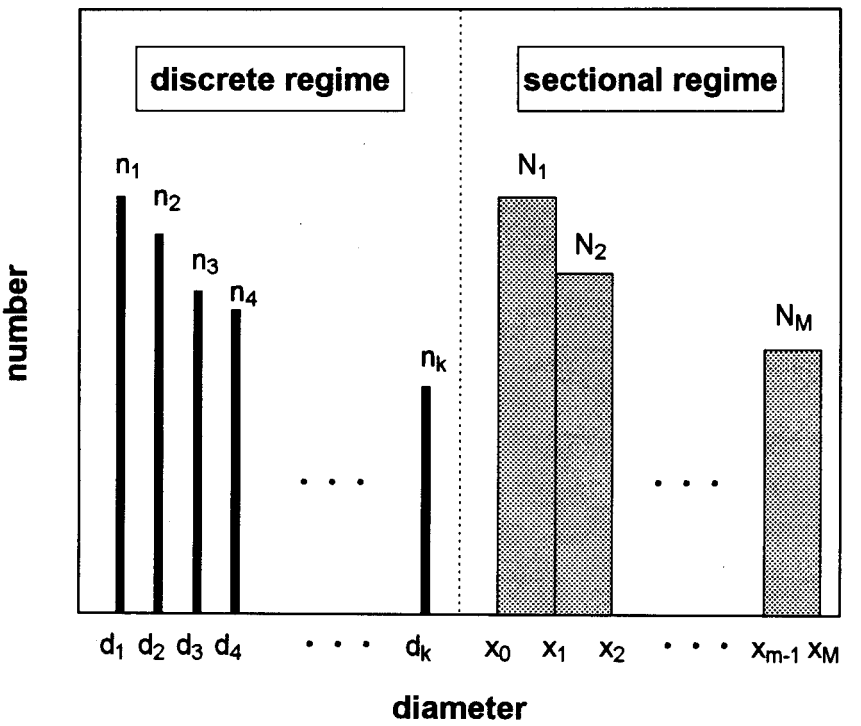

Fig. 6-3 Outline of the Discrete Sectional Model

When the DSM is applied to the liquid pulse injection technique, the population balance equations can be rewritten as follows (see **Appendix** for details).

(Discrete Regime)

For the number of clusters, n_1, which have a volume of v^*,

$$\frac{dn_1}{dt} = V\left[r_{v^*} - \sum_{i=1}^{k} \beta_{1i} \frac{n_1}{V}\frac{n_i}{V} - \left\{\sum_{r=1}^{M} {}^{1}\overline{\overline{\beta}}_{1r} \frac{N_r}{V}\right\}\frac{n_1}{V}\right] \tag{6-9}$$

for the number of i-mer particles, n_i, which have a volume of $i \times v^*$,

$$\frac{dn_i}{dt} = V\left[\frac{1}{2}\sum_{j=1}^{i} \beta_{(i-j)j} \frac{n_{(i-j)}}{V}\frac{n_j}{V} - \sum_{j=1}^{k} \beta_{ij} \frac{n_i}{V}\frac{n_j}{V} - \left\{\sum_{r=1}^{M} {}^{1}\overline{\overline{\beta}}_{ir} \frac{N_r}{V}\right\}\frac{n_i}{V}\right], \ (2 \le i \le k) \tag{6-10}$$

(Sectional Regime)

For the number of particles which belong to the l th section, N_l,

$$\begin{aligned}\frac{dN_l}{dt} = V\Bigg[&\frac{1}{2}\sum_{r=1}^{l-1}\sum_{s=1}^{l-1} {}^{1}\overline{\beta}_{rsl} \frac{N_r}{V}\frac{N_s}{V} - \left\{\sum_{r=1}^{l-1} {}^{2}\overline{\beta}_{rl} \frac{N_r}{V}\right\}\frac{N_l}{V} - \frac{1}{2} {}^{3}\overline{\beta}_{ll}\left(\frac{N_l}{V}\right)^2 \\ &- \left\{\sum_{r=l+1}^{M} {}^{4}\overline{\beta}_{rl} \frac{N_r}{V}\right\}\frac{N_l}{V} - \left\{\sum_{i=1}^{k} {}^{2}\overline{\overline{\beta}}_{il} \frac{n_i}{V}\right\}\frac{N_l}{V} + \sum_{i=1}^{k}\sum_{s=1}^{l-1} {}^{3}\overline{\overline{\beta}}_{irl} \frac{n_i}{V}\frac{N_r}{V} \\ &+ \frac{1}{2}\sum_{i=1}^{k}\sum_{j=1}^{k} {}^{4}\overline{\overline{\beta}}_{ijl} \frac{n_i n_j}{V V}\Bigg], \quad (1 \le l \le M)\end{aligned} \tag{6-11}$$

where β_{ij} is the rate coefficient of the coagulation between a particle of volume $i \times v^*$ and volume $j \times v^*$, ${}^1\overline{\beta}_{rsl}, {}^2\overline{\beta}_{rl}, {}^3\overline{\beta}_{ll}, {}^4\overline{\beta}_{rl}$ the inter- and intra-sectional coagulation coefficients to count the interactions of particles inside the sectional regime, and ${}^1\overline{\overline{\beta}}_{ir}, {}^2\overline{\overline{\beta}}_{rl}, {}^3\overline{\overline{\beta}}_{irl}, {}^4\overline{\overline{\beta}}_{ijl}$ the discrete-sectional coagulation coefficients accounting for the interactions of particles between the discrete and sectional regimes.

In calculations, the largest particle in the discrete regime was taken to be formed by 10 clusters, and the maximum diameter of the sectional regime was taken to be 500 nm. The sectional regime was divided into 50 sections.

Parameter a was determined by adjusting its value so that the peak position of the calculated distribution curve would match that of the experimentally obtained curve.

6.4 Results and Discussion

From TEM observation, the frequency of each range of particle size was obtained. Using the frequency and the amount of catalyst material introduced into the reactor, the total number of particles per pulse were calculated. The product of the total number of particles and the frequency gives the number of particles corresponding to particle size, yielding the number distribution of the catalyst particles. This allows one to directly compare the number of particles obtained per pulse at different reaction conditions.

Figure 6-4 shows the influence of the concentration of the catalyst particle material on the number distribution of the obtained particles. The amount of catalyst particle material per pulse, and the carrier gas line velocity were fixed in this series to 0.02 cm^3 and 2.55 (mm-NTP) s^{-1}, respectively. The position of the peak of the distribution shifts to a larger diameter region with the increase in concentration of the catalyst particle material. The total number of particles also increases. This is due

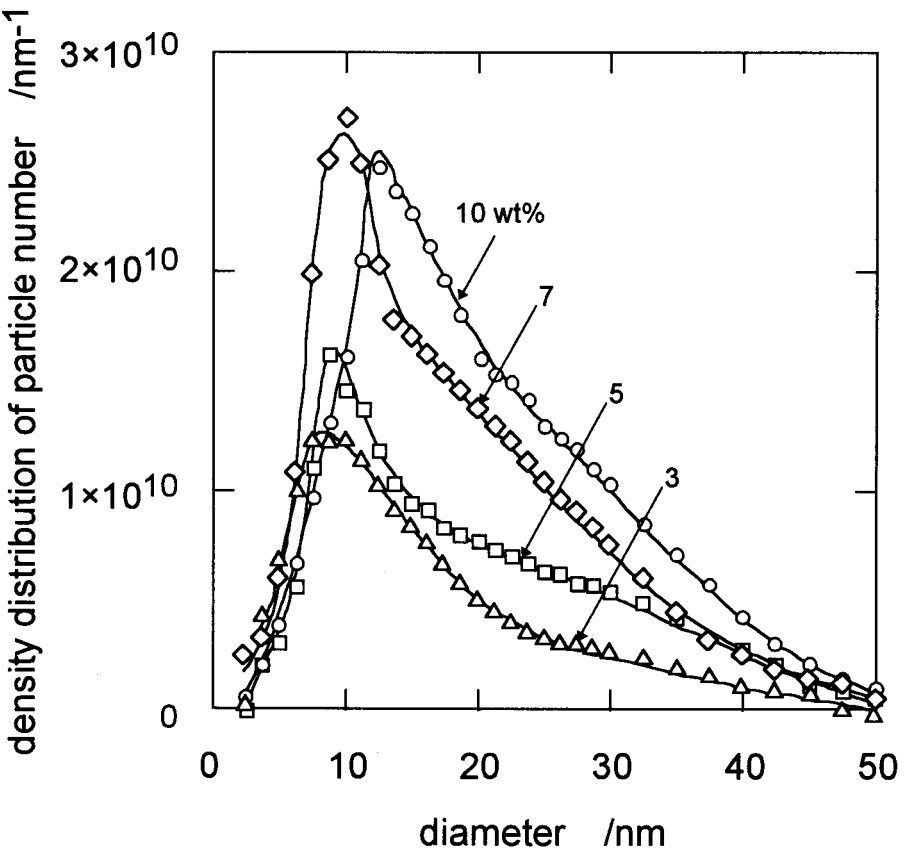

Fig. 6-4 Influence of the Concentration of the Catalyst Particle Material on the Distribution Curve of the Obtained Particles

(Catalyst Source Amount per Pulse: 0.020 cm^3
Carrier Gas Line Velocity: 2.55 (mm-NTP) s^{-1})

to the increase in the concentration of ferrocene in the initial cell. A higher concentration leads to more particles and a higher coagulation rate. The number of particles which have diameters between 20 and 30 nm increases with the increase in the concentration of the catalyst material.

Figure 6-5 shows an example of the influence of the amount of catalyst particle material per pulse on the number distribution of the obtained particles. The concentration of the catalyst particle material, and the carrier gas line velocity were fixed in this series to 10 wt% and 2.55 (mm-NTP) s^{-1}, respectively. The total amount of particles increases with the increase in the amount of catalyst particle material. Moreover, the position of the peak of the distribution slightly shifts to a smaller diameter region. This may be attributed to the drop of the initial temperature of the cell because of the limit of heat conduction at the reactor wall. A lower temperature leads to slower decomposition and coagulation rates. The number of particles which have diameters in the range 20 and 30 nm increases with the increase in the amount of catalyst particle material. However, even though the particles have the suitable size for rapid fiber production, their temperature may not be high enough to show a high activity for fiber production. In fact, the yield of VGCFs increase with the increase in the amount of catalyst particle material per pulse, but after reaching a maximum value, it drastically decreases as was shown in chapter 3.

Figure 6-6 shows the influence of the line velocity of the carrier gas on the distribution curve of the obtained particles. The concentration and the amount per pulse of the catalyst particle material were fixed in this series to 10 wt% and 0.02 cm^3, respectively. The peak position of the distribution curves shift to a smaller diameter region with the increase in the line velocity of the carrier gas. A higher line velocity leads to a shorter coagulation time, resulting in the production of smaller particles. Note that an optimal line velocity exists, which gives the maximum number of catalyst particles in the range of 20 to 30 nm.

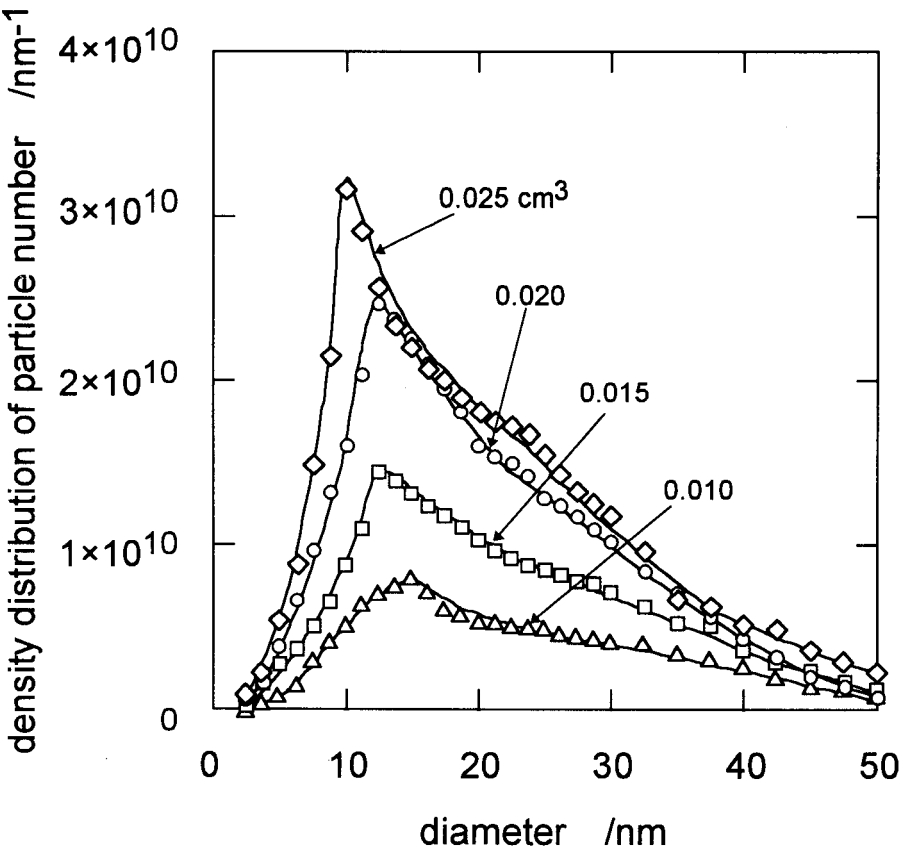

Fig. 6-5 Influence of the Catalyst Source Amount per Pulse on the Distribution Curve of the Obtained Particles

(Catalyst Source Concentration: 10 wt%
Carrier Gas Line Velocity: 2.55 (mm-NTP) s^{-1})

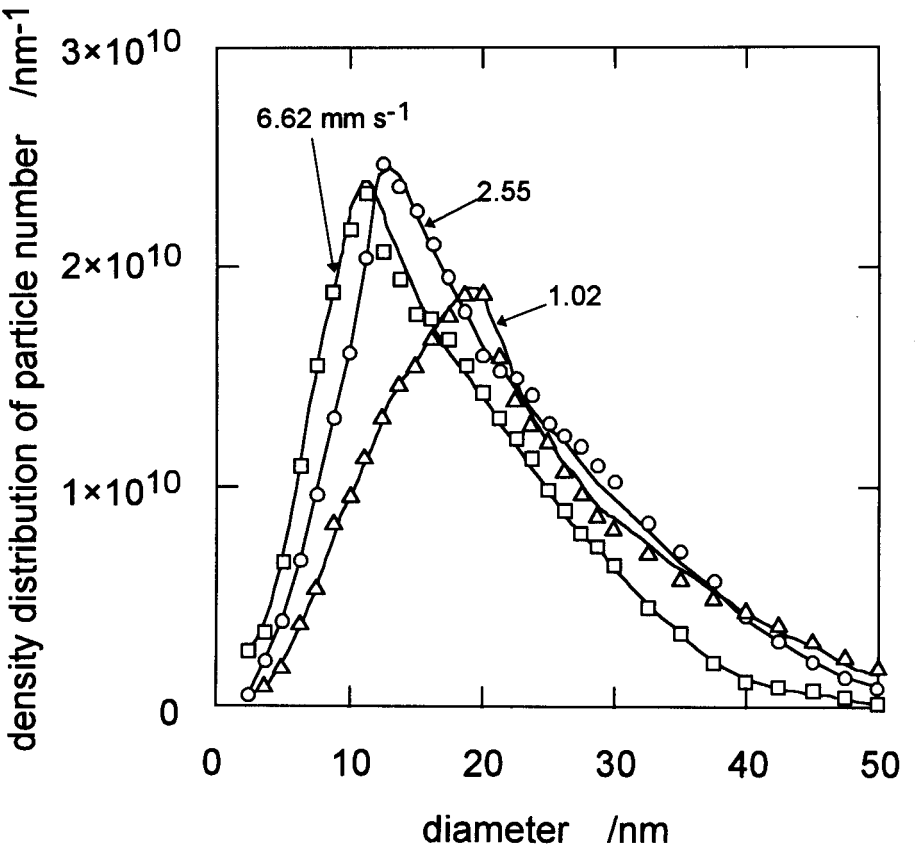

Fig. 6-6 Influence of the Line Velocity of the Carrier Gas on the Distribution Curve of the Obtained Particles

(Catalyst Source Concentration: 10 wt%
Catalyst Source Amount per Pulse: 0.020 cm^3)

VGCFs were produced under the same reaction conditions of which particle size distributions were investigated, and the yield of the amount of fibers produced were measured. As the number of fibers produced is roughly proportional to the number of active catalyst particles, a linear relationship should hold between the number of catalyst particles which have the suitable size for fiber growth, and the VGCF yield. Indeed, Fig. 6-7 shows that the VGCF yield is well proportional to the number of catalyst particles which have diameters between 20 and 30 nm. This linear relationship confirms the assumed suitable particle size range for VGCF production.

The size distributions of catalyst particles produced at various reaction conditions were predicted using the model described in the previous section. First, the only unknown parameter, a of the coagulation coefficient $\beta(u,v)$, was determined as 1.08×10^{-16} $m^{2.5}s^{-1}K^{-0.5}$ by adjusting its value so that the peak position of the calculated distribution curve matches that of the experimentally obtained curve in Fig. 6-8. The solid curve in Fig. 6-8 shows the re-calculated distribution curve using the proposed model, and well expresses experimental data.

Substituting the obtained a value into Eq. (6-6), the size distribution curves of catalyst particles obtained under other reaction conditions can be predicted using Eqs. (6-9) to (6-11). Figure 6-9 shows a typical result where the line velocity of the carrier gas was changed from 2.55 (mm-NTP) s^{-1} (Fig. 6-8) to 1.02 (mm-NTP) s^{-1}. The predicted curve well represents experimental data, indicating that it is possible to predict the size distribution curves of catalyst particles obtained under various reaction conditions by using the developed model.

Finally we propose a procedure to predict the optimal reaction conditions to obtain VGCFs at high yields using the liquid pulse injection technique. First, the concentration of the catalyst material should be high. However, as there is a limit in the solubility of ferrocene in benzene, 10 wt% seems to be an adequate concentration. Next, the amount of catalyst material should be determined from the heat transfer

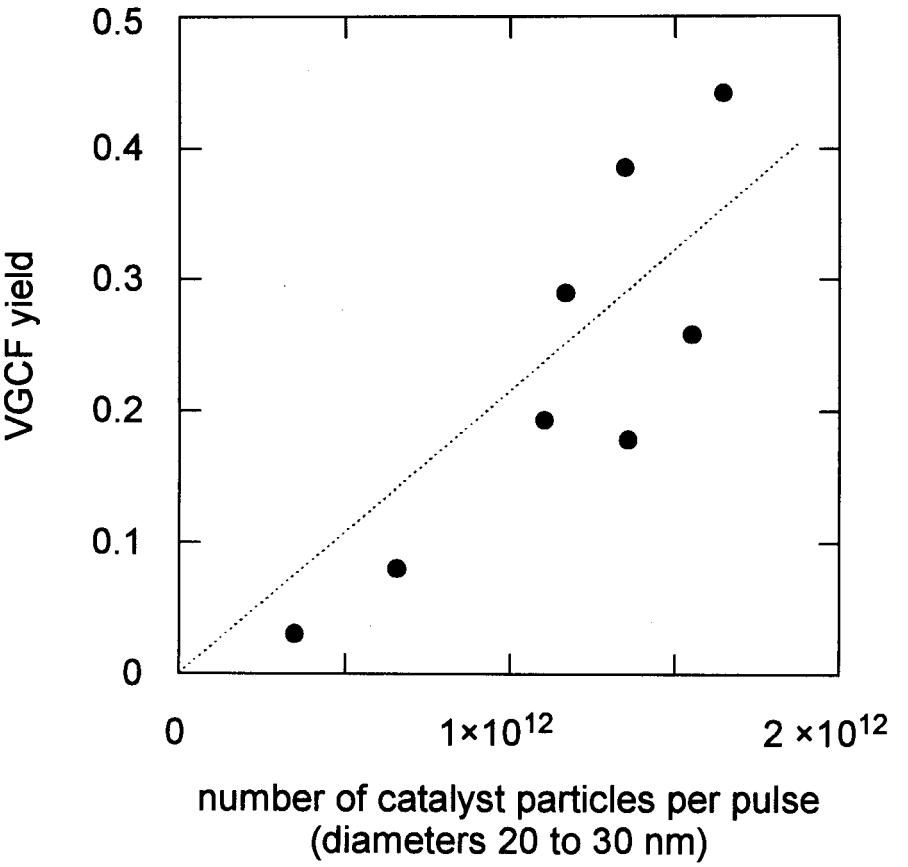

Fig. 6-7 Relationship between VGCF Yield and Number of Catalyst Particles which Have Diameters between 20 and 30 nm

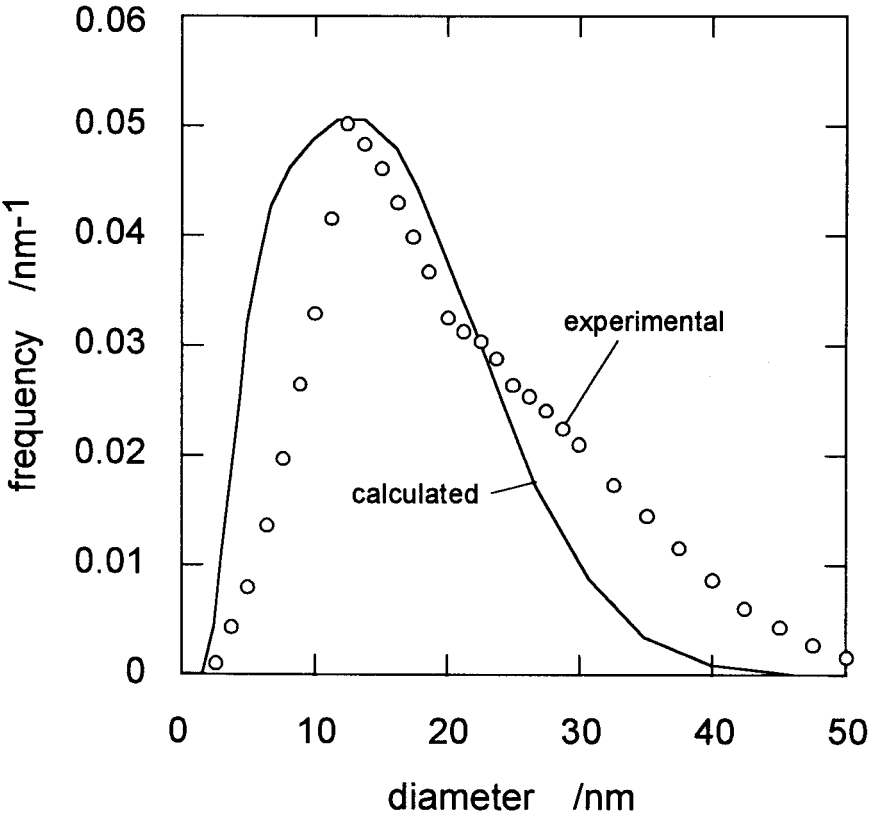

Fig. 6-8 Calculated Distribution Curve

(Catalyst Source Concentration: 10 wt%
Catalyst Source Amount per Pulse: 0.020 cm^3
Carrier Gas Line Velocity: 2.55 (mm-NTP) s^{-1})

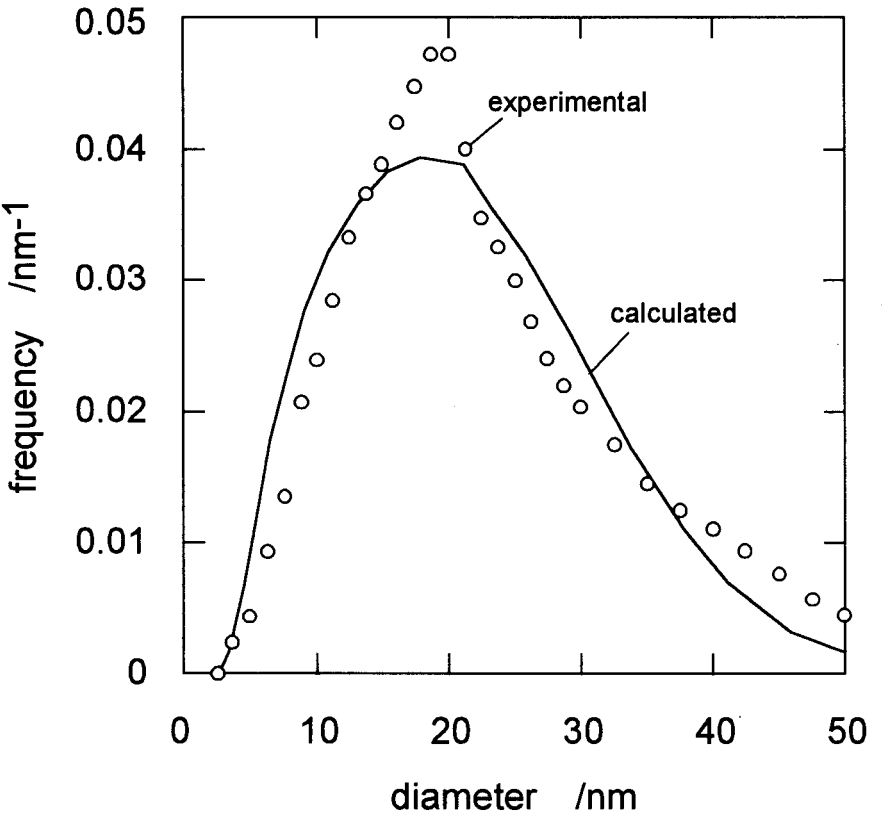

Fig. 6-9 Calculated Distribution Curve

(Catalyst Source Concentration: 10 wt%
Catalyst Source Amount per Pulse: 0.020 cm^3
Carrier Gas Line Velocity: 1.02 (mm-NTP) s^{-1})

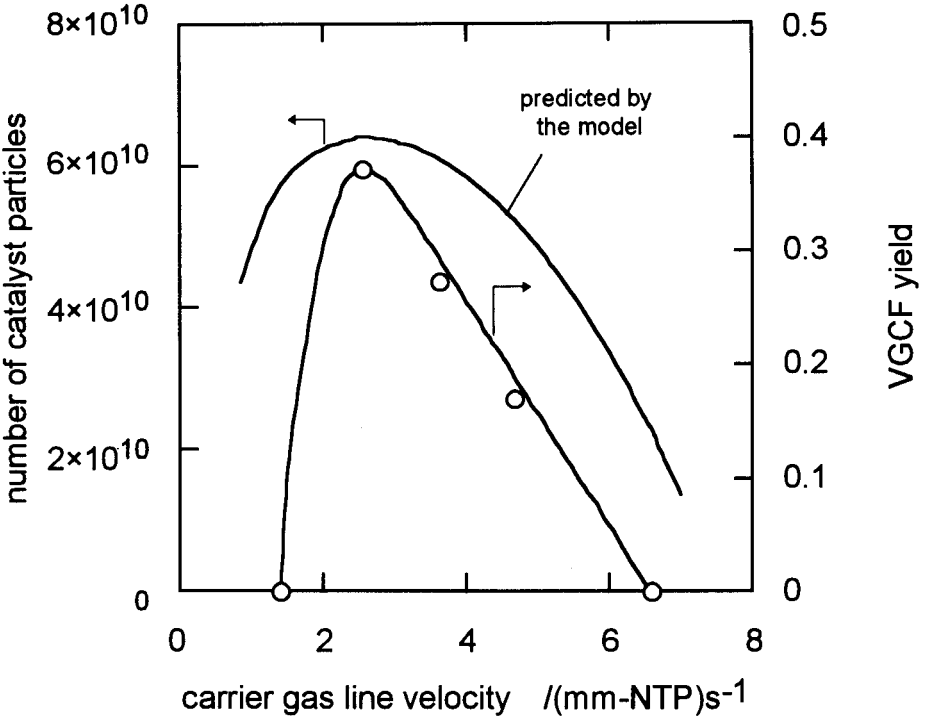

Fig. 6-10 Relationship between the Calculated Number of Catalyst Particles with Sizes between 20 and 30 nm and Carrier Gas Line Velocity

ability from the reactor wall to the liquid pulse. As was shown in chapter 3, in the reactor employed in this work, 0.020 cm^3 was the optimal value. Finally, the carrier gas line velocity should be determined by employing the proposed model, so as to obtain the maximum amount of catalyst particles with sizes between 20 and 30 nm. Figure 6-10 shows the relationship between the predicted number of catalyst particles with sizes between 20 and 30 nm, and the line velocity. This figure also shows the experimental data of the yields of VGCFs produced under the same carrier gas line velocities. The number of catalyst particles with sizes between 20 and 30 nm reaches a maximum value at the line velocity of 2.55 (mm-NTP) s^{-1}. As predicted, this line velocity also gives a maximum VGCF yield.

6.5 Conclusion

The influence of the reaction conditions on the size distribution of ultra-fine iron catalyst particles produced using the liquid pulse injection technique was investigated. Each of the selected reaction conditions, the concentration and amount of the catalyst material and the line velocity of the carrier gas, affected the distribution. It was found that VGCF yield increases with the increase in the number of catalyst particles in the size range of 20 to 30 nm. Finally, a model based on population balance equations, was developed to predict the size distribution of particles produced under various reaction conditions. This model was numerically solved using the discrete-sectional model, and was found to well represent experimental data. This allows us to predict optimal reaction conditions for the production of VGCFs.

Nomenclature

$C_{ferrocene}$	=	number of ferrocene molecules per unit volume within cell	$[m^{-3}]$
k	=	decomposition rate constant of ferrocene	$[s^{-1}]$
$n(v)$	=	distribution function	$[m^{-3}]$
$n(v,t)$	=	distribution function at time t	$[m^{-3}]$
n_i	=	number of particles containing i monomers	
N_l	=	number of particles within the lth section	
$m(x)$	=	distribution function	
r_{birth}	=	birth rate of clusters	$[m^{-6}\ s^{-1}]$
r_{v^*}	=	decomposition rate of ferrocene	$[m^{-3}\ s^{-1}]$
t	=	time from injection of catalyst material	[s]
T	=	temperature of cell	[K]
T_0	=	initial temperature of cell	[K]
v	=	volume of particle	$[m^3]$
v^*	=	volume of iron cluster (atom)	$[m^3]$
V	=	volume of cell	$[m^3]$
V_0	=	initial volume of cell	$[m^3]$
a	=	adjustable parameter	$[m^{2.5}s^{-1}K^{-0.5}]$
$\beta(u,v)$	=	coagulation coefficient	$[m^3s^{-1}]$
β_{ij}	=	coagulation coefficient of discrete regime	$[m^3s^{-1}]$
$^1\overline{\beta}_{rsl}, ^2\overline{\beta}_{rl}, ^3\overline{\beta}_{ll}, ^4\overline{\beta}_{rl}$	=	inter- and intrasectional coagulation coefficients	$[m^3s^{-1}]$
$^1\overline{\overline{\beta}}_{ir}, ^2\overline{\overline{\beta}}_{rl}, ^3\overline{\overline{\beta}}_{irl}, ^4\overline{\overline{\beta}}_{ijl}$	=	discrete-sectional coagulation coefficients	$[m^3s^{-1}]$

Literature Cited

Baker, R. T. K. and Harris, P. S., *Chemistry and physics of carbon* vol. **14**, 83 (1978)

Baker, R. T. K., *Carbon* **27**, 315 (1989)

Benissad, F., Gadelle, P., Coulon, M. and Bonnetain, L., *Carbon* **26**, 61 (1988)

Dyagileva, L. M., Mar'in, V. P., Tsyganova, E. I. and Razuvaev, G. A., *J. Organometal. Chem.* **175**, 63 (1979)

Endo, M., *CHEMTECH* **Sept.**, 568 (1988)

Friedlander, S. K., Smoke, Dust and Haze, Wiley-Interscience (1977)

Ishioka, M., Okada, T and Matsubara, K., *Carbon* **31**, 699 (1993)

Lewis, K. E. and Smith, G. P., *J. Am. Chem. Soc.* **106**, 4650 (1984)

Wu, J. J. and Flagan, R. C., *J. Colloid Interface Sci.* **123**, 339 (1988)

Appendix

Transformation of Population Balance Equations According to the Discrete-Sectional Model (DSM)

Here a new variable $\overline{n}_l$ is introduced to establish the relationship between $n(v)$ and N_l. $\overline{n}_l$ fulfills the following relationship.

$$n(v)\mathrm{d}v = \overline{n}_l \mathrm{d}x \tag{a-1}$$

Under the assumption that the x range for each section is small compared to the entire x range, the number of particles in the lth section, N_l, can be expressed as,

$$N_l = \int_{v_{l-1}}^{v_l} n(v)\mathrm{d}v = \overline{n}_l \int_{x_{l-1}}^{x_l} \mathrm{d}x = \overline{n}_l \, (x_l - x_{l-1}) = n(v)(x_l - x_{l-1})\frac{\mathrm{d}v}{\mathrm{d}x} \tag{a-2}$$

(Population Balance Equation of Iron Clusters (Atoms))

(a) The generation of clusters due to the decomposition of the particle material can be expressed by Eqs. (6-4) and (6-5).

(b) The disappearance of clusters due to the coagulation of clusters with particles within the discrete regime can be expressed as,

$$-\sum_{i=1}^{k} \beta_{1i} \frac{n_1}{V} \frac{n_i}{V} \tag{a-3}$$

(c) The disappearance of clusters due to the coagulation of clusters with particles in the sectional regime can be derived as follows using Eq. (a-2).

$$-\int_{v_0}^{v_M}\beta(v^*,v)\frac{n_1}{V}\frac{n(v)}{V}\mathrm{d}v = -\left[\sum_{r=1}^{M}{}^{1}\overline{\overline{\beta}}_{1r}\frac{N_r}{V}\right]\frac{n_1}{V} \tag{a-4}$$

where,

$${}^{1}\overline{\overline{\beta}}_{1r} = \int_{x_{r-1}}^{x_r}\frac{\beta(v^*,v(x))}{x_r - x_{r-1}}\mathrm{d}x,\ (1 \le r \le M) \tag{a-5}$$

Therefore, the population balance equation corresponding to clusters can be expressed by Eq. (6-9).

(Population Balance Equations of the Number of *i*-mers in the Discrete Regime)

(d) The appearance of *i*-mers due to the coagulation of two particles in the discrete regime can be expressed as,

$$\frac{1}{2}\sum_{j=1}^{i}\beta_{(i-j)j}\frac{n_{(i-j)}}{V}\frac{n_j}{V} \tag{a-6}$$

The factor 1/2 is employed to avoid double counting.

(e) The disappearance of *i*-mers due to the coagulation of *i*-mers with particles within the discrete regime is given as,

$$-\sum_{j=1}^{k}\beta_{ij}\frac{n_i}{V}\frac{n_j}{V} \tag{a-7}$$

(f) The disappearance of *i*-mers due to the coagulation of *i*-mers with particles in the sectional regime can be expressed using Eq. (a-2) as,

$$-\int_{v_0}^{v_M}\beta(i\times v^*,v)\frac{n_1}{V}\frac{n(v)}{V}\mathrm{d}v = -\left[\sum_{r=1}^{M}{}^{1}\overline{\overline{\beta}}_{ir}\frac{N_r}{V}\right]\frac{n_i}{V} \tag{a-8}$$

where,

$$ {}^{1}\overline{\overline{\beta}}_{ir} = \int_{x_{r-1}}^{x_r} \frac{\beta(i \times v^*, v(x))}{x_r - x_{r-1}} \mathrm{d}x, \quad \begin{pmatrix} 1 \le i \le k \\ 1 \le r \le M \end{pmatrix} \tag{a-9} $$

From the above equations, the population balance equation for i-mers in the discrete regime can be expressed by Eq. (6-10).

(Population Balance Equation for the Sectional Regime)

(g) The formation of particles of the lth section by the coagulation of two particles of sections lower than l can be expressed by,

$$ \frac{1}{2}\int_{v_0}^{v_{l-1}}\int_{v_0}^{v_{l-1}} \theta(v_{l-1} \le u+v \le v_l)\beta(u,v)\frac{n(u)}{V}\frac{n(v)}{V}\mathrm{d}u\mathrm{d}v = \frac{1}{2}\sum_{r=1}^{l-1}\sum_{s=1}^{l-1} {}^{1}\overline{\beta}_{rsl}\frac{N_r}{V}\frac{N_s}{V} \tag{a-10} $$

where,

$$ {}^{1}\overline{\beta}_{rsl} = \int_{x_{r-1}}^{x_r}\int_{x_{s-1}}^{x_s} \frac{\theta(v_{l-1} \le u(y)+v(x) \le v_l)\beta(u(y),v(x))}{(x_r - x_{r-1})(x_s - x_{s-1})}\mathrm{d}y\mathrm{d}x, \quad \begin{pmatrix} 2 \le l \le M \\ 1 \le r \le l-1 \\ 1 \le s \le l-1 \end{pmatrix} \tag{a-11} $$

and,

$$ \theta\,(statement) = \begin{cases} 1 & (statement; TRUE) \\ 0 & (statement; FALSE) \end{cases} \tag{a-12} $$

(h) The disappearance of particles in the lth section by the coagulation of particles in the lth section with particles in sections lower than l is given by,

$$-\int_{v_0}^{v_{l-1}}\int_{v_{l-1}}^{v_l}\theta(u+v\geq v_l)\beta(u,v)\frac{n(u)}{V}\frac{n(v)}{V}\mathrm{d}u\mathrm{d}v=-\sum_{r=1}^{l-1}{}^{2}\overline{\beta}_{rl}\frac{N_r}{V}\frac{N_l}{V}$$

(a-13)

where,

$${}^{2}\overline{\beta}_{rl}=\int_{x_{r-1}}^{x_r}\int_{x_{l-1}}^{x_l}\frac{\theta(u(y)+v(x)\geq v_l)\beta(u(y),v(x))}{(x_r-x_{r-1})(x_l-x_{l-1})}\mathrm{d}y\mathrm{d}x,\quad\begin{pmatrix}2\leq l\leq M\\1\leq r<l-1\end{pmatrix}$$

(a-14)

(i) The disappearance of particles in the *l*th section due to the coagulation of two particles which both belong to the lth section can be derived as,

$$-\frac{1}{2}\int_{v_{l-1}}^{v_l}\int_{v_{l-1}}^{v_l}[\theta(u+v<v_l)+2\theta(u+v\geq v_l)]\beta(u,v)\frac{n(u)}{V}\frac{n(v)}{V}dudv$$
$$=-\frac{1}{2}{}^{3}\overline{\beta}_{ll}\frac{N_l{}^{2}}{V}$$

(a-15)

where,

$${}^{3}\overline{\beta}_{ll}=\int_{x_{l-1}}^{x_l}\int_{x_{l-1}}^{x_l}\frac{[\theta(u(y)+v(x)<v_l)+2\theta(u(y)+v(x)\geq v_l)]\beta(u(y),v(x))}{(x_l-x_{l-1})^2}\mathrm{d}y\mathrm{d}x$$

$$(1\leq l\leq M)$$

(a-16)

(j) The disappearance of particles in the *l*th section due to the coagulation of particles in the *l*th section with particles in sections higher than *l* can be expressed as,

$$-\int_{v_l}^{v_M}\int_{v_{l-1}}^{v_l}\beta(u,v)\frac{n(u)}{V}\frac{n(v)}{V}\mathrm{d}u\mathrm{d}v=-\sum_{r=l+1}^{M}{}^{4}\bar{\beta}_{rl}\frac{N_r}{V}\frac{N_l}{V} \qquad \text{(a-17)}$$

where,

$${}^{4}\bar{\beta}_{rl}=\int_{x_{r-1}}^{x_r}\int_{x_{l-1}}^{x_l}\frac{\beta(u(y),v(x))}{(x_r-x_{r-1})(x_l-x_{l-1})}\mathrm{d}y\mathrm{d}x,\quad \begin{pmatrix}1\le l\le M-1\\ l+1\le r\le M\end{pmatrix} \qquad \text{(a-18)}$$

(k) The disappearance of particles in the lth section due to the coagulation of particles in the lth section with particles in the discrete regime is given by,

$$-\sum_{i=1}^{k}\int_{v_{l-1}}^{v_l}\theta(i\times v^{*}+v\ge v_l)\beta(i\times v^{*},v)\frac{n_i}{V}\frac{n(v)}{V}\mathrm{d}v=-\sum_{i=1}^{k}{}^{2}\bar{\bar{\beta}}_{il}\frac{n_i}{V}\frac{N_l}{V} \qquad \text{(a-19)}$$

where,

$${}^{2}\bar{\bar{\beta}}_{il}=\int_{x_{l-1}}^{x_l}\frac{\theta(i\times v^{*}+v(x)\ge v_l)\beta(i\times v^{*},v(x))}{x_l-x_{l-1}}\mathrm{d}x,\quad \begin{pmatrix}1\le i\le k\\ 1\le l\le M\end{pmatrix} \qquad \text{(a-20)}$$

(l) The generation of particles in the lth section due to the coagulation of particles in sections lower than l with particles in the discrete regime is expressed as,

$$\sum_{i=1}^{k}\int_{0}^{v_{l-1}}\theta(v_{l-1}\le i\times v^{*}+v<v_l)\beta(i\times v^{*},v)\frac{n_i}{V}\frac{n(v)}{V}\mathrm{d}v=\sum_{i=1}^{k}\sum_{r=1}^{l-1}{}^{3}\bar{\bar{\beta}}_{irl}\frac{n_i}{V}\frac{N_r}{V} \qquad \text{(a-21)}$$

where,

$$ {}^{3}\overline{\overline{\beta}}_{irl} = \int_{x_{r-1}}^{x_r} \frac{\theta(v_{l-1} \le i \times v^* + v(x) < v_l)\beta(i \times v^*, v(x))}{x_r - x_{r-1}} \mathrm{d}x, \quad \begin{pmatrix} 1 \le i \le k \\ 1 \le r \le l-1 \\ 2 \le l \le M \end{pmatrix} \tag{a-22} $$

(m)The generation of particles in the *l*th section due to the coagulation of two particles which both belong to the discrete regime becomes,

$$ \frac{1}{2}\sum_{i=1}^{k}\sum_{j=1}^{k} {}^{4}\overline{\overline{\beta}}_{ijl} \frac{n_i}{V}\frac{n_j}{V} \tag{a-23} $$

where,

$$ {}^{4}\overline{\overline{\beta}}_{ijl} = \theta(v_{l-1} \le i \times v^* + j \times v^* < v_l)\beta(i \times v^*, j \times v^*), \quad \begin{pmatrix} 1 \le i \le k \\ 1 \le j \le k \\ 1 \le l \le M \end{pmatrix} \tag{a-24} $$

Therefore, the population balance equation corresponding to the particles in the sectional regime can be expressed by Eq. (6-11).

CHAPTER 7

General Summary

This thesis was dedicated to develop a new method to produce long vapor grown carbon fibers at high growth rates. The key point was how to generate active ultra-fine catalyst particles, which are inevitable for the elongation of the fibers. This was achieved by introducing the catalyst material into the reactor as a liquid pulse. Through experimental studies, the following conclusions were obtained.

The introduction of the catalyst material to the reactor as a liquid pulse enables the rapid raising of the pulse temperature above its decomposition temperature. This leads to the generation of catalyst particles in a highly dense state. Moreover liquid pulse introduction allows the controlling of the contacting pattern between the generated catalyst particles and the carbon source. Therefore the sizes of the catalyst particles can be controlled before they make contact with the carbon source, as they grow through the coalescence among themselves. The size of the catalyst particles is a critical factor for the rapid growth of the fibers. It was found that fibers with lengths up to 55 mm could be obtained within 30 s by the proposed method. Empirical equations which well represent the growth behavior of the fibers were also proposed. It was also found that fibers obtained through this new method possess the same structure as those produced by conventional methods. Due to this structure, the obtained fibers show high electrical conductivities, tensile strengths and oxidation resisitivities.

The effect of reaction conditions when employing this new production method were also investigated. Considering the reaction temperature, a higher temperature is favorable to increase the activity of the catalyst particles. However, if the temperature is too high, the carbon source will tend to thermally decompose, resulting

in the decrease in its concentration. This leads to the decrease in the growth rate, and the yield of the fibers. Therefore, an optimal reaction temperature exists. This is also the case with the initial carbon source concentration. The initial growth rate of the fibers increases with the increase in the initial carbon source concentration, but after reaching a maximum value, it starts to decrease. At high reaction temperatures, which are inevitable to activate the catalyst particles, the carbon source will usually thermally decompose. In this new production method, this decomposition is suppressed by hydrogen. However, the suppression effect of hydrogen decreases with the increase in the concentration of the carbon source. Therefore, an optimal initial carbon source concentration, which maximizes the carbon source concentration at the reaction zone exists.

The axial growth rate of the fibers highly depends on the size of the catalyst particle. In this new production method, these particles are formed through the coalescence of iron clusters generated by the thermal decomposition of ferrocene. Therefore, reaction conditions which alter the size distribution of the particles, such as the carrier gas line velocity, and amount of catalyst source injection must be adjusted to increase the number of catalyst particles which have the size suitable for rapid fiber growth.

In order to realize a new production process using this new method, it is necessary to continuously produce VGCFs. It was shown that this could be done by intermittently injecting liquid pulses of the catalyst source into the reactor. However, one must be sure that the interval of injection must be long enough so that the pulses do not interfere with one another.

Presently, benzene is the most popular carbon source for the production of VGCFs. It was experimentally shown that fibers could also be rapidly grown using aromatic compounds such as toluene and xylene. This implies that a low cost mixture of benzene, toluene and xylene could be used as the carbon source for VGCF production which was also proved experimentally. It was also found that the methyl group has a

growth inhibiting effect, therefore the fiber growth rate constants of the three aromatic compounds decrease in the order benzene, toluene and xylene. Furthermore, it was shown that fiber growth rate constants of mixtures of the three aromatic compounds are predictable.

VGCFs were rapidly obtained from light paraffins, such as *i*-butane, *n*-pentane and *n*-hexane. As it is unlikely that fibers grow directly from the initial carbon source considering the high reaction temperature, the actual hydrocarbon(s) which exists at the reaction zone were collected and analyzed. It was found that when light paraffins were used as the initial carbon source, the hydrocarbons which actually exist at the reaction zone were mainly benzene, methane and ethylene. It was also found that among these hydrocarbons, benzene is the actual contributor to fiber growth. Therefore, VGCFs can be produced from a wide variety of hydrocarbons which generate benzene under the conditions used for fiber production. The key point for efficient fiber production is to prepare active catalyst particles where the concentration of the generated benzene is high. This can be easily achieved using the newly developed method.

The influence of the reaction conditions on the size distribution of catalyst particles using this new production technique was also investigated. Reaction conditions which affect the coalescence behavior of the catalyst material, such as concentration and amount of the catalyst material and the line velocity of the carrier gas, significantly affected the size distribution. It was also found that the yield of fibers increases with the increase in the number of catalyst particles in the size range of 20 to 30 nm. Therefore, reaction conditions must be optimized to maximize the number of the catalyst particles which sizes are in this range.

A model based on population balance equations was developed to predict the size distribution of particles produced under various reaction conditions. The discrete-sectional model was found to be a powerful tool for actual calculations based on this

model. This model was found to well represent experimental data. Therefore, optimal reaction conditions to maximize the yield of fibers are predictable by employing this model.

The key factors for efficient fiber production in a laboratory scale by using this new method were clarified through the works presented in this thesis. However, for the realization of this new process in a commercial scale, further analysis of the reactor as well as reaction conditions must be done. Firstly, in the reactor employed in this work, the maximum attainable yield of the fibers was about 40 %, as approximately 60 % of the carbon source is consumed by thermal decomposition. This carbon loss may be decreased by changing the configuration of the reactor, for example by decreasing the ratio between the surface area and volume of the reactor, but lowering the production temperature is a more effective way to increase fiber yield. This may be realized by preparing catalyst particles which activate at a lower temperature. Lowering the melting point of the catalyst particle by adding another metal to it is one way to achieve this. Secondly, the flow pattern in the reactor is not realistic for commercial production as the Reynolds number of the flow is about unity. Factors, which were not problematic in laboratory scale reactors, such as heat convection, may be critical for efficient fiber growth. Therefore, precise analysis of the gas flow in the reactor must be conducted to produce fibers in a different flow pattern must be done in order to up-scale this process.

List of Publications

The studies in this thesis have been presented in the following publications.

Chapter 2

THE PRODUCTION OF LONG VAPOR GROWN CARBON FIBERS AT HIGH GROWTH RATES

T. Masuda, S. R. Mukai and K. Hashimoto, *Carbon* **30**, 124-125 (1992)

THE LIQUID PULSE INJECTION TECHNIQUE: A NEW METHOD TO OBTAIN LONG VAPOR GROWN CARBON FIBERS AT HIGH GROWTH RATES

T. Masuda, S. R. Mukai and K. Hashimoto, *Carbon* **31**, 783-787 (1992)

Chapter 3

RAPID VAPOR GROWN CARBON FIBER PRODUCTION USING THE INTERMITTENT LIQUID PULSE INJECTION TECHNIQUE

T. Masuda, S. R. Mukai, H. Fujikawa, Y. Fujikata and K. Hashimoto, *Materials and Manufacturing Processes* **9**, 237-247 (1994)

Chapter 4

THE PRODUCTION OF VAPOR GROWN CARBON FIBERS FROM A MIXTURE OF BENZENE, TOLUENE AND XYLENE USING THE LIQUID PULSE INJECTION TECHNIQUE

S. R. Mukai, T. Masuda, Y. Fujikata and K. Hashimoto, *Chemical Engineering Science* **49**, 4909-4916 (1994)

Chapter 5

THE PRODUCTION OF VAPOR GROWN CARBON FIBERS FROM LIGHT PARAFFINS USING THE LIQUID PULSE INJECTION TECHNIQUE

S. R. Mukai, T. Masuda, Y. Fujikata, T. Harada and K. Hashimoto, *Carbon* **33**, 733-735 (1995)

DOMINANT HYDROCARBON WHICH CONTRIBUTES TO THE GROWTH OF VAPOR GROWN CARBON FIBERS

S. R. Mukai, T. Masuda, T. Harada and K. Hashimoto, *Carbon* **34**, 645-648 (1996)

Chapter 6

THE INFLUENCE OF CATALYST PARTICLE SIZE DISTRIBUTION ON THE YIELD OF VAPOR GROWN CARBON FIBERS PRODUCED USING THE LIQUID PULSE INJECTION TECHNIQUE

S. R. Mukai, T. Masuda, Y. Matsuzawa and K. Hashimoto, *Chemical Engineering Science*, in press

Acknowledgment

Work on this study has been conducted at the Laboratory of Chemical Reaction Engineering, Division of Chemical Engineering, Graduate School of Engineering, Kyoto University from 1989 to 1997.

The author would like to express his sincere gratitude to Dr. Kenji Hashimoto, Professor of Kyoto University, not only for his constant supervision and encouragement throughout the course of this study, but also for giving the author a chance to become an academic staff of his laboratory, and continue work on this challenging topic.

It was a great pleasure and honor to have two supervisors for this thesis, Dr. Kouichi Miura and Dr. Masataka Tanigaki, Professors of Kyoto University. The author would like to express his sincere appreciation for their critical reading of the manuscript and valuable suggestions.

The author would like to express his sincere gratitude to Dr. Takao Masuda, Associate Professor of Kyoto University, for his kind guidance and encouragement throughout this study. The author would also like to express his gratitude to Dr. Motoaki Kawase. It was a great pleasure and stimulating experience to work together with both Doctors at the Laboratory of Chemical Reaction Engineering.

This thesis could not be submitted without the help and assistance of Messrs. Manabu Kano, Hiroyuki Fujikawa, Yoshihiro Fujikata, Yoshiaki Matsuzawa and Takeshi Harada. The author would like to express his sincere appreciation to them for their efforts and ideas on conducting this work.

Much analytical work, which all does not appear in this thesis, was conducted using the equipment of the Laboratory of Environmental Process Engineering, Division of Chemical Engineering, Graduate School of Engineering, Kyoto University. Sincere acknowledgments are due to Dr. Kazuhiro Mae, Associate Professor of Kyoto University, and Mr. Hiroyuki Nakagawa, Research Instructor of Kyoto University, not only for their guidance in using the equipment, but also for their kind suggestions about the handling of carbon materials. The author is also indebted to Dr. Kuniaki Gotoh, presently Associate Professor of Yamaguchi University, for suggestions about obtaining the size distributions of catalyst particles, and comments about the development of the model, both results shown in chapter 6. Sincere acknowledgments are also due to Messrs. Toshio Kawaguchi, Kiyoshi Nakai and Tatsuya Suzuki of Sumitomo Chemical Co., Ltd., for the transmission electron microscopy observations to obtain the frequency of the catalyst particles in chapter 6.

The author would like to express his sincere appreciation to the generous financial support by Grant-in-Aid for Scientific Research from the Ministry of Education, Science and Culture, by Research Development Corporation of Japan, and by Sumitomo Bakelite Co., Ltd. Sincere acknowledgments are due to Mr. Masaki Saitoh of Research Development Corporation of Japan, and Messrs. Tsuneo Moriya and Yoshinobu Ohtake of Sumitomo Bakelite Co., Ltd.

The author was very fortunate to obtain the opportunity to meet and discuss with the "Giants" in the field of Vapor Grown Carbon Fibers during the course of this study, Dr. Terry Baker, Professor of Northeastern University, Dr. Gary Tibbetts of General Motors and Dr. Morinobu Endo, Professor of Shinshu University. Their outstanding contributions along with those of many researcher who devoted much of their time to research on Vapor Grown Carbon Fibers led the author to many new ideas and to the development of this new production method.

The author can't forget how happy his father looked when he heard his son's intention

to continue research to achieve the degree of Doctor of Engineering. It was only a few days after this incident that he passed away. It is beyond imagination how tough it was for the author's mother to live on her own after her husband's death. Although it was a situation that she should rely on her son, she never did so. The author would like to express his deepest gratitude to his parents for their encouragement and support, and would like to dedicate this thesis to them.